8-2009

Creation of Defined Single Cell Resolution Neuronal Circuits on Microelectrode Arrays

Russell Pirlo
Clemson University, rpirlo@gmail.com

CREATION OF DEFINED SINGLE CELL RESOLUTION NEURONAL CIRCUITS ON MICROELECTRODE ARRAYS

A Dissertation
Presented to
the Graduate School of
Clemson University

In Partial Fulfillment
of the Requirements for the Degree
Doctor of Philosophy
Bioengineering

---

by
Russell Kirk Pirlo
August 2009

Approved by:
Dr. Bruce Gao, Committee Chair
Dr. Ken Webb
Dr. James Colacino
Dr. Mark Kindy

ABSTRACT

The way cell-cell organization of neuronal networks influences activity and facilitates function is not well understood. Microelectrode arrays (MEAs) and advancing cell patterning technologies have enabled access to and control of *in vitro* neuronal networks spawning much new research in neuroscience and neuroengineering. We propose that small, simple networks of neurons with defined circuitry may serve as valuable research models where every connection can be analyzed, controlled and manipulated.

Towards the goal of creating such neuronal networks we have applied microfabricated elastomeric membranes, surface modification and our unique laser cell patterning system to create defined neuronal circuits with single-cell precision on MEAs.

Definition of synaptic connectivity was imposed by the 3D physical constraints of polydimethylsiloxane elastomeric membranes. The membranes had 20µm clear-through holes and 2-3µm deep channels which when applied to the surface of the MEA formed microwells to confine neurons to electrodes connected via shallow tunnels to direct neurite outgrowth. Tapering and turning of channels was used to influence neurite polarity. Biocompatibility of the membranes was increased by vacuum baking, oligomer extraction, and autoclaving. Membranes were bound to the MEA by oxygen plasma treatment and heated pressure.

The MEA/membrane surface was treated with oxygen plasma, poly-D-lysine and laminin to improve neuron attachment, survival and neurite outgrowth. Prior to cell patterning the outer edge of culture area was seeded with $5x10^5$ cells per cm and

incubated for 2 days. Single embryonic day 7 chick forebrain neurons were then patterned into the microwells and onto the electrodes using our laser cell patterning system.

Patterned neurons successfully attached to and were confined to the electrodes. Neurites extended through the interconnecting channels and connected with adjacent neurons. These results demonstrate that neuronal circuits can be created with clearly defined circuitry and a one-to-one neuron-electrode ratio. The techniques and processes described here may be used in future research to create defined neuronal circuits to model *in vivo* circuits and study neuronal network processing.

DEDICATION

This work is dedicated to my parents Russell and Mary Ann Pirlo. It is not only by one's own hard work, but also by the help of others that a person achieves success I am blessed to have their love and support. They encouraged me to become a scientist from my earliest memories. Looking back, it's funny, maybe even scary, how significantly they molded my mind. Today I can see the intent and the worth of the things they worked hard to give me and teach me.

Throughout my life, my parents have shown me the value of problem solving and ingenuity. In my youth I received building toys and wrench sets as an adult. I learned diligence and capability through observing my father build our house. I have never forgotten his encouragement to provide for myself through invention and discovery.

I am thankful to my mother for encouraging me to read and helping me with academics. She also got me involved in 4-H which was invaluable to my social confidence and inspiring with projects like building an electric motor out of wire and nails.

Later my parents put me through college and supported me even when I dropped out, though not *too* much. When I decided to go to graduate school they were extremely supportive and helped me move to Clemson. I am very happy to have this way of thanking them for all they have done. I love You Mom and Dad.

ACKNOWLEDGMENTS

I would like to acknowledge my advisor or Dr. Bruce Gao. I did not come to Clemson to work with Bruce, but I liked him immediately and was excited by the laser cell patterning project which has been central to our work these past 5 years. In our individual meetings he would occasionally use a Chinese metaphor to explain the larger more abstract ideas of work ethic and research approach. As an advisor he encouraged me to develop an autonomous, confident and robust approach to research which I will apply to future projects, scientific and otherwise.

I would like to thank my committee, Dr. Ken Webb, Dr. James Colacino and Dr. Mark Kindy for their time, advice, guidance and patience.

I would like to acknowledge my labmates in the Clemson Biophotonics Lab especially Andrew Sweeny who besides being a master of laboratory organization, offered the kind of support only another graduate student can. I am lucky to have been a teaching assistant for Professor Delphine Dean and to count her as friend. Cassie Gregory was always ready to offer me research advice and assistance. I would also like to acknowledge my first friend, roommate and labmate in Clemson, Sriram Narasimhan.

Finally, I would like to acknowledge my friends in Clemson who had nothing to do with engineering but everything to do with my life the past 5 years. My girlfriend Claudia Dishon, who brightened my life and eased my burdens. Cam Whiteside and his twisted stories. Nathaniel Edwards and his beats, films and jokes. Nikki Dodd. My friends Heath Combs, Brianne Ferguson, Jason Koepke, and Matt Landreth who came to visit me in Clemson. Places- The Joint, the reservoir, the RooPlex, the old MoeJoes

TABLE OF CONTENTS

Page

Table of Contents (Continued)

Page

LIST OF TABLES

LIST OF FIGURES

List of Figures (Continued)

Figure Page

List of Figures (Continued)

List of Figures (Continued)

Figure Page

List of Figures (Continued)

Figure Page

List of Figures (Continued)

List of Figures (Continued)

Figure Page

CHAPTER I
INTRODUCTION

The mammalian brain is an enormously complex organ with immense parallelism, adaptability, and pattern recognition capabilities. There are great rewards if we can understand, repair, mimic, interface or repurpose the machinery behind these abilities. Still, our interests go deeper than just the concrete computational functions; embodied within the human brain are the abilities to create, think and decide as well as our personalities and ultimately, consciousness. The advancing field of neuroscience and our growing knowledge of how our brains and minds work is having an increasingly large impact or our society, and this trend will accelerate as the field of neuroengineering develops.

Historically, the study of the brain has been approached from two directions, the anatomical and the cellular/molecular or as Kandel and Pittenger divide the study of memory[6], the systems level and the molecular level. These two approaches were shaped by the available tools and previous knowledge, (or limits thereof).

Neuroscience at the Anatomical Level

The effort to localize mental processes to specific regions of the brain began in the early 1800s, with Gall (phrenology). While the 35 mental faculties ascribed by Gall to specific cortical regions may seem ill conceived from today's perspective, there is still a consensus that different regions of the brain perform certain specific tasks and communicate with other regions to operate as a system. At the anatomical level, brain damage, open brain surgery, and functional magnetic resonance imaging(fMRI) have

enabled us to map cognitive functions to specific regions of the brain[6]. One region of particular interest has been the hippocampal region of the brain which has been implicated in learning and memory. Much of what we have learned about the hippocampus has come from electrophysiological studies of *ex vivo* slices of the tissue via patch clamp or MEA. The hippocampus is also notable because of its implication in Alzheimer's disease.

Neuroscience at the Cellular Level

Using Camillo Golgi's sliver chromate stain Ramón y Cajal was able to resolve the fine structures of the brain and concluded that nervous tissue was comprised of individual autonomous cells, "neurons" rather than a continuous web as previously thought. For this discovery Cajal shared the 1906 Nobel Prize in Physiology with Golgi. This marks the start studying neuroscience at the cellular level. Confocal and two-photon microscopy techniques and fluorescent labeling techniques such as antibody staining and transgenic labeling are enabling a clearer vision of how individual neurons connect to form neuronal networks *in vitro* and *in vivo*[7] . Yet examining a neuronal networks electrical activity and synapse characteristics at a single cell level is a challenge even today.

Towards understanding the newfound cellular components of the brain, a large part of neuroscience research in the 20th century investigated the activities and mechanisms of single neurons or single synapses. By mid-century the voltage clamp technique was allowing scientists to probe the electrical activity of single neurons, a

crucial tool in understanding the ionic and molecular mechanisms of these cells and the electrical activities so important to transmission and processing of information.

Famously John Eccles applied these tools to the reflex arc to study synaptic transmission. Hodgkin and Huxley who shared the 1963 Nobel Prize in Physiology with Eccles were some of the first to perform intracellular electrophysiology using the voltage clamp method to understand and model the initiation and propagation of action potentials in the neuron. Using multiple patch clamps as well as chemical stimulation methods scientists like Eric Kandel probed the learning mechanisms of individual synapses. This experimental method could electrically probe simple invertebrate neuronal circuits, *in vitro* neuronal circuits, or circuits within brain slices. The patch clamp technique has enabled our understanding about how single neurons and individual synapses behave, including the various receptors, gated ion channels and secondary messengers related to learning and memory.

Unknown Fundamentals of Neuroscience

While neuroscience has made immense progress in elucidating the biology and function of the brain and neurons there are still many unanswered fundamental questions. We have yet to explain the relation between organization and activity at the intermediate level of the brains structure: how do the higher cognitive functions of the brain arise from the individual connections between single neurons? Furthermore it is still not clear if neurons or synapses are the basic computational unit of the brain[8] or whether the complex functions of the brain can even be broken down into a machine composed of fundamental units. It may be impossible to simplify the neural activity in such a manner

as the characteristics and activities of neurons, synapses, astrocytes, and non-synaptic extracellular signals all contribute. For example, Astrocytes were until recently considered only a passive component of the brains signal processing functions. However, it is known that astrocytes increase the number of synapses, and that increase in synapses leads to an exponential increase[9] in network activity[10]. Astrocytes also play important roles in the recycling of neurotransmitters at synapses and may be important to synaptic information processing[11]. Neurons and glia communicate intimately [12-14] yet astrocytes have largely been left out of *in vitro* neuronal network models, and the mathematical modeling of synapses and neuronal networks. We believe that the field of neuroscience lacks a practical tool for creating defined and simplified heterotypic (including astrocytes) neuronal networks in which every intercellular connection is identifiable, and every cell has a dedicated electrophysiological, input and output. For a full and good understanding of neuronal network processing it is absolutely necessary to include astrocyte components in the investigation of neuronal network structure/function.

Neural Connections Give Way to Function

Even if we disregard the indefinite roles of astrocytes and concentrate only on neuron to neuron connections, understanding the architecture of neuronal circuitry is still a tremendous challenge. The human brain contains and estimated 100 billion neurons, each connected with 5,000-10,000 other neurons for a grand total of a quadrillion neural connections[15]. This complexity is unrivaled by any other biological system and facilitates similarly unrivaled mental capabilities. It is the complex connections between neurons that give rise to the incredible sensing, learning, memory and thinking abilities as

well as consciousness. While we are beginning to understand certain circuits, such as those which produce vision, other higher levels of thought, decision making, and memory are not understood. One problem is the difficulty in monitoring the activity the individual neurons that make up complex networks. Tools and techniques that enable reduced complexity and/or increased access in order to explore the roles of cell-contact and network architecture in computational capability are extremely important. The ability to identify single cells and individual connections is a key prerequisite to understanding the components and conditions needed to produce computational networks with specific functions. In this way it is possible to decipher, test and prove models for neuronal network logic. By manipulating and monitoring individual neurons and neuronal networks we can understand how single cell/connection changes shape network development and operation. This same process may also be applied toward neurodegenerative diseases. The initial causes and mechanisms of disease progression from a single cell/location through neuronal circuitry or regions of the brain are still unknown for Alzheimer's disease and Amyotrophic lateral sclerosis. Simplified heterotypic neuronal circuit models could provide a valuable research models for these diseases which cannot be monitored or manipulated at such a scale *in vivo* or even with conventional *in vitro* cultures.

Cell Patterning Technology

To create *in vitro* research models which offer control over geometry, cell types, and cell-cell interactions researchers have developed many cell patterning techniques by borrowing, bending and building upon microfabrication techniques of the microelectronic

industry. Photolithography may be used to create surface patterns of cytophilic or cytophobic chemicals to control areas of cell attachment. Photolithography may also be used as a first step to create molds for elastomeric devices including stamps for microcontact printing (μCP), elastomeric membranes, and microfluidics. Additionally there are jet-based printing techniques and laser printing and manipulation techniques for controlling the geometry of cells cultures. In native tissues cells are highly ordered, especially neuronal networks, these technologies offer the ability to organize cells in order to mimic, isolate, and study how the geometry and organization of cells shape their development and function[16].

Microelectrode Arrays

The patch clamp technique remains an important and useful electrophysiological tool with the unique ability to probe single ion channels with its micropipette and examine actual electrical properties of the membrane including conductance, potential, and capacitance. Yet it is the micropipette and the associated headstage and micromanipulators that limit the number of electrodes that can physically be employed. To investigate neuronal network activity, many simultaneous recordings are required. Microelectrode arrays, like cell patterning techniques, borrow microelectronics technology for the study of cell biology. Neuroscience has reached this stage of inquiry by building upon our knowledge of neurons at the cellular and molecular level and through the development of microelectronic devices.

In contrast to the patch clamp technique MEAs are only capable of recording of extracellular potentials produced by a cells ionic current as they travel through the

extracellular environment. For this reason, MEAs are used only to examine the action potential or spike activity from neurons and neuronal networks. However, a prevailing concept is that neuronal information is processed, transmitted and stored as a code of spikes. A typical MEA may have 60 electrodes versus the 2-3 electrodes that may be employed simultaneously with a patch clamp set up. This allows for recording many more points in the network, but does not allow for specific neurons to be probed, as the neurons are usually randomly cultured at high density over the electrodes.

Engineering Neuronal Networks

Combining cell patterning technology with microelectrode arrays in order to study neuronal networks is an obvious idea at least a decade old. In this time it has been demonstrated to be a powerful tool with clear potential, but it is still relatively new and our abilities are still advancing. Because the electrodes of a planar MEA cannot be brought to a cell the way a patch clamp micropipette can be, patterning not only allows for refining network structure, but bringing it to and keeping it on the electrodes. Microcontact printing is the most popular method and has been used to create more and more restricted networks. Bruce Wheeler's group has worked extensively with μCP to create rows and lattices of neuronal circuitry [17-19]. The use of elastomeric membranes with microtunnels has been gaining interest[20], but has not yet been employed for single cell resolution circuits. Among research which does achieve single cells resolution [21, 22] the cells must be actively deposited into the microwells. This deposition is traditionally achieved via a micro-manipulated micropipette, which is tedious, risks contamination, and is limited in its ability to securely seat cells in 3d microstructures. The

direction that neuronal network engineering is advancing is clear, though success has been limited.

Research Goal

During the course of the research presented in this dissertation, our guiding goal has been to establish a method for producing fully-defined, heterotypic, single-cell-resolution neuronal networks with full electrophysiological access. Toward this end the objectives of our research were : - (a) to develop a laser cell patterning system capable of depositing single neurons to the electrodes of an MEA, (b) create elastomeric membranes to confine neurons to the electrodes of the MEA and direct neurite outgrowth towards adjacent electrodes, (c) use these systems to create viable heterotypic neuron-astrocyte circuits with defined connectivity and single cell resolution (d) demonstrate electrophysiological stimulation and recording of these circuits with the microelectrode array and assess signal propagation characteristics.

This dissertation will discuss the history, methods and motivation of defining neuronal networks on microelectrode arrays, as well as briefly reviewing pertinent background information on neurons, astrocytes, neuronal network electrophysiology, surface modification, contact guidance, optical force manipulation and microfabrication techniques. We will create various laser patterned neuronal circuits with single cell resolution and examine the complications involved with creating, culturing and electrophysiological probing single cell resolution neuronal circuits. We will complete our analysis by examining the viability and polarity and synapse formation of neuronal circuits with different cell types, cell numbers, and with or without astrocyte contact.

Finally we will discuss the limitations of the current process and future possibilities for these processes and for creating defined neuronal circuits.

CHAPTER II
LITERATURE REVIEW

Neuronal Network and Cell Components

Neurons

Neurons are electrically active cells which convey electrical signaling throughout the body and brain. They are the primary computational cells of the brain. Neurons are polar cells with four specialized regions, the axon, terminals, cell body (soma) and dendrites. Neurons are polarized cells which send signals out along their axons which form synapses at terminals upon all regions of other neurons to form axodendritic, axosomatic, axoaxonic synapses. This polarity is a crucial aspect in neuronal circuitry. Both axons and dendrites may be called neurites, which are the slender outgrowths which develop as a neuron matures. Neurites may be highly branched allowing for a single neuron to synapse with thousands of others neurons.

Synapses are points where neurons connect with other cells by translating an electrical action potential into a chemical signal. Although the previously mentioned axodendritic, axosomatic, and axoaxonic synapses are the most numerous, synapses may be formed between dendrites (dendrodendritic) and cell bodies (somasomatic). The location of synapses has an effect on its influence or weight in contributing to or inhibiting and action potential. Synapses are small open spaces where vesicles of neurotransmitters are released from the presynaptic neuron into the synaptic cleft which is between 20-30nm across. The vesicles activate ligand-gated ion channels (receptors) in

the postsynaptic neuron (or other cell), which may activate more ion channels or secondary messengers through a cascading mechanism.

The electrical signal produced in the postsynaptic neuron is a postsynaptic potential (PSP). Synapses may be excitatory or inhibitory depending neurotransmitter of the presyanptic neuron and the receptors of the postsynaptic neurons, and PSPs can be inhibitory (IPSP, hyperpolarizing), or excitatory (EPSP, depolarizing). A neuron may receive many inputs, and integrate the resulting PSPs (Figure 2.1). If the summation and integration of all PSPs sufficiently depolarizes the neuron from the resting potential (65-70mv) beyond a threshold (40-50mv) an all-or-nothing action potential is initiated by positive feedback from voltage gated ion channels in the membrane of the neuron. An increased density of these ion channels at the area on the soma adjacent to the axon termed the hillock makes it an originating point for action potentials. The action potential travels along the membrane via saltatory conduction, along the axon until voltage gated channels in the axon bulb trigger the release of synaptic vesicles.

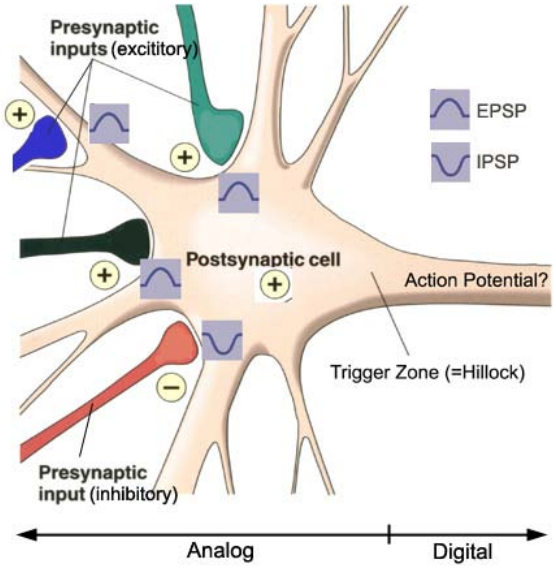

Figure 2.1: The cell membrane of a neuron integrates the PSP from several synapses. Carlson, 2007[2]

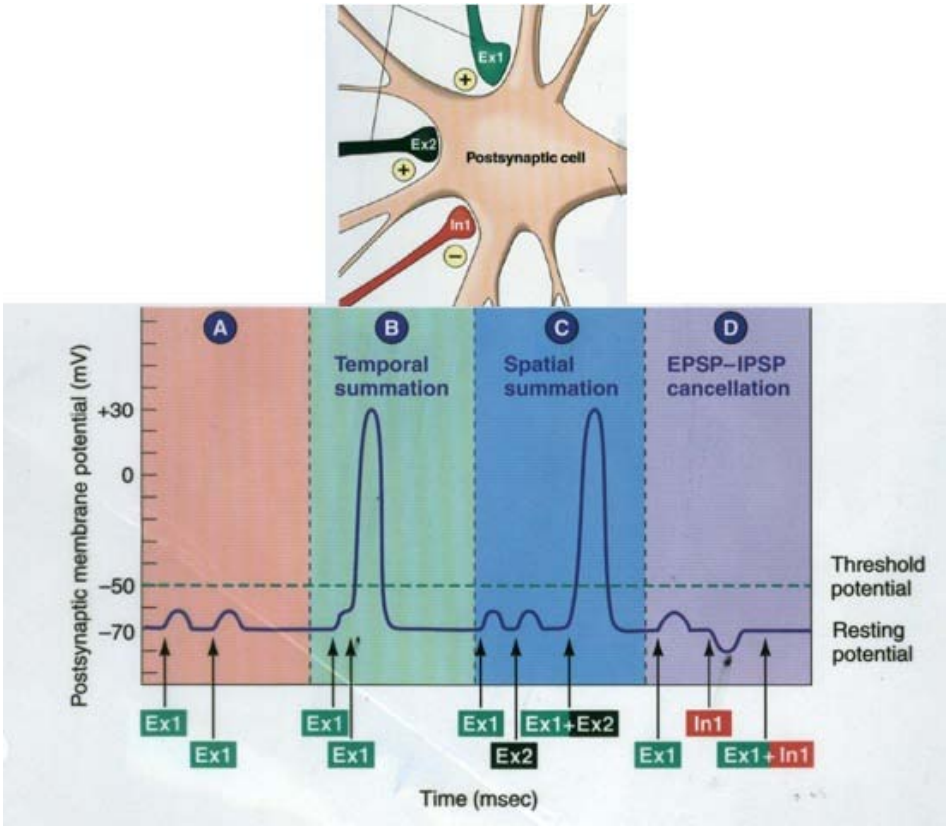

Figure 2.2[2]: A postsynaptic neuron performs spatial and temporal summation of excitatory and inhibitory PSPs. Individual PSPs have small amplitudes (0.1-10mV) and slow attack (0.4mV/ms) rates which are singularly are usually in sufficient to trigger an action potential. If the summed membrane potential exceeds a threshold an action potential results. Carlson, 2007[2]

Because the action potential is an all-or-nothing signal, it is not graded and no information is believed to be conveyed in its amplitude. Rather, information is coded in the spike rate and timing, and in the characteristics and strengths of the synapse. Synapse strengths may be modified by synchronized firing (Hebbian[23]) and back-propagation of signals, as in pyramidal hippocampal neurons [12]. This modification of synapse strength is termed plasticity. Hebbian plasticity and back-propagation of signals are important mechanisms of learning and memory. Information is interpreted by summing and

integrating a large number of inhibitory and excitatory PSPs as depicted in Figure 2.2. Typically several excitatory potentials are required to generate a spike, however a single presynaptic neuron can have many synapses with a single postsynaptic neuron making it capable of triggering a spike in a postsynaptic neuron[21]? Neuroscience has yet to determine the basic computational unit of the brain, whether it is the neuron, or the individual synapse[8]. The ability to visualize what connections are present in a circuit, test their individual responses, and compare these with the dynamic activity of the entire circuit or network is vital to clarifying the issue.

Glial Cells

Neurons are supported by glial cells and in the brain astrocytes are the primary glial cell and outnumber neurons 10 to1. Astrocytes support neurons by providing growth factors, recycling neurotransmitters, regulating metabolism, protecting form excitotoxic factors and maintaining homeostasis. Astrocytes have been shown to play an important role in synaptic plasticity, including LTP, and have long been known as a factor in electrical activity through their vital role in axon physiology (saltatory conduction). Glial cells are important in neuronal network development including the control of neural stem cell differentiation, neuron guidance, and synaptogenesis. In some instances such as the neuromuscular junction[24], glial cells are required for efficient innervations.

Developmental Role of Glia

Glial cells play important roles in development, influencing the fate of differentiating cells, guiding neuron motility and neurite extension, and even acting as

stem cells. Glial cells release factors that can induce a change in cell fate toward neurogenesis[25]. During development, radial glia are an important guide for neurons to follow to their destination in the cortex[26]. Glia cells are required for efficient innervation at the neuromuscular junction *in vitro* [24]. In fact some cells we refer to as glia cells can function as neuron stem cells.[27]

Support and Protection by Glia

Glial cells play an important role in protecting neurons from damage. In fact, malfunction of the glial system has been closely linked in the physiopathology of many neurodegenerative diseases. Astrocytes protect neurons from oxidative stress[28] through several activities including the release of catalase[29] glutathione precursors[30] ceruloplasmin[31] and the recycling of vitamin C[28]. The neuron-protective effects of astrocytes begin at astrocyte/neuron ratios as low as 1/20[29].

Glial cells support neurons in many ways. Glial cells are a mediator between the vasculature in the brain and neurons, playing an important role in neurovascular function[32]. This includes regulating dilation of arteries to increase nutrients to active neurons as well as forming and release energetic substrates including glycogen and lactate and uptaking glucose[33]. Astrocytes are vital to maintaining healthy glutamate levels. Glial glutamate (Glu) transporters are the primary pathway for actively removing extracellular Glu, maintaining it at a low level, below 1 mM [34]. Through excitatory amino acid transporters (EAATs) glial cells terminated excitatory synaptic transmission and protect cells from prolonged influx of a calcium and excitotoxicity. Because of their

protective activities, and a related role in inflammation, glial cells are implicated in several neurodegenerative diseases including AD and ALS[35].

Excitability of Glia

There is still some debate weather glial cells are[36] or are not[37] excitable. It is clear that glial cells release neurotransmitters when stimulated by neurons and have a variety of neurotransmitter receptors[38]. Physically glial are have intimate contact with the neuron-neuron synapse[39] and are ultimately responsible for removal of glutamate from the synaptic cleft, and stopping synaptic excitation. Additionally glial cells can modulate the level synaptic transmission, releasing a glutamate receptor agonist to enhance excitatory transmission or releasing ATP to suppress transmission[40]. If one considers an action potential and saltatory conduction as the requirements for 'excitability' than glial cells are not excitable. However, if a transient electrical depolarization in response to receptor activation leading to neurotransmitter release from voltage-gated[41] channels is the requirement than glial cells are excitable, basing their excitability on intracellular Ca_2^+ variations[42]. Even if astrocytes are not excitable, that does not mean they do not play a role in transmitting signals through neuronal networks (Figure 2.3).

Modulation of Synaptic Plasticity by Glia

While it is not agreed whether glia are excitable, there is consensus that they are synaptically active. The 'tripartite synapses' between a pre- and postsynaptic neurons and the adjacent glia may be considered a functional unit[43]. Astrocytes my release

glutamate at neuronal synapses, extending the influx of calcium which can have potentiating effects. Glial cells also release soluble N-ethylmaleimide–sensitive factor attachment protein receptor (SNARE) protein which activates metabotropic glutamate receptors (mGluRs)[44]. Glial cells regulate post-synaptic AMPA receptor density, and by the release of D-serine can help induce LTP and LTD[45]. It has been shown that astrocytes are actively involved in the transfer and storage of synaptic information[44]. In Haydon's review of the glial role in synaptic activity[5] he calls for the inclusion of glial cells in our models of neuronal network activity. The glial role in synaptic plasticity has been reviewed recently[46, 47] and it is clear that glial cells not passive as once believed. Consequently, it is important to study how they affect neuronal network activity and

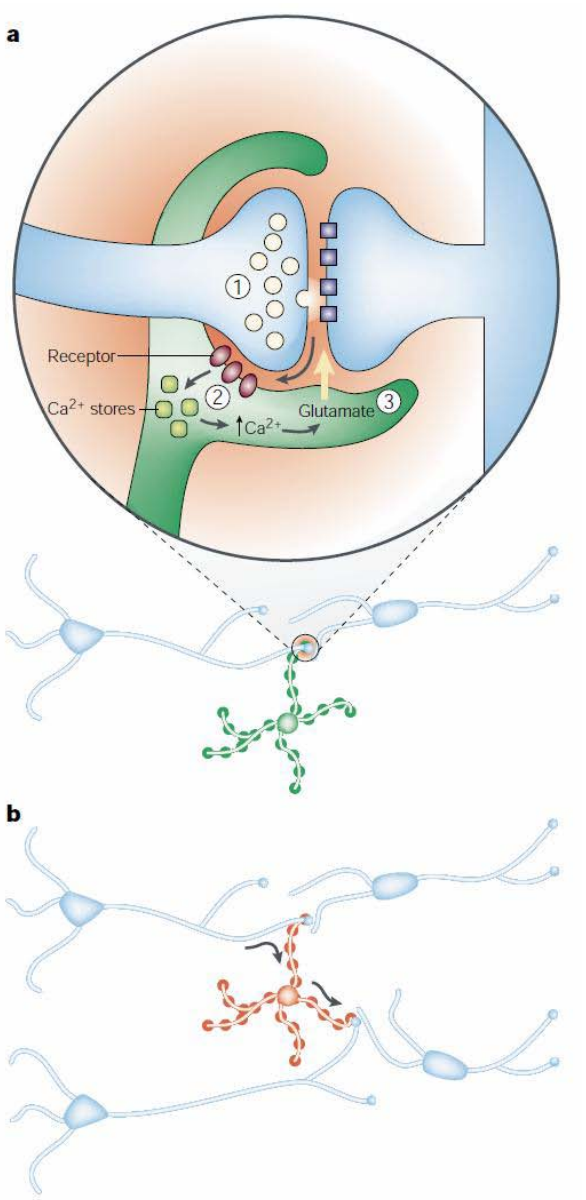

Figure 2.3: The role of astrocytes in neurosignalling. A) Astrocytes remove and release Glutamate at synapses. B) Astrocytes can transmit intercellular signaling between neurons. Haydon, 2001[5]

include them in neuronal network models.

Cell Culture

Our research required considerable time and development of culturing practices for primary neurons and astrocytes from both chick and rat. While we were compelled to study the literature reporting on these techniques we believe a full review of the subject is not warranted here. However, there are two specific issues which influenced our research choices and should be briefly addressed. These have to do with differences between chick and rat neurons, and the use of glial conditioned media.

Culture of Neurons

For *in vitro* dissociated neuron cultures, rat cells are the most widely used and chick cells are also popular. The advantages of using chick neurons are the ease of use and cost efficiency. Because the animal develops inside an egg, and cells are harvested from embryonic chicks, specimen can be kept in a counter top incubator with only water and electricity required and minimum upkeep. There are two primary disadvantages of the chick as a model, the short cell lifetime and the questionable relevance of an avian, rather than a mammalian model. To date, there have been no published research investigating or using chick neurons cultured on MEAs, though their activity has been studied with patch clamp[48]. Chick neurons have been used repeatedly in non-electrophysiological *in vitro* studies of DRG, motor neurons, and cortical (forebrain) neurons. Heidemann et al describe the techniques for chick forebrain culturing in chapter four of Methods in Cell Biology volume 71[49], which is an invaluable source for anyone

culturing chick neurons. One great advantage of the forebrain neuron culture is that it is nearly pure, removing a purifying step, and the nuisance of overwhelming glial or fibroblast proliferation. In chapter two of the same text He and Baas give a good review of culturing peripheral neurons, including rat and chick DRG. And Chapter 5 Kuhn describes the techniques for culturing chick spinal motor neurons (SMN).

The use of chick neurons in MEA experiments has not been reported, there are a few possible reasons. While chick forebrain neurons have many morphological similarities to embryonic rat hippocampal neurons, the fine processes do not fully develop into dendrites seen stage 4 and 5 hippocampal cells[50]. Another limiting factor may be the unsuitability of the cells for long term culture, or possibly a lack of appropriate long term culture techniques. For neuronal network experiments on MEA most researchers have chosen to study the activity of rat cortical cells[51] or hippocampal cells[52] which are usually harvested from embryonic day 18 (E18) rats. Because of the popularity of this cell source, there is a wealth of harvesting and culturing protocols, and the larger size of the animal makes many dissections (i.e. DRG) easier than in chick. However the cost of housing animals is substantial. An interesting alternative is available through Brain Bits LLC, a company that sells micro-dissected brain regions from embryonic rats, which can be a cost effective alternative.

Glial Contribution

In light of the wide range of important activities performed by glia (glial section), a glial co-culture or conditioned media approach should be considered when modeling the nervous system for *in vitro* investigation. Such preparations are likely to improve

culture viability and function, and improve the model by more closely mimicking the *in vivo* environment. More importantly, when investigating neurodegenerative disease or the learning process and synaptic plasticity of neuronal networks inclusion of glial cells is vital, if not the focus of the research.

Astrocyte Conditioned media

Conditioned media is essentially used media. The media is 'conditioned' by exposure to a cell culture, accumulating trophic factors and soluble signals, as well as waste products. The use of media conditioned by a higher density cell culture, or culture of a different cell type can be used to re-introduce trophic factors that may be to diffuse due to low density cell culture or missing because of lack of a supporting cell type in the culture. Specifically, astrocyte conditioned media has been shown to improve synapse formation [53]. Additionally, conditioned media can help to regulate density dependant[54] proliferation that is mediated by autocrine signaling[55] (i.e. glial and myoblast). Conditioned media may also be beneficial for what it doesn't have. Glial conditioned media has been used to deplete a serum supplemented media of glutamate, improving cell survival[56]. Conditioned media is generally exchanged before the normal lifespan of the media, so as to retain nutrients and reduce waste products. It may also be mixed with unconditioned media.[57].

However, not all cell signaling and trophic effects are carried out via soluble, diffusible, global factors. Cell-cell contact can be very important to the function of a cell type. For example astrocytes extend processes that contact neuronal synapses where they remove excitatory amino acids[58]. Blocking of EAA transporters has been

shown to result in neuronal and glial cell death[59]. Ultimately, one must consider the processes being studied when choosing whether or not to use a conditioned media, or a co-culture system in the experimental design.

Cell Patterning Techniques

Almost all tissues and organs are comprised of cells with an organized structure which facilitates function. The brain itself has many different functions and regions made up of different neuron types with distinct morphologies and unique network architectures. Due to the tricky access to and enormous complexity of brain circuitry, the task of correlating the neuronal morphologies and network architecture of specific regions with their function is difficult and largely undone[60]. A reduction in complexity and increased access are both achieved by *in vitro* cultures of dissociated neurons. However, in random 2d *in vitro* neuronal networks, it is not possible to monitor every neuron separately, nor is it possible to observe and map all physical connections between cells. To achieve these goals some type of cell patterning must be implemented to reduce the number of cells and the complexity of the network.

There are many different cell patterning techniques, most of which are adaptations from other technologies including photolithography and inkjet printing. These techniques may be employed for neuronal and non-neuronal cells alike. Here we describe only a few cell patterning techniques which are used or particularly relevant for neuronal network definition. These include surface patterning with chemicals that modify the attachment of cells, microfluidic/elastomeric membrane patterning which uses physical restriction and contact guidance, and finally optical force patterning techniques. Microfabrication has

become a significant tool in cell biology and tissue engineering. In fact a high impact journal devoted to microfabricated devices (lab-on-a-chip) was created in 2001 and publishes research including surface patterning, microfluidic, and microelectrode array techniques.

The most common patterning method used with MEAs is to surface pattern cytophilic and/or cytophobic factors (determined by a cell's adhesive properties) using microcontact printing. Typically, in this technique a PDMS stamp is primed with a cytophilic molecule such as Laminin. The stamp is then aligned to the features of the MEA and brought into contact with the MEA surface, transferring the Laminin. Randomly deposited neurons will selectively adhere to the Laminin pattern and develop into a patterned network. Because there is still a random component to the patterning process, each electrode does not necessarily receive the same number o neurons, which may also attach onto bars of the pattern. Furthermore, the fidelity of this type of patterning degrades overtime. Most importantly, controlling the placement multiple cell types is difficult and limited by the number of cell specific adhesion molecules.

Cell Patterning Techniques - Surface Patterning

During development neurons are guided by repulsive and attractive cues arising from contact with other cells and/or the extracellular matrix (ECM) or by diffusible molecules. It has been shown that both surface bound and diffusible molecules are responsible for survival and guidance of neurite outgrowth, and that they work in a synergistic way. Surface bound molecules may be used to promote or reduce cell attachment to a substrate by making it cytophilic or cytophobic. By patterning attractive

or repulsive chemicals to the surface with a technique such as photolithography researchers may control cell attachment, migration and neurite extension. Kleinfeld and colleagues used photolithography to pattern self-assembled monolayers of alkyl- and aminosilanes in a pioneering example of this technique[61]. The contrasting cytophilic and cytophobic regions produced defined electrically excitable networks of cerebellar granule cells and Purkinje neurons. This kind of surface patterning combines the use of a patterning technique (photolithography), and a surface modification technique (silanization).

Cell patterning Techniques - Surface Modification

Surface modification may be employed for a number of reasons including implant and biomedical device biocompatibility or to create self assembled monolayers to model surface interactions or to create biochemical assays[62]. Here we are reviewing two of the most common reasons pertaining to *in vitro* cell culture, to increase or decrease cell adhesion. Many surface patterning methods to control neuronal network geometry use a cytophilic/cytophobic surface modification contrast[63].Cell adhesion is influenced by several factors including topography, surface charge, surface hydrophobicity, surface chemistry, and protein interactions. The basic chemistries used for surface modification are oxidation, reduction, addition and elimination. Oxidation is convenient and can be used on most of the common materials used in cell culture including glass, polystyrene, PDMS, and the MEA electrodes made of indium tin-oxide (ITO) and the insulating layer of silicon nitride (Si_3N_4).

Surface Modification - Oxidation

Once PDMS is polymerized and crosslinked into a solid form, it surface is hydrophobic, which may require surface modification for proper wetting in microfluidic techniques[64] and improved cell attachment. Oxidizing the surface is usually done via O_2 plasma treatment, which replaces the –CH3 groups with –OH groups converting the surface from hydrophobic to hydrophilic and adds some $–O^-$ groups which give the surface a negative charge. Vickers have developed a extraction/oxidation process to generate hydrophilic PDMS[65]. This process combines the use of solvents (triethylamine, ethylacetate and acetone) to remove PDMS oligomers and the subsequent treatment with O2 plasma to convert the surface groups to SiO_2. They found that the extraction process increase the lifetime of hydrophilic surface groups from 3 hours on non-extracted PDMS to 7 days in extracted PDMS. This resulted in increased efficiency for electro-osmotic flow and electrochemical detection in the microfluidic device. Besides increasing wetting to allow for better and more uniform coverage, and improving cell adhesion by making the surface hydrophilic, and the –OH groups added by oxidation are useful for silanization.

Other groups have used the extraction process to treat microfluidics and improve biocompatibility. Millet and colleges compared the survival and neurite outgrowth of neurons cultured in either untreated, extracted, or autoclaved PDMS microfluidic tunnels[66]. They found that the extraction process improved neuron survival, with lesser improvement seen in autoclaved PDMS versus the untreated PDMS. They believe the

short chain oligomers may be cytotoxic and extraction removes them while autoclaving increases the degree of polymerization, also reducing oligomers.

Oxidation of polymers may also be achieved via chemical means with acids or bases, with the advantage that specific functional groups are created on the surface which can be used in further covalent modification. However, these acids and bases may be damaging to electrodes and can leave behind unwanted salts. Because of the wide publication and excellent results of plasma oxidation, these will not be reviewed.

Surface Modification - Physiosorption

Physiosorption can be used to attach proteins to a surface, the proteins adhere via Van der Waals or electrostatic forces only [67] in physiosorption. Physiosorption is a very simple technique for modifying surfaces because it requires no specified chemical reaction, only a clean and activated substrate. This can be achieved by sonication in a cleaning solvent such as acetone for hydrophilic surfaces or by oxidation or ashing in plasma cleaner. Activation via plasma treatment is achieved when weak boundary layers (especially organic molecules) with the lowest molecular weight are removed, and the surface becomes oxidized, increasing polar groups and increasing adhesion and wetting properties. Oxygen radicals may also break bonds to promote 3D cross bonding. A limitation of physiosorption is a possibly shorter lifetime of the modified surface because of weak interactions.

Surface Modification - Functionalization

Functionalization is the altering functional group to enhance attachment of macro molecules [68]. When functionalizing a polymer surface the goal is to create a surface layer of well-defined functional groups. This can be achieved by the use of oxidizing solutions such as sulfuric or nitric acid, or by hydrolysis using a base such as sodium hydroxide when an electron deficient carbon group is present. In the case of microelectrode arrays, these acids and bases may not be appropriate because of their reaction with the metal electrodes. PDMS[69] ITO functionalization [70]

Surface Modification - Polyethylenimine (PEI)

Polyethylenimine $(CH_2CH_2NH)_n$ is an organic cationic polymer. Possessing a high density of amino groups that can be protonated, PEI has a positive charge and has been shown to increase the attachment of cells such as neurons [71], which would otherwise attach only weakly to a glass substrate. However PEI has been shown to be unfavorable to human Schwann cell proliferation, at least in comparison to PDL, Fibronectin, Laminin or cross linked gelatin.[72]. Lakard and colleagues coated fluorine-doped tin oxide (FTO) with several polymeric films, and found PEI to improve attachment most[73]. When compared with other polymeric amines such as polyornithine for the culturing of fetal rat neurons, its effectiveness was equal[74]. While native PEI is water soluble, it is possible to hydrophobize PEI by combining the branched form with octadecanyl groups bound to 2 mol% of the amino groups of the PEI. This form of PEI, *polymer AB-30*, is soluble in ethanol, but not in water or cell media. This modified PEI film may be especially effective for long-term studies because it has a sustained coating

lifetime, and sustained cell attachment effects.[75] PEI has shown good cell adhesion results for neurons *in vitro* when used with Laminin in a layer-by-layer (LbL) coating technique[76]. The same group used this method to coat electrodes implanted into the brains of rats, in an attempt to improve the long-term reliability of implanted electrodes[77], one of the major challenges facing chronic implantation. The LBL technique has also been employed with Heparin to create a surface that repels cell adhesion[78]. PEI is easily coated on indium-tin oxide (ITO)[79], a common electrode material. Though the use of PEI is well documented, it is its use is not consistent. It has been used at concentrations as low as 0.001% w/v[80] and as high as 0.1% w/v[81, 82]. Another group tested several concentrations of PEI (0.025, 0.25, 2.5, 25 and 250ug/ml) found that 25ug/ml (0.0025%) was optimal for retaining the most HEK-293 (human embryonic kidney) cells subjected to repeated washings. [71] Furthermore, some have used it diluted in nanopore filtered water[71], while it is also commonly diluted in a borate buffer.

Surface Modification - Poly-L-lysine (PLL)

Poly-L-Lysine is a synthetic cationic poly-amino acid. Poly-amino acids including Poly-D-lysine (PDL) and Poly-L-Ornithine (PLO) have properties that mimic proteins, which can be exploited for increasing the adhesiveness of cell culture and tissue engineering substrates. Cell adhesion is improved by non-specific binding due to increasing electrostatic interactions. Glass and oxidized surfaces have a negative charge, as does the cell membrane; the protonated (positively charged) amino groups of PLL increase the electrostatic interactions. Poly-amino acids may also be used for drug

delivery and the delivery of nucleic acids. PDL differs from PLL in its d-enantiomer, which, produced in plants is less prone to animal protease-mediated breakdown, extending its lifetime in culture. PLL can be toxic to cells if it is unattached from the surface or present in too high of a concentration. PLL is applied to a cell culture surface at a concentration of 0.1- 1.0 mg/ml. A higher concentration of PLL can be used in media containing serum than in serum free media. PLL can inhibit neurite outgrowth in sympathetic neurons[83], possibly because it is too 'sticky'. Low molecular weight (average) 27,000 is more effective at promoting neuritogenesis than high molecular weight poly-lysine (130,000) when tested at concentration of 5micrograms/ml[84].

In addition to being applied to glass or oxidized polymer surfaces PLL may be attached to a SAM[85]. Layered films have also been implemented with PLL and poly(L-glutamic acid) (PGA)[86]. PLL is often used as an intermediate layer between glass and a natural protein such as Laminin, and can even be conjugated to Laminin before deposition[87].

Surface Modification - Natural Adhesive Proteins

Cells naturally contact proteins in the extra-cellular matrix (ECM), they have evolved to specifically bind to target proteins via integrins, and interpret trophic signals from their interaction with ECM proteins[88, 89]. It is therefore logical and wise to use biological proteins on a surface when possible. This can not only improve attachment and viability, but may improve cell health and function such as accelerated neurite outgrowth.

Natural Adhesive Proteins - Collagen

Collagen is a fibrous protein made up of smaller collagen rods about 300 nm long and 1.5nm in. It is a triple helix formed from polypeptide strands. These rods are packed together to form fibrils, which in turn are combined to make collagen fibers. There are many types of collagen, collagen IV is found in the basal lamina, which is crucial to neuronal development. It is often employed as a gel for exploring neuronal phenomenon in 3D cultures[90, 91]. The presence of collagen in a 3D extracellular matrix and its effect on neurite out growth are complex[92]. Alignment of collagen fibers can be used to influence the direction of axon extension and glial migration[93].

Natural Adhesive Proteins - Laminin

Laminin is a cross shaped glycoprotein and ligand that helps make up the extra-cellular matrix (ECM). It is an 800kDa heterotrimeric ECM molecule, composed of three chains, alpha, beta, and gamma. The Laminin family of heterotrimers play a role in many areas of the body including the muscle, brain and kidney[94]. Receptor mediated polymerization of Laminin networks are important to the formation of basement membranes[95]. High resolution video microscopy has shown that Laminin has rapid effects on the growth cone, dramatically accelerating the transport of membranous organelles microtubules to the lemellipodium, increasing extension rate[96]. Laminin and its ligand Nidogen have been found to be essential for growth cone turning *in vivo*[88]. It is the most commonly employed ECM protein in neuronal cultures.

Natural Adhesive Proteins - Entactin/Nidogen

Entactin also known as Nidogen binds Laminin to Collagen in the ECM along with Perlecan. It is important in directing the migration of neurons and Schwann cells, and is a pro-survival cue for Schwann cells[89]. As mentioned above, it facilitates the some neural functions of Laminin[96].

Natural Adhesive Proteins - ECL

All the above proteins are part of the extracellular matrix. Instead of just employing one of these proteins it may be beneficial to provide an extracellular environment that more closely resembles the real extracellular matrix. ECL is a commercially available mixture of Entactin, Collagen, and Laminin, The role of the ECM extends beyond direct interaction with cells, and it also mediates communication between cell types. For example, ECM proteins provide important cues for Schwann cell proliferation, migration, and activation, and induce Schwann cells to release trophic signals improving neurite outgrowth[97].

Microfluidic/Elastomeric Membrane Techniques

Extraction of Short Oligomers from PDMS Membranes

As mentioned in the biocompatibility section extraction of short oligomers can improve cell viability, and help extend the life surface modifications. This is relatively easy process that can be achieved using a number of polar solvents. A detailed analysis of the compatibility of different solvents with PDMS has been performed Lee et al[98]. Effective solvents include triethylamine, ethyl acetate, pentane, xylene isomers, ethylbenzene, acetone and ethanol. These solvents do cause swelling which can be

advantageous in removing PDMS membranes form rigid molds. However, when extracting oligomers, to avoid cracking and tearing from uneven shrinkage the PDMS structures should be soaked in progressively lower solubility solvents[99]. Lee and others from Whiteside's group at Harvard examined the influence of PDMS with varying treatments and compositions on the attachment and growth of several mammalian cell types.[100] they found that PDMS with excess curing agent was the allowed the most cells to attach and survive, followed by PDMS with excess curing agent and then PDMS that was extracted. Normal PDMS was the worst. They did not test PDMS with excess curing agent and extraction. They found oxidation (without physiosorption) to reduce the number of cells that attached and grew. Finally while short-chain oligomer extraction improves the viability of most cell types cultured on PDMS, it may be best not to use extracted PDMS with microcontact printing techniques as short chain oligomer contamination has been shown to improve oligonucleotide and consequently transfer. absorption[101].

Microfluidic/Elastomeric Devices

Microfluidic devices are an attractive technology for creating networks with pre-determined connectivity for several reasons. If properly constructed microfluidic channels and compartments are capable providing patterning definition and retention well beyond the lifetime of a neuronal culture allowing for longer pattern fidelity than attainable with degradable surface patterns as well as adding the ability to be reused. Recognizing this strength Morin and colleagues have employed PDMS microfluidics on MEAs to define connectivity, but did so with very large (600μm^2) microwells[102],

which were far too large to acquire the single cell resolution networks. Work by Dworak and Bruce Wheeler's group employs a similar approach using microtunnels in a PDMS membrane to guide the neurites of large neuron cultures over a set of electrodes[20]. PDMS microstencil[103]. Employing such elastomeric membranes Claverol-Tinture and colleagues were able to guide the axon of a single invertebrate neuron over a series of electrodes[104].

The small volumes inside microfluidic channels can aid in culturing neurons at very low densities. Millet and coworkers have successfully cultured neurons in a simple microfluidic channels at densities not possible otherwise[66]. The channels were also used to coat the substrate with PDL and Laminin and to slowly flow media over the neurons which improved viability.

Finally, the shape of microfluidic channels may be used to influence the turning of neurite outgrowths. Francisco and colleagues cultured neurons in non-microfluidic 3D structures to study the effects of channel geometries on neurite extension. They were able to regulate the axon guidance and by varying the angle turns in channels[105]. These topographical guidance cues were shown to influence neurite outgrowth as early as 1987[106].

While the strengths of microfluidic devices are applicable to maintaining low density neuronal network health and structure, they are not well suited to initial pattern formation. Placing cells to specific points on a substrate will require a different approach.

Optical Force Manipulation

In all of the neuronal network patterning previously discussed, placement of individual cells to specific wells or electrodes was performed by contact manipulation with a micropipette. This process is time consuming and involves cumbersome micromanipulators which usually necessitate an open environment prone to contamination. Additionally, the access angles available when using a micropipette and micromanipulator may not allow easy placement of cells in a 3D structure, as manipulation is achieved by dropping, nudging or flowing a cell using the micropipette.

When one applies laser guidance and laser trapping systems for biological use, a wavelength of 800nm is usually used to reduce cell damage. Work by both Vorobjev[107] and Liang[108] has shown that optical traps using lasers with wavelengths in the 800nm range have little effect on cellular processes for exposure times less than 3 minutes. When Odde and Renn used and 800nm wavelength laser in their first laser guided direct writing of chick neurons they found that the cells remained viable even after hour long exposures at high intensities of over $100W/m^2$ [109]. In 2002 Mohanty used the COMET assay to assess the DNA damage to cells exposed to micro-focused laser radiation over wavelengths form 750nm-1064nm, they found that the least damage occurred over the 800nm-1064nm range with little variation in that range.[110] Over the past decade it has been demonstrated optical force manipulation using 800nm wavelength radiation causes very little damage to cells if any.

Optical Force Manipulation - Background and History

(For an in depth history and review of optical trapping please read “History of Optical Trapping and Manipulation of Small-Neutral Particle, Atoms, and Molecules” [111] For an exhaustive list and guide to literature see “Laser-based optical tweezers” [112])

Here we discuss two patterning techniques using optical force; laser tweezers, and laser guided direct writing. Optically, laser cell patterning is the same technique as laser guided direct writing. These techniques are derived from a single phenomenon first reported by Ashkin[1] in 1970, who discovered the phenomenon while working at Bell Labs. In this publication Ashkin examines how micron sized dielectric particles become trapped in stable optical potential wells by radiation pressure.

Laser Guidance - Theory and Optics

The forces of laser guidance can be explained in different ways depending on the size of the guided particle relative to the wavelength of the laser. If the particle diameter is much larger than the wavelength this is the Mie regime, and can be explained using ray optics. If the particle is much smaller than the wavelength of the incident light, than the electromagnetic wave (Rayleigh) approach must be used. A third model, the generalized Lorenz–Mie theory (GLMT) can describe particles in the intermediate range. While this is a strong approach, and best for particles that are not much larger, or much smaller than the wavelength, it is complex and computationally demanding. The ray optics approach to calculating the forces on a trapped particle is simpler, and when using a near IR laser with wavelength of 800nm and cells which have a diameter no less than about 8μm, the

cell is an order of magnitude large than the wavelength. Therefore, I will not delve into the electromagnetic wave approach or GMLT. To illustrate the phenomenon I will use the ray optics approach which is the way Ashkin first explained it.

In the ray optics approach we can define two forces, a radial force, which pulls the cell toward the center of the laser, and an axial force, which, if the laser is weakly focused can push the cell in the direction of the beams propagation.

Modeling the cell as a sphere with an index of refraction higher than the surrounding media is valid for most embryonic cells which are round, including neurons. Using a single mode (TEM_{00}) laser beam with a Gaussian intensity profile the initial off-axis cell can be modeled as in this Figure2.4 from Ashkin's publication[1].

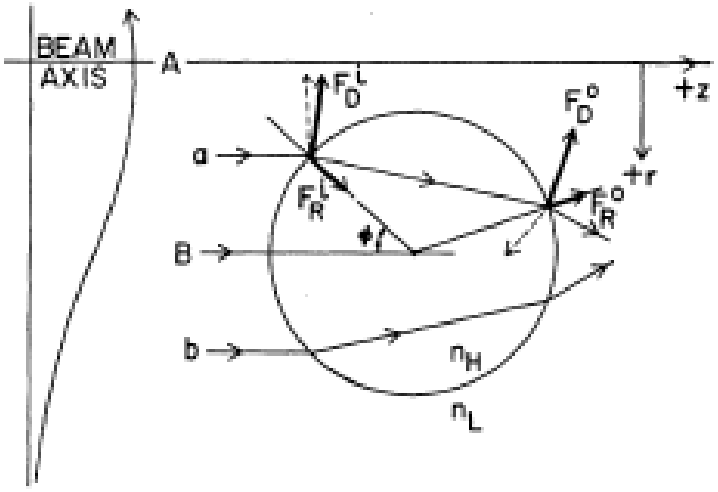

Figure 2.4: Ray optics model of optical force guidance of a dielectric sphere by Ashkin. 1970 [1]

The rays a and b represent just some of the many rays of the laser beam which increase in intensity toward the beams axis A. The index of refraction of the cell is

roughly n_H =1.35 and the index of the surrounding media, without an excessive amount of serum or other supplements near that of water with n_L = 1.333. As the cell is off axis, beam a has a higher intensity, than beam b. At the interface between the cell and the media, the rays undergo Fresnel reflection and refraction. Using Snell's law $\frac{\sin\theta_1}{\sin\theta_2} = \frac{n_2}{n_1}$, where θ_1 is the angle between the incident ray and the vector normal to the interface and θ_2 is the angle between the refracted ray and the normal vector. The beams are refracted as they enter the cell, and again as they exit. The photons of light in rays a and b have momentum p= h/λ, where h is Planck's constant and λ is the wavelength of the photon. As the photons are refracted, a radial momentum is imparted to the photon, which must be compensated by a opposite radial momentum in the cell as per conservation of momentum. Because of the Gaussian intensity profile and the off axis position of the cell ray a has more momentum than ray b. In order to conserve momentum a net force on the cell toward the beams axis arises. This force will pull the cell toward the center of the beam. Once in the center ray a and ray b will have equal momentum and the net radial force will be zero.

The axial force arises from scattering of photons, and reflection. If the laser is weakly focused then these forces will be greater than the any forces due to refraction or radiation pressure. In strongly focused beam, the radiation forces will overcome the scattering forces and trap the cell in all three dimensions. This difference in the way the beam is focused is what separates optical trapping (trapped in 3 dimensions) form optical guidance (trapped in 2 dimensions). To strongly focus a beam, an objective with a high

numerical aperture (NA) is used, a weakly focused beam is produced by an objective with a lower NA. A crucial parameter that is correlated with the NA of an objective is the working distance (the distance between the lens and the focal point). The objectives with high NAs used in optical trapping have short working distances, which can limit their applications.

The first publication by Ashkin does not mention the NA of the focusing lens or characteristics of the focused laser beam, but describes a laser trap using two coaxial laser beams from opposing directions. In 1986 Ashkin reports on a single beam trap (Figure 2.5), using a higher NA(1.25) focusing lens and "demonstrate the existence of negative radiation pressure, or backward force component, that is due to an axial

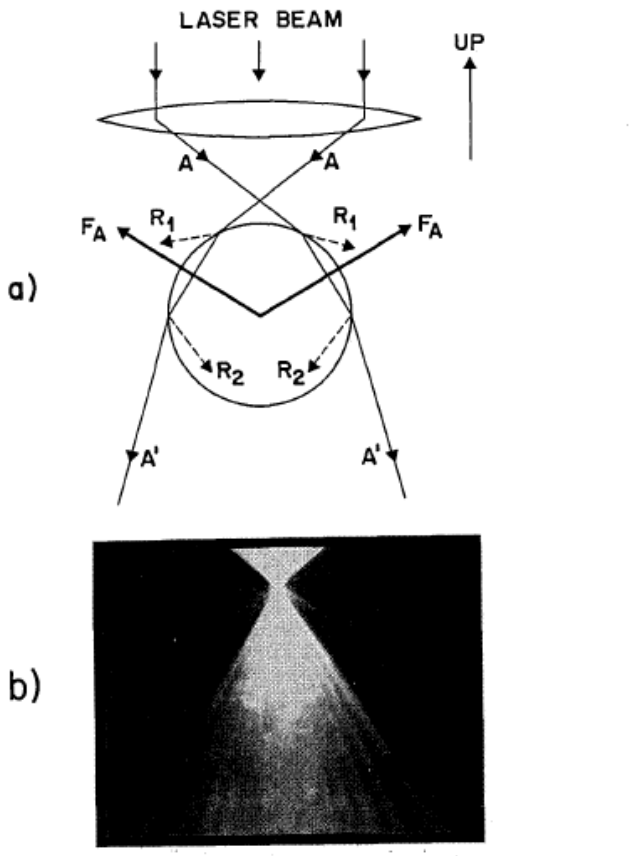

Figure 2.5: a) Ray optics of a single beam optical trap resulting from a high NA objective. b) Photograph of a trapped particle in water showing incident and refracted light. Ashkin, 1986 [3]

intensity gradient." [3] "Although the tweezer trap at first sight seems counter-intuitive, it is axially stable because of the dominance of the backward axial gradient force over the forward-scattering force"[111]

At some point Ashkin and his colleagues had accidentally trapped what they believed to be bacteria in a laser trap which inspired tem to try it on purpose. "We could trap, observe, and manipulate bacteria which we grew from bits of Joe Dziedzic's ham sandwich. We readily confirmed our hypothesis. Our paper in Science [103] on laser trapping of viruses and bacteria was the first report of optical manipulation of living cells, although optical damage to bacteria cells was apparent."[113] This experiment was with a 514.5 nm laser, so they tried other wavelengths that might be less damaging . In 1987 Ashkin and colleagues reported their application of this phenomenon for the manipulation of single cells using an infrared laser beam[114]. The 1060nm YAG laser and could trap bacteria that actual reproduced inside the 50mw trap.

Optical Force Patterning - Cell Damage Considerations

A reasonable concern is that exposure to the laser radiation, especially in its focus may cause cell damage. Because of the strength and popularity of optical tweezers as a biological tool, there have been several studies investigating the optimal wavelength of laser radiation that should be used for minimum biological damage, and what effects it may have.

Vorobjev and coworkers first reported on their investigations of biological damage versus radiation wavelength effects in 1993[107]. They found that laser irradiation caused chromosomal shoulders to stick together during separation. They

assessed the amount of ‘sticking’ in relation to radiation wavelengths from 700nm to 840nm at 130mW power for times up to 5 minutes. They found that the wavelengths producing minimal chromosomal separation abnormalities were 700nm and 800-820nm. They also found that the maximum chromosomal sticking occurred with exposure to the 760-765nm wavelength.

In a 1996 Studying different optical trapping wavelengths on human spermatozoa, Konig et al found that wavelengths below 800nm induced UVA type oxidative stress and cell death[115]. They also suggested the use of a single frequency laser, to reduce cytotoxic effects. In 1996 Liang investigated the effects of optical trap wavelength on cloning efficiency, and came to a similar conclusion, adding that for exposure times less than 3 minutes, there was little effect[108].

When Odde and Renn used and 800nm wavelength laser in their first laser guided direct writing of chick neurons they found that the cells remained viable even after hour long exposures at high intensities of over $100W/m^2$ [109]. In 2002 Mohanty used the COMET assay to assess the DNA damage to cells exposed to micro-focused laser radiation over wavelengths form 750nm-1064nm, they found that the least damage occurred over the 800nm-1064nm range with little variation in that range[110]. Their data for 30s exposure times at 120mW showed the least damaging wavelength was 800nm resulting in a mean DNA damage of 12%. Besides the direct effects of radiation on cellular DNA, the effect of heating was also considered. Liu et al examined the change in the temperature of Chinese hamster ovary (CHO) cells when exposed to the focus of a 1064nm laser, finding that the heat generated was roughly 1.15±0.25°C/100mW[116].

With laser guidance and trapping powers between 100-150mW, the amount of heat generated is likely not harmful.

Laser Guided Direct Writing (LGDW)

Some reviews have named LGDW as the fist 'cell printing'[117]. LGDW can be used to droplets of material, including biomolecules, or cells to a substrate with very high accuracy. It employs the laser guidance force created by a weakly focused Gaussian beam described above. Renn and Pastel first published on this technique in 1998, where they patterned NaCl droplets which were suspended in atmosphere by a ultrasonic nebulizer[118]. The focusing optics were aligned to guide the particles through a hollow optical fiber and onto a substrate. One year later they reported patterning a wide variety of particles including water droplets, polystyrene spheres, glycerin droplets, salt, sugar, KI, CdTe, Si, and Ge crystals, and Au and Ag metal particles with sizes ranging from 50 nm to 10 mm using a 0.5-W laser of 800nm.[119]

According to some, the first reported 'cell printing' was performed using LGDW[117]. While optical traps had been demonstrated on living cells for over a decade, they were not guided with LGDW until 2000[109]. Here Odde and Renn guided embryonic chick spinal cord neurons through a hollow fiber and onto a substrate.. They were able to 10–100 cells in a continuous process, at with a resolution <1μm, and to various substrates. LGDW has been shown to be an effective tool in 3d patterning of small population sizes for a variety of different cells[120]. In this publication they published a table that indicates how laser guidance parameters change with cell type.

Electrophysiology

Electrophysiology

Introduction

Before we can really discuss neuronal networks and neuronal network electrophysiology, an introduction of the tools used will be helpful. As previously mentioned, the activity of neuronal networks is built upon the mechanisms involved in single neuron and synapse activity. Most of what we have described about the basic electrophysiological activities of single neurons was learned using patch clamp.

Patch Clamp

The conventional tool for electrophysiology experiments has been the patch clamp. The patch clamp uses a micropipette, which is usually a fire polished, pulled glass capillary tube with an electrode and intracellular-like fluid inside. While observed under a microscope the micropipette is carefully maneuvered into contact with a cell by a micromanipulator. In the whole-cell type patch suction is applied to the micropipette, rupturing the cell membrane and allowing for intra-cellular recordings. This process of obtaining a patch takes hundreds of hours of practice and experience to perform successfully. The patch clamp can act in voltage or current clamp modes, allowing for detailed recordings of currents and membrane potentials, membrane resistance, and membrane capacitance. With ability to control membrane potential while measuring current, it is possible to deduce the characteristics of voltage gated channels and of ion concentrations. Because of its ability to analyze the detailed electrical activity of a cell patch clamp is often employed to test the health or functionality of an altered cell or a

differentiated stem cell. Furthermore in ex vivo slice studies or with very low density *in vitro* cultures you can bring the electrode to the cell.

Detail in resolving membrane potentials and ion currents are a major advantage of the patch clamp. Another advantage of patch clamp is that the micropipette is moveable and can be brought into contact with a cell of choice, where as the MEA electrodes are fixed and can only record from neurons which are growing on or near them. However, the disadvantages of the patch clamp method are primarily related to the micropipette. Its use implies an open air culture, which even with an onstage incubator may experience significant changes in osmolarity due to evaporation. The micropipette and micromanipulation head-stage are relatively cumbersome, and limit the number of simultaneous electrodes that can be used to 3 or 4. Finally, to achieve intracellular recordings the cell membrane must be ruptured, which ultimately kills the cell and making long term studies impossible.

While the patch clamp technique has yielded many insights into the electrical activity and memory mechanisms of single cells and synapses, it is inadequate for monitoring many cells at once or for recording from cells multiple times over several days or weeks. When studying neuronal network activity many more electrodes are required and the non-destructive extracellular recording allows studying network development and training phenomenon.

Microelectrode Arrays - Introduction

In 1972 Thomas and colleagues first published their invention of a planar multielectrode array [121] that had 2 rows of 15 electrodes made of gold and plated with

platinum black. At first they were not successful in recording from neurons, but could record from chick myocytes. In 1979, without knowledge of Thomas's work Gross et al. took advantage of emerging integrated circuit microfabrication technologies to form planar arrays of microelectrodes which could be used to stimulate or record the electrical activity of cells cultured on such arrays (a single snail ganglion)[122]. The third MEA pioneer, who also developed an MEA system for neuronal electrophysiology without reference to previous work was Pine in 1980 [123]. MEAs have been used for large and long-term *in vitro* network studies[124], explanted hippocampal brain slices [125], as well as *in vivo*, implanted into the brain and spinal cord[126].

In the last 30 years the MEA has become a powerful and popular tool to study electrically active cells (nerve and muscle cells), *in vitro* and *in vivo*. Stemming from and leading to the growing popularity of MEA electrophysiology, complete commercial systems (MEAs, amplifiers, AD cards, Stimulators, and Control/Recording software) are available, and individual components, including specialized analysis software are can also be obtained from commercial sources. However, many labs still produce their own MEAs, exploring custom configurations and materials; this is especially true for *in vivo* applications, as long-term biocompatibility is still a limiting factor to therapeutic use. There is a growing selection of MEA types that are commercially available including flexible planar arrays for *in vivo* use, perforated arrays to increase nutrient and waste transport and 3D arrays with spikes that can reach further into brain slice preparations, past the dead cell layer.

However, for the study of neuronal networks of dissociated neurons there is a popular standard. This MEA design starts with a glass substrate about 3mm thick with indium tin-oxide (ITO) electrode leads, insulated by a thin silicon nitride layer. The electrodes themselves are usually coated with Titanium nitride (TiN) to reduce impedance. The standard array of electrodes is composed of 60 or 59 electrodes (1 electrode lead may be used as an internal reference). Each electrode is 30μm in diameter and they are arranged in a pseudo 8x8 square array (corners missing) with an inter-electrode spacing of 200μm. Other options are available, but this configuration is very popular and almost all the experiments reviewed here are performed on this type of array. Most groups have chosen to modify these arrays with surface patterning, microfluidic overlays, or with custom stimulation and recording hardware and software. This standard MEA is inserted into a compatible amplifier, which contacts all the ends of the electrode leads, and amplifies the small (mV) signal. The amplifier is connected to a computer for simultaneous recording from all the electrodes. A stimulation system is can be purchased or built, and leads from this apparatus can be plugged into pin holes on the amplifier board for stimulation of the same electrodes used in recording. Some groups have built their own control cards and used alternative AD/DA cards to perform simultaneous stimulation of larger electrode arrays. Additionally, open source software has been developed in C++ and runs on a Linux system. This software adds some functionality and efficiency that is not available in commercial software.

Microelectrode Arrays - Advantages

There are two primary advantages of MEAs for studying the electrophysiology of *in vitro* neuronal networks. MEAs are non-invasive and allow for long-term studies involving electrical stimulation and recording, and they allow simultaneous multi-site recording, far exceeding the number of electrode that can be employed in patch clamp setups.

Micro/multi-electrode arrays are the standard for studying neuronal network activity *in vitro.* Unlike patch clamp which is limited by the physical space required for headstages, and the skill required attaining patches, a typical MEAs can stimulate and record from 60 electrodes at one time. Furthermore, extracellular electrodes do not puncture the cell membrane the way a micropipette does during a whole cell patch clamp experiment, which ultimately leads to cell death. A major disadvantage has been that the electrodes are fixed in place, and alignment with specific cells in a network is difficult or impossible.

Microelectrode Arrays - Disadvantages

While the MEA has some clear advantages over patch clamp, it also has drawbacks. MEAs can be used to measure only the extracellular electric field potential at an electrode. The extracellular ion currents which occur during an action potential generate a spiked waveform. The magnitude of this waveform is mostly a product of the extracellular matrix components and the distance from the electrode, and offers no information other than that a spike has occurred. Furthermore, this dependence on electrode contact or separation and the decreases yields a lower signal-to-noise ratio than

patch clamp. Additionally, the field potential at an electrode may be the summation of currents from several local neurons, with different spike timing and magnitudes. In this case discerning the activity of a single neuron requires complex signal processing and spike sorting algorithms. This ambiguous mode of interpretation is not ideal for studying the signal propagation through single cells. Finally, the micropipette used in a patch clamp system is brought into intimate contact with the cell, where as the electrodes of an MEA are not movable, and can only record from cells growing on or near them.

Microelectrode Arrays - Applications

Work with neuronal tissue in culture can be classified as part of two major mechanistic domains: (1) receptor-dependent studies and (2) circuit-dependent studies (pg193)[127]. As one would expect, the domain being investigated influences the experimental design. Generally, when investigating a receptor-dependant phenomenon on an MEA, random 2D cultures of neurons are used. By applying different chemical agonists or antagonists to a culture, one can study the change in network activity resulting from stimulating or blocking a receptor. This may be applied to study the relation of certain receptors and synapse types on network activity and learning phenomenon, or it may be used employed as a biosensor for detecting substances. Gramowski et al[128] created a database of 30 extracted activity states of neuronal networks on MEA to profile the effects of different substances, which could then be used to identify unknown substances based on their activity state profile. This illustrates not only the application of the neuronal network/MEA hybrid devices as a biosensor, but shows how network activity can be interpreted without reference to the circuitry.

When investigating circuit-dependent phenomenon there are few experiments that can be performed with a fully random 2D culture. The density of cells may be manipulated and should have an effect on circuitry which arises, and can be studied by looking at neuronal network activity. At extremely low densities simple networks may automatically arise, which has been the case with some *in vitro* invertebrate neuron cultures. However, this extremely low cell density significantly reduces the chance of neuron-electrode contact. In fact, most of the invertebrate studies of simple circuits have been studied with patch clamp.

In order to really study the circuitry of a neuronal culture, some connectivity restrictions must be imposed, as the connectivity in random 2D cultures is to complex and dense for direct monitoring. Toward this end researchers have employed the cell patterning and neurite guidance techniques. The most popular technique is surface patterning via microcontact printing; the second most popular technique is the use of microfluidic overlays for physical restriction. Thus far applications of these techniques have still fallen short of an ideal system for investigating circuit-dependent phenomenon *in vitro.* As one researcher in the field has put it:

"The most challenging area in neural engineering today is to determine the formation of memory at the cellular level. In order to achieve this, it is essential to acquire electrical recordings from individual neurons."[129]

Only Suzuki and colleagues, using their stepwise photothermal etching technique, have successfully created a directionally and geometrically controlled linear neuronal circuit with a one-to-one neuron electrode pairing[21].

Microelectrode Arrays - Stimulation Parameters and Protocols

Appropriate stimulation protocols for *in vitro* cultures of neurons vary depending not just on the cell type but also for electrode (material, size, and coatings), the ECM(artificial), and microstructures such as elastomeric membranes, as the stimulation voltage varies with the resistance of the medium between the electrode and the cell. These relationships are easiest to model using a current driven stimulus as the electric field is most simply described as $I_{extra} = \frac{1}{R_s}[U_{stim} - U_{extra}]$ [130].

When choosing stimulation parameters one must also consider the electrode material properties, as an excessive stimulation can damage the electrodes and/or insulation layer as well as causing electrochemical fouling of the electrode. To reduce the electrochemical effects, a biphasic pulse should be used, that leaves the electrode with a net charge of zero. To avoid excessive electrode voltages that may damage the electrode or cell, voltage controlled stimulation is preferred to current control. Wagenaar and colleagues published an in depth review of various stimulation parameters in which both current and voltage control are tested with several profiles[131]. They found that a negative current was most effective, and can be achieved with a biphasic voltage pulse that begins with a positive voltage, followed by a negative voltage. They also found that the ideal pulse width is around 400 μs, enough time to allow the cell membrane and parasitic capacitances of the system to charge. They tested the evoked response of a random monolayer of E18 rat cortical neurons. In this model they found a linear relationship between the numbers of neurons directly stimulated by a voltage controlled

pulse and the pulse amplitude. Here they tested between -900mV and 900mV, however these values are very dependent on the experimental setup.

Microelectrode Arrays - Stimulation artifacts

With stimulation voltages in the range of Volts and recorded signals in the 10-100µV range, stimulation artifacts may make recorded action potentials imperceptible. To overcome the stimulus artifact problem, newer MEA amplifiers from Multi Channel systems include a blanking circuit which grounds the amplifier during stimulation. However, a new artifact may result from re-inclusion of the amplifier, a problem reported by Jimbo et al [132]. They addressed the stimulus artifact with a custom built "hold + discharge" circuit, which employs a sample and hold circuit which keeps the amplifier input at its pre-stimulus level for the duration of the pulse, and an electrode in the media which acts as a sink for the electrode/electrolyte capacitive charge. However, purchasing a commercial amplifier system with blanking circuit can be very expensive, and many researchers do not have the time or training to build their own circuits. Luckily and free and open source software solution has been developed called MEABench (D.A. Wagenaar, <http://www.its.caltech.edu/~pinelab/wagenaar/meabench.html>). This system employs Suppression of Artifacts by Local Polynomial Approximation (SALPA), which models and removes the stimulus artifact for each electrode individually, allowing for spike detection from directly stimulated neurons within 2ms of the stimulus[133].

Neuronal Network Electrophysiology

In a biological neuronal network the connections between neurons are real and must exist in some spatial form. The physical geometry of the network restricts synaptic possibilities. Additionally, the physical layout affects our ability to monitor areas of the network, and insert stimulation. It is logical to expect that in our investigation of neuronal networks *in vitro* that we would start with simple models first, increasing the size and complexity of networks as our understanding grew. Yet the cell patterning technologies for implementing such simple circuits were developed after the advent of the MEA. Consequently, the use of MEAs to study *in vitro* neuronal networks began with experiments monitoring random 2D (monolayer) neuronal networks. As cell patterning technologies evolved they were then applied to neuronal network research.

Quantification of Neuronal Network Activity Features

The dynamic network activity of 2D neuronal networks on MEAs has been studied under several conditions including development[134], chemical antagonists[128], and stimulation protocols intended to train[52] the networks, eliciting a defined change in activity. While exact definition of activity features may vary between researchers, some general activity features are commonly quantified. The fundamental activity that can be recorded on an mea is an spike, caused by a an action potential from a cell or group of cells, the simple and effective way to recognize a spike is to set a threshold from 3 – 8 times the RMS noise level. A spike train is a series of spikes, many believe the inter-spike interval is how neural information is encoded[135]. A burst is a period of high activity, which can be defined as attaining a certain number of spikes and a given window

of time. Bursts are not isolated to one electrode, rather they happen over a burst area, which can be quantified by the number or percentage of electrode over which it takes place. Bursts propagate throughout a culture and this propagation can be characterized by a vector, and a speed[136]. It should be noted that bursting activity of 2D *in vitro* neuronal networks is not associated with an analogous activity *in vivo*. This activity is especially abundant during network development, and can be greatly reduced by introducing programmed stimulation simulating input from other brain regions[137]. The basic features of bursts and spike rates can be quantified by their rate or frequency. Bursts can also be quantified by their duration. Furthermore one can quantify the interval between spikes and bursts, the spike rates during bursting and during intervals, the peak and mean values of spike rates and bursting rates, and the change in values. Additionally a coefficient of variation (CV) can be assessed. CV is a statistical term which measures the dispersion of the probability distribution, it is equal to σ/μ, where to σ is the standard deviation and μ is the mean. The meaningfulness of all these quantification methods may be questionable as one tries to relate them to events and mechanisms *in vivo*. Usually the results are related to a baseline activity of the 2D network without chemical or electrical manipulation. The 'normal' activity of a 2D culture has been characterized as it develops over the lifetime of the culture by multiple groups [134, 138].

Spontaneous firing is a normal part of neuronal network development[139]. Spontaneous release of neurotransmitters like glutamate contribute to spontaneous firing of cells[140, 141]. Ion channel fluctuations may also cause such firing[142]. This spontaneous activity may be an indicator of neuronal network development.

Electrophysiology of 2D Neuronal Networks

Most of what we know about neurons and synapses has been gleaned from their isolated function rather that the concerted functions they perform in networks. The two dimensional arrangement of neuronal networks on MEAs may be seen in two ways; The model may be seen as inadequate to mimic *in vivo* networks and reveal meaningful properties of 3D *in vivo*. Or it may be seen as a simplified scenario, which is easier to access with chemical and electrophysiological tools, and easier to test against a mathematical model. As stated by Michele Giugliano "such an approach makes it possible to dissect the interactions among individual neurons of a network and to look for collective mechanism as the cellular and sub-cellular levels, through manipulation of the physiochemical conditions[127]." In random 2D neuronal networks, the primary methods of manipulation will be chemical (or genetic) and electrical. By applying chemicals to an *in vitro* neuronal culture on MEA, such as specific receptor antagonists or altering the levels of a certain ion, researchers can isolate and investigate the activity of receptors, and study how they influence network behavior[143]. Relating changes in network activity in response to chemical or electrical manipulation can shed some insight into what role certain receptors play in signal processing and memory, as well as more general mechanisms of neuronal network activity. However, in random 2d neuronal networks, it is not possible to monitor every neuron nor to observe and map all physical connections.

2D Neuronal Networks - Electrical Manipulation and 'Training'

Much of the research with MEAs and neuronal networks is focused on the effects different stimulation parameters on the activity of the neuronal network, as an alternative or in addition to chemical manipulation.

An example of an electrical manipulation only experiment, which is not aimed at learning is the Wagenaar et al 2005 publication on controlling bursting behavior with closed-loop multi-electrode stimulation. Building on the idea that networks with a large fraction of intrinsically spiking neurons have a lower bursting rate[144], they investigated different stimulation protocols to see if they reduced bursting behavior[137]. They began by injecting spikes at single electrodes are various frequencies, eventually finding that injecting spikes at frequencies of 50hz distributed over 25 electrodes suppressed bursting completely. However, this high rate of stimulation can interfere with other experiments and introduces more artifacts. Furthermore, many MEA experimental setups do not allow for stimulation at 25 electrodes. By employing a closed loop, where stimulation rate and electrode depended on the culture activity, they could achieve similar results with lower stimulation frequencies across only 10 electrodes. One advantage of this method of burst suppression is that it does not impede the networks response to other stimulation protocols the way partially blocking excitatory synaptic transmission with an antagonist such as AP5 or CNQX does[145]. Training protocols may be superimposed over the background burst suppression. An attractive aspect of this technique is that it more closely mimics natural modes of activity where constant stimulation comes from sensory afferents.

Demarse et al took the closed-loop stimulation concept one step further, to embody the neuronal network in a virtual environment[146] so that activity vectors in the culture would control the movement of the 'animat' in a square room. A program interpreted and learned the activity vectors to translate them into movement. The animat would then receive 5 inputs, 1 for each direction of motion, and 1 for collision detection. The results did not indicate that the animat learned that it was in a confined space or that it had real control over its direction. Nor did the group "know in detail how the complex patterns of activity were affected by the stimulation we provided, nor what changes within the network are responsible for producing the different patterns." However, this experiment does introduce an experimental design that is likely to be revisited and improved upon when we have a better understanding of the complex activity patterns of neuronal networks, and it illustrates how complex the challenge of appropriately stimulating and analyzing the activity of random 2D neuronal networks is.

Shahof and Marom have demonstrated the ability of MEA networks to 'learn' an activity by stimulating a coupled pair of electrodes in the network at a low frequency (0.3–1 Hz) until a desired predefined response (activity at an initially unresponsive electrode pair) was observed 50±10 milliseconds after the stimulus or 10 minutes, whichever came first at which point stimulation was immediately removed. Then after a 5 min rest the teaching cycle was repeated, this process lead to a specific response elicited by the stimulus[147]. Importantly, this 'learning' was achieved without a reward mechanism or other chemical treatment which is a novel achievement. They relate this achievement to a psychological theories by Hull and Guthrie, that "it is not necessary to

assume a separate mechanism for the biological realization of a reward in distinction from the process of exploration for solutions; the behavioral concept of reward might be considered as a change (removal) in the drive underlying the exploration in the space of possible modes of network response. A drive to explore that is removed when a desired state is achieved is an intentionless natural principle for adaptation to rich and unlabeled environment." However, even if this type of learning can be shown to have an *in vivo* correlate, the idea of learning through reward is no less important [148-150]. The analysis employed in this experiment, correlating the firing of two electrodes is an important concept carried over to experiments involving reward.

2D Neuronal Networks - Conditional firing probabilities (CFP)

Building of the work of Shahof and Marom[147] in 2004 Eytan et al[151] employed CFP as a neuronal network analysis tool in their investigation of Dopamine's effects on in learning in *in vitro* cortical neuron populations, calling it functional association strength. They observed that in the random monolayer approach to MEA neuronal network studies, several synaptic pathways may be present between each pair of electrodes. They looked at the effects of Dopamine on CFPs, finding that Dopamine is a catalyst for change in CFPs rather than stability. It has been found that Dopamine is released in animals when they experience an unpredicted stimuli, Eytan and colleagues propose that change in neuron population associations is enhanced because the current associations are in adequate[151].

In 2007, Feber et al improved upon this approach, looking at the relationships for every pair of electrodes (i, j) they defined "the conditional firing probability ($CFP_{i,j}[\tau]$)

as the probability that electrode *j* records a spike at $t = \tau$, given that an action potential was recorded at electrode *i* at $t = 0$..

" "If a CFP*i,j* [τ] distribution clearly deviated from a flat one, electrodes *i* and *j* were considered to be related."[152]. Using the CFP they characterized the strength of the relationship between electrodes as the maximum probability of a paired firing, and the propagation time as the delay between t=0 and the time when CFP was maximum. CFP is an important concept if one considers Feber's remark, "The formation and development of connections is assumed to be crucial in the process of learning, their conservation is assumed to be essential for memory. To demonstrate either memory or learning, one needs to monitor the connections in neuronal networks."[152]

While there are many similarities of 2D random cultures of neurons with *in vivo* networks, there are inherent differences. Foremost, neuronal networks in the brain are 3D, with the neurons enclosed in a matrix of astrocytes and ECM which affects chemical and electrical signaling. Additionally, *in vivo* neuronal networks have a more engineered order due to developmental cues. Furthermore, local neuronal networks in the brain receive input from other areas of the brain and from other neuron types, rather than existing as a homogenous self-contained network.

2D Neuronal Network s- Computational Modeling

However, by developing models to explain the general role of cellular and synaptic organization on network function and of chemical and genetic factors on overall network activity, we may reveal some lower level universal concepts that can be extrapolated to models based on the physiological organization of neuronal networks.

There have been several efforts toward this goal, most of which are mathematically involved and may require a strong understanding of statistics and network theory. Most models start with a simplified model of the neuron, a popular model is the integrate-and-fire (IF) model[153]. In the IF model, or leaky IF model, a neuron is represented as a leaky capacitor which fires when a threshold membrane potential is exceeded. By creating a network of such inputs has been possible to simulate the input a single neuron receives from a cultured network and inject a corresponding current via patch clam[154]. When modeling a neural network, complex reverberations of activity spontaneously emerge with sufficient feedback. Donald Hebb proposed that these reverberations may be used to encode and store information in the nervous system. Such reverberations of activity are commonly observed in 2D neuronal networks[155]. Depending on the initial conditions, (a perturbations of network activity from stimulation) network activity may 'settle' to a specific activity state, or a persistent dynamic attractors. Several network models of memory embrace these dynamic attractors[156]. In this manner a single network may have several end attractor states or memories based on the pattern of stimulation. Many of these dynamic attractor models are based on the work of Hopfield and the Hopfield network[157], which bases its synaptic weight calculations on a Hebbian model[158] commonly stated as "fire together, wire together." Attractor-based models of memory may include as little as 8 neurons[159]. There is indirect evidence that attractor states are responsible for hippocampal spatial maps (place cells). However, "Since hippocampus is a multimodal integration area and hippocampal place cells are driven by a variety of sensory inputs and intrinsically generated path-integration signals,

one considerable hurdle is to design a controlled situation where the hippocampus is disconnected from all external influences."[160]

Finally, percolation theory, employed in many scientific fields, has been suggested by a few researchers attempting to model 2D neuronal networks [161, 162]. Here, the specific connections may be overlooked in order to address an overall activity of the network, such as "the critical distance that dendrites and axons have to travel in order to make the network percolate, i.e., to establish a path from one neuron of the network to any other, or the number of bonds (connections) or sites (cell bodies) that can be removed without critically damaging the functionality of the circuit."[163]

Electrophysiology of Patterned Neuronal Networks

While MEA research with 2D neuronal networks is an expanding field with interesting phenomena and provocative models, connecting 2D neuronal network phenomenon with the anatomical or single cell level of current knowledge is often difficult. It may seem that the random 2D realm is at best, floating between these two levels, without a firm attachment to either side. Every neuron in a neuronal network makes tens to hundreds of connections with other neurons. With confluent monolayers especially, it is impossible to discern the detailed connectivity of a randomly cultured neuronal network. Though the activity of such networks can be interrogated by the previously described techniques, unambiguous testing of these models is virtually impossible. Towards removing the ambiguity of neuronal network architecture and recordings scientists have worked to simplify these networks by reducing and restricting

the connectivity. The earliest attempts at spatial organization of cells on electrode array surfaces used surface patterned chemical cues [164, 165].

Chang, who used microcontact printing to create patterned neuronal networks on MEAs takes a cautious approach to interpreting network activity as he chose to"…assess the level of activity with the percentage of electrodes active rather than applying spike sorting or burst analysis because physical connectivity and extended network activity should be established for spike and burst analysis to be meaningful."[166] In this set of experiments, 40μm wide lines PDL were stamped onto the array, inducing several 1D neuronal networks across the array. In these patterned networks neuronal activity was increased compared to random cultures of the same cell density, in agreement with earlier results[167]. Additional observations included accelerated gliogenesis and synaptogenesis, and an increase in glial proliferation, in the absence of serum. This final result may reflect the findings of other groups that glia increase neuronal activity. Chang acknowledges that their patented networks lacked the desired regulation of neurite extension, not yet realizing full control over network geometry. Finally, an important question is raised with crucial implications on neuronal network design; what is "the minimum network size, in terms of cell number that results in network activity"?

Maeda et all cultured a random 2d network, and then partitioned it into pieces with a UV laser to investigate if synchronized bursting behavior was due electrical excitation or a diffusive chemical factor[136]. They found when the larger network was sectioned into pieces that synchronized bursting was isolated for each division, and that the frequency of spontaneous bursts did not change significantly. However, they did find

that propagation velocity was decreased after sectioning, implying that projection (neurite) density is a determinant propagation velocity.

Feinerman and colleagues have published several different experiments all using a quasi 1D neuronal network. They pattern rat hippocampal neurons into long >17mm lines that are170μm wide. The cell activity is observed optically using calcium sensitive dyes. This model allows them to easily monitor the propagation of signals and bursts along the line[168] leading to a more 'behaved' culture resembling a hippocampal slice. In one experiment investigating bursting activity[169], they could temporarily partition the cultures (in contrast to work by Maeda[136]) with TTX applied to only a center portion of the line. In this fashion they could analyze the independent activity of burst initiation zones (BIZs). They found that BIZs compete to drive the global bursting behavior, and the BIZ with the shortest refractory time is the winner. Essentially, after every burst, cells begin to recover, and the first BIZ to do so will initiate a burst. They also correlated BIZs with a higher cell density, and lower ratio of inhibitory synapses. This makes sense in light of Chang's work[166], where a restricted linear network increases activity, possibly by a decrease in refractory time with an increase in glial cell contact. In other work they used a similar model (8.5cm long, 170μm wide) to investigate the propagation speed of signals through the network, and the stability of rate coded information[168]. Here they found that signal propagation along the line fits precisely with an information theory model of Gaussian communication channels and that rate coded information fails with in a 3mm distance from synaptic noise of a layered network.

Truly 1D neuronal networks with single cell resolution have only been achieved by only 1 group. In 2005 Suzuki et al employed their unique stepwise photothermal etching method to etch micro-wells and connecting channels in an agarose substrate covering an MEA. They achieved not only a linear 3 cell circuit, but by creating the channels in a stepwise fashion, controlled the direction of neurite outgrowth. They found these directionally controlled circuits had a one-way propagation of signal transmission as opposed to conventional open channel preparations[21]. One problem with this technique was that not all neurons they placed down were recorded, though signal still propagated through to the next electrode. This may be because of the etching procedure leaves a fouled electrode with a poor SNR. Thus far the group has not published any more results, expanding the technique to more mature experiments or complex circuits. One other group has prepared system for 1D networks with single cell resolution, however they have only reported its use with a single cell at a time. Using an elastomeric membrane method to confine the neuron to the electrode and direct the neurite Claverol-Tinture and co-workers [104] grew Helix aspersa neurons on electrodes and stimulated them pharmacologically. They then recorded the signal propagation through the neurite as it passed several electrodes. More recently Dworak has demonstrated a similar application of PDMS microtunnels, directing the axons of large populations of neurons over microelectrode wires[20].

CHAPTER III
PROJECT RATIONALE

Overall Goal

The previously described cell patterning techniques and research approaches to studying and defining *in vitro* neuronal networks have lead the way for the work described in this dissertation. Previous research has opened a path and provided important stepping stones that make this research possible. We believe that the ability to create defined heterotypic neuronal circuits with single-cell-resolution and one-to-one neuron electrode access is a significant advancement in neuronal network research which may similarly clear the path for more complex fully-defined neuronal network research models.

It is clear from the brief literature review that there is no shortage of techniques for patterning cells. For neurons specifically, the most widely used method of controlling cell placement and neurite outgrowth is surface patterning of cytophilic molecules via microcontact printing. While surface patterning has been a successful approach, it does not offer direct placement of neurons on electrodes, but requires the neurons to preferentially migrate to the larger cytophilic area of a stamped electrode. Furthermore, complex multi-stamping procedures are required to achieve heterotypic, cell-type-specific patterning. To bypass these drawbacks we have chosen to use an optical force manipulation technique cultivated in our lab to place cells to specific points on the substrate. However, this technique alone provides no control over cell migration which quickly undoes patterns created by precise cell placement. To compensate we have

employed elastomeric membranes with micro-holes and micro-channels which serve as micro-wells and micro-tunnels when aligned and attached to a flat substrate such as a coverslip or an MEA. These microwells of the elastomeric membranes are used to confine cells to the electrodes of the mea and the micro-tunnels direct neurite outgrowth between specific neuron/electrode pairs. The elastomeric membranes address the additional challenge of survival of neurons cultured at the very low densities implied by single-cell-resolution circuits. The microstructures of the elastomeric membranes closely resemble microfluidic channels which have been shown to aid in the culturing of neurons at very low densities[66].

The guiding goal of this design based research project was to establish a method for producing fully-defined, heterotypic, single-cell-resolution neuronal circuits with electrophysiological access to individual neurons. Successful achievement of this goal may be marked by milestones which are reflected in the specific aims of the research plan. These aims were:

1. **Develop a Laser patterning System with capability to pattern various cell types to various substrates with greater than 10µm accuracy.**
2. **Develop the microfabrication techniques, and microstructure designs to impose 'defined' neuronal circuitry.**
3. **Use the laser cell patterning system to place individual neurons and or astrocytes into the elastomeric membrane microstructure and on microelectrode arrays.**
4. **Determine the rate of patterned neuron viability, the success rate of neurite polarity control.**

These aims provide a template for neuronal biochip construction which can be used in a variety of neuronal network research applications. Successful realization of these aims will serve as proof that a defined neuronal network can be implemented into a

microfluidic and electrophysiological device and serve as a guide for the construction of future defined neuronal network biochips. The flexibility of the systems in Aims 1 and 2 will allow different configurations and different cell types to be easily included at low cost, yielding a productive research tool which can be applied to several different diseases including ALS and AD.

Rationale of Specific Aims

Aim 1

Develop a Laser patterning System with capability to pattern various cell types to various substrates with greater than 10µm accuracy.

A method for depositing single cells to specific points on a substrate is central to creating neuronal networks with single cell definition. The method must have sufficient accuracy and precision to place neuronal cells with a diameter of 8 µm into microwells as small as 10 µm in diameter (Aim 2). The method chosen must also meet the requirement of creating heterotypic (i.e. neuron and astrocyte) cell patterns to enable the proposed, as well as future, research scenarios. Optical force manipulation systems have proven to be very useful in manipulation, separation, and patterning of individual cells and can meet the above requirements.

Factors influencing the optical properties of the system include the cell medium, the size and index of refraction of the cell which varies for each cell type, as well as factors arising from the cell deposition chamber. The laser patterning process must take place in a sealed chamber to eliminate turbulence inducing leaks and contamination.

This laser deposition chamber must be biocompatible, allow for the minimally altered passage of light for imaging and laser guidance, and incorporate various substrates including a microelectrode array (MEA) and any microstructures attached to it.

Aim 2

Develop the microfabrication techniques, and microstructure designs to impose 'defined' neuronal circuitry

Neurons, like many cell types, tend to migrate. To keep cells in their initial patterned positions, especially neurons patterned to electrodes, some mechanism must be employed to control cell migration. Furthermore, it is also desirable to control the direction in which neurons extend their axons and dendrites in order to fully define the neuronal circuits cultured on the chip. We propose using 3D microstructures to confine cell bodies and guide neurite extension. This choice of methods also addresses the additional challenge of maintaining neuronal cultures with very low cell densities (<2500cells/cm^2). The incorporation of microfluidic structures creates a very low-volume culture space which can aid in the survival of low density neuronal cultures[66, 84] due to a decrease in autocrine and paracrine signal diffusion.

Aim 3

Use the laser cell patterning system to place individual neurons and or astrocytes into the elastomeric membrane microstructure and on microelectrode arrays

In order to create a neuronal biochip which can be used as a research tool, creating patterns of neurons on the microelectrode array and microstructure substrate is not enough. The neurons must develop into a healthy network which can serve as a meaningful model for the way neurons would behave *in vivo*. Toward this end a crucial

part of this project will be to determine what fabrication and culturing methods will yield arrays of healthy neurons that extend neurites and connect to neighboring neurons to create a network. Specifically we must succeed in inducing the following sequence of neuronal culture states.

- Cells attach to the substrate and extend neurites
- Cells survive for at least 1 week.
- Neurites fully extend to neighboring cells, showing visible contact

Initial success of the neuronal circuit creation systems will be evaluated by observing cell and network morphology with microscopic techniques. Survival, outgrowth, and synapse formation must be achieved before electrical activity and signal propagation can be expected. Live-cell phase microscopy will be used to quickly assess the rate of neuron survival and neurite extension. Immunocytochemical antibody staining and fluorescent microscopy will be used to assess neurite outgrowth and synapse formation which may be difficult to observe because of debris or substrate features.

Aim 4

Determine the rate of patterned neuron viability, the success rate of neurite polarity control.

Once the laser cell patterning, microfabrication, and culture techniques are sufficiently refined to support neurite outgrowth we will begin to assess two characteristics of the patterned neurons. In normal randomly seeded cultures of neurons only a fraction of the cells plated survive and extend neurites. Therefore, we do not expect every patterned neuron to survive and extend neurites. The success rate of a patterned neuron to survive and extend neurites will affect the efficiency of the system to create single the intended fully defined single cell circuits. We would like to optimize the

laser cell patterning, microfabrication, and culture methods to maximize the fraction of patterned cells which survive and extend neurites. Therefore we will assess the viability of neurons laser patterned into the PDMS microstructure.

We hypothesize that channel geometries can be used to influence polarity of neurons. The fabrication process employed permits a feature resolution no smaller than 8μm which is not ideal for restricting the path of neurite elongation in a single direction. Working with this limitation we instead used a combination of channel width tapering and sharp or obtuse channel turns to influence the direction of neurite extension and neuron polarity. To test the effectiveness of this method we will observe the path of polar processes, axons and dendrites, by time interval live-cell microscopy and immunocytochemical staining.

CHAPTER IV
LASER CELL PATTERNING SYSTEM

Introduction

Conventional manipulation of cells in space is performed with a micropipette and micromanipulators similar to those used in a patch clamp experiment. This is a time consuming process that can expose the culture to contamination and is not amenable to placing cells firmly into the bottom of a microwell. We have chosen to use an optical force cell patterning method which has the advantages of keeping the cells in an air/water tight chamber reducing contamination, is easier and faster than contact manipulation, and can firmly press a cell into contact with a surface without damaging pressure.

While the inherent qualities of optical force manipulation may suffice the requirements for achieving Aim 1 there are other points of concern that must be addressed during development of the laser cell patterning system. There are three major points; 1) The laser cell patterning system including all cell contacting components must be biocompatible and provide the means for cell support such as media and gas exchange and temperature control. 2) The laser patterning system must be compatible with the substrate; specifically it must be able to pattern cells inside the microwells of a PDMS membrane and onto the electrodes of an MEA without damaging the electrodes. 3) It must pattern cells in a time efficient manner so that arrays of cells (60) can be patterned in a practical time period (~1hour). These issues are addressed by the proposed system design which will first be briefly summarized and is illustrated in Figure 13. The laser cell pattern system[170] is faster, easier, and more sterile than conventional methods

using a micropipette, and more adept at placing cells fully onto electrodes inside a 3D microwell. Together, these advantages amount to a major increase in practicality. Additionally, the laser patterning system can be used to pattern multiple cell types enabling heterotypic neuronal circuits which can be used to model *in vivo* circuits between different brain regions, to test the effect of different cell types on a circuit, and to investigate how cells form transgenic disease model animals behave and affect circuits

The laser guidance phenomenon used in our laser cell patterning system exploits the same radial gradient force that is used in laser tweezers systems. When a laser beam with a Gaussian intensity profile passes through a particle, the particle experiences a force pulling it toward the center of the beam. In laser trapping, the laser is focused so tightly that a gradient force also pulls the cell toward the center of the beams waist. In laser guidance, the weakly focused beam does not produce a strong enough gradient to overcome the predominate scattering force which pushes the cell in the direction of the beam. This begets two advantages of laser guidance over laser trapping. The weakly focused beam may be achieved with a long-working-distance objective, allowing for an extended 3D space to work in. Additionally, forward pushing axial force of a weakly focused beam allows for cells to be pushed onto the substrate, ensuring good cell electrode contact.

Overview

The entire laser cell patterning system, illustrated in Figure 4.1 was built around a stationary downward propagating laser beam. This laser beam was weakly focused to produce a guidance region where a cell would become physically trapped in the

horizontal plane and pushed downward in the direction of the beams propagation. Cells suspended in a culturing media within the cell deposition chamber could be brought into the guidance region by moving the chamber relative to the focused laser's guidance region. Once a cell was trapped and guided, the chamber and the attached substrate could then be moved so as to bring the guidance region and the guided cell into alignment with

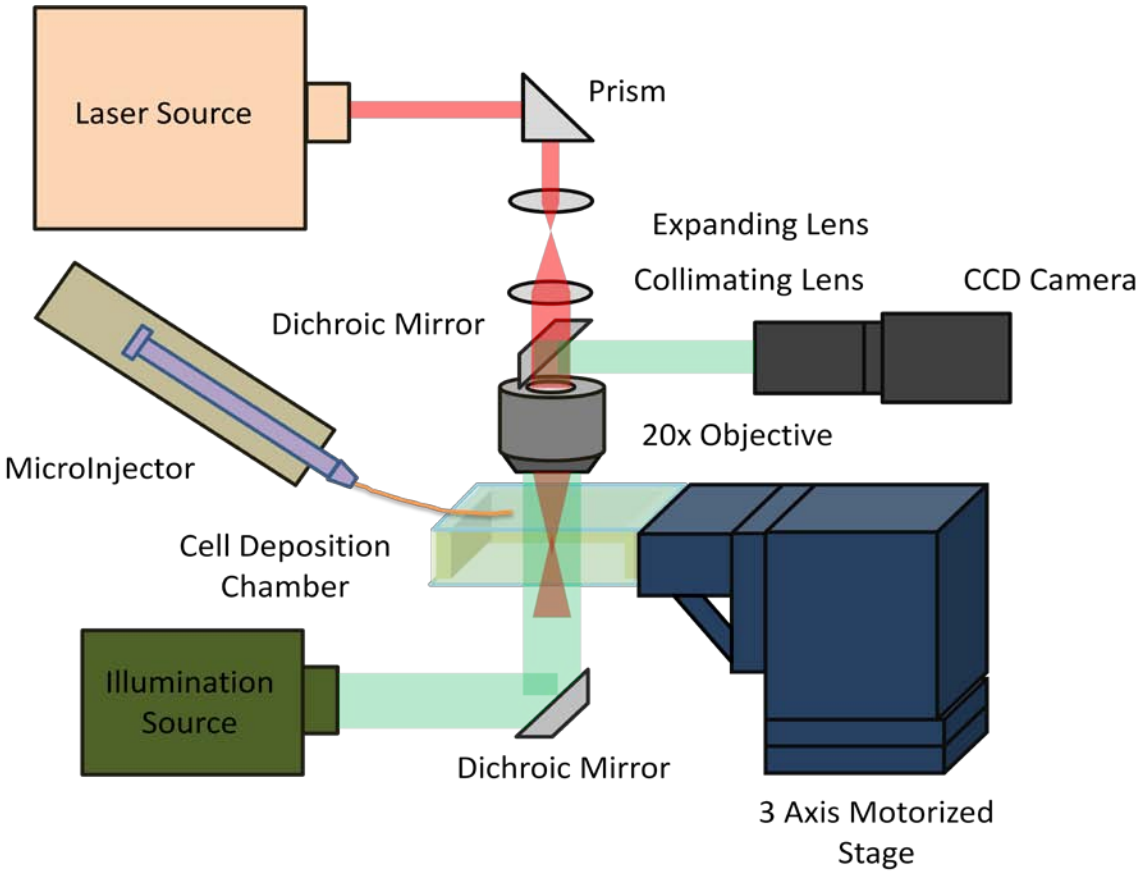

Figure 4.1: Schematic of laser cell patterning system hardware (not to scale).

a desired point on the substrate. The process was imaged using the same stationary objective used to focus the beam.

Materials and Methods

Optics

The laser source used was a Spectra-Physics 3900S CW Tunable Ti:sapphire laser pumped by a Millennia Vs and tuned to produce an 800nm wavelength single mode beam with a Gaussian intensity profile. The beam was passed through 3 prisms with antireflective coating optimized for 800nm to bring the beam parallel to the table up, over, and down as shown in figure x. The beam was then focused and expanded using an f = 17mm, D=10mm lens and collimated using an f = 48mm, D=10mm lens. The expanding lens was mounted on a motorized translational stage and used to steer the beam's focus point so that the guidance region of the beam coincided with the object plane of the imaging system. The beam then passed through a 45º dichroic mirror which was used to reflect the visible image to the CCD camera while allowing passage of the 800nm beam. The beam was then focused using an EPI L Plan Apo 20x long working distance objective with NA = 0.35 and f= 200. The illumination source was a simple incandescent light source with a green pass filter. The illumination was passed through an iris to control brightness and aid in system alignment. The illumination beam was reflected upwards with a dichroic mirror and through the bottom of the laser cell deposition chamber; it passed through the 20x objective and was reflected to the side by the dichroic mirror. The image was then passed through several IR filters to remove artifacts from the guidance beam, before it hit the Sony CCD camera. The CCD camera was mounted on 3 orthogonal translational stages to allow for the center of the CCD to be aligned to the laser guidance region.

Laser Cell Patterning Chamber

Living cells require media to survive. In the long term the media must provide nutrients and growth factors as well as aiding in transport of waste material. In the short term the media provides a hydrating source with the proper osmolarity and pH to keep cells healthy. During the cell patterning process cells must be kept in such an environment. To satisfy this need laser guidance and cell patterning took place inside the cell deposition chamber. This component of the system held media in an air and water tight seal over the substrate (MEA with microfluidic structure overlay) and allowed the laser beam and the imagining illumination to pass through.

During the course of this research the laser deposition chamber underwent many revisions, but there were two general designs that were employed. The earlier design (stacked) was more modular and centered around a stacked design which would allow for interchangeable and customizable parts, and compatibility with different substrates. The later design (patternscope) removed the use of a PDMS wall component which was found to be susceptible to fungal contamination. We will discuss both designs as each has some advantages, and a understanding of the patternscope design advantages is improved with comparison to the stacked design.

Stacked Chamber

An exploded view of the chamber with substrate is illustrated in Figure 4.2. The chamber consisted of a custom 0.5-3mm thick PDMS gasket and a ‘ventblock’(Figure 4.3) which was made from a #1 glass coverslip glued to a stainless steel block with an inlet, outlet and an optical window. Through-holes were drilled in the coverslip with a

high-speed dremmel and a 2.3mm diamond bur ball drill bit (diamondburs.net LLC). The PDSM gasket was formed by molding PDMS over several small fibers glued to the bottom of a 200mm glass Petri dish. Once cured, the PDMS was removed, cut in 22mmX22mm squares and holes were punched for the center chamber and the connecting inlet and outlet ports. The fibers in the mold produced small grooves or channels which accommodated the 360µm diameter PEEK tubing which was part of the microinjection system used to deliver cells into the chamber for patterning. These components were all clamped together by two round stainless steel plates fastened with 10-32 thumb screws, creating a sealed chamber.

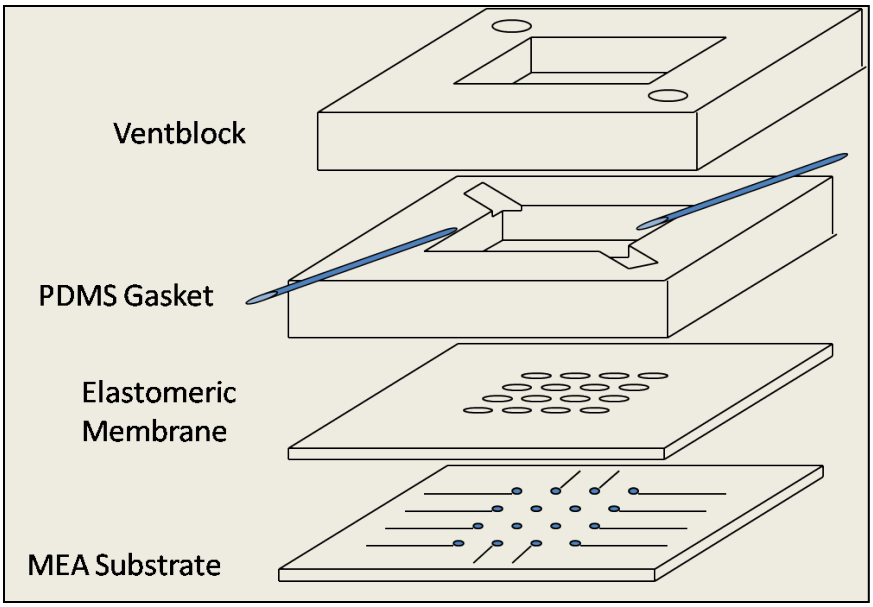

Figure 4.2: Stacked chamber illustration. The Ventblock and PDMS Gasket are stacked on top of the substrate (an MEA with Elastomeric Membrane).

Figure 4.3: Ventblock bottom view.

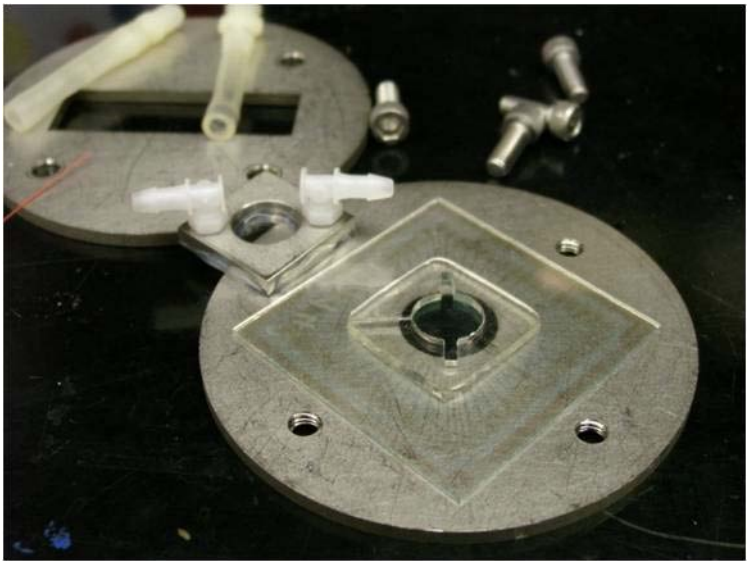

Figure 4.4: Stacked chamber disassembled. The MEA has a PDMS Gasket bound to it.

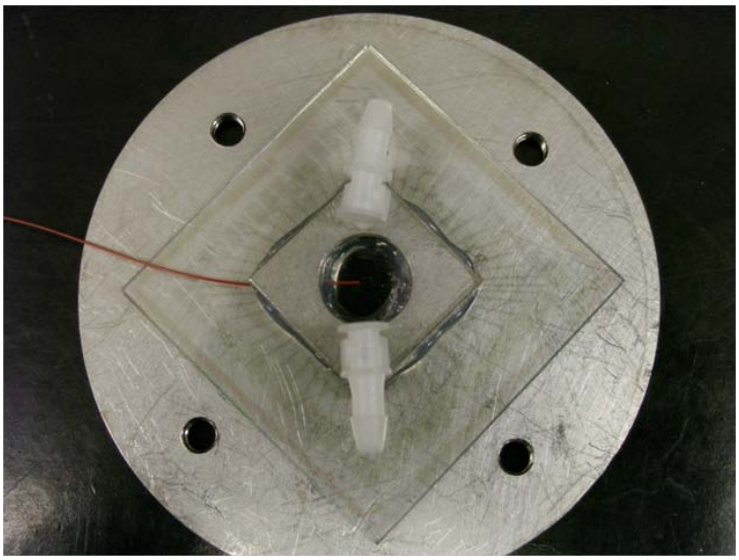

Figure 4.5: Stacked chamber partially assembled. The red microinjection fiber (PEEK tubing) can be seen protruding into the center of the chamber.

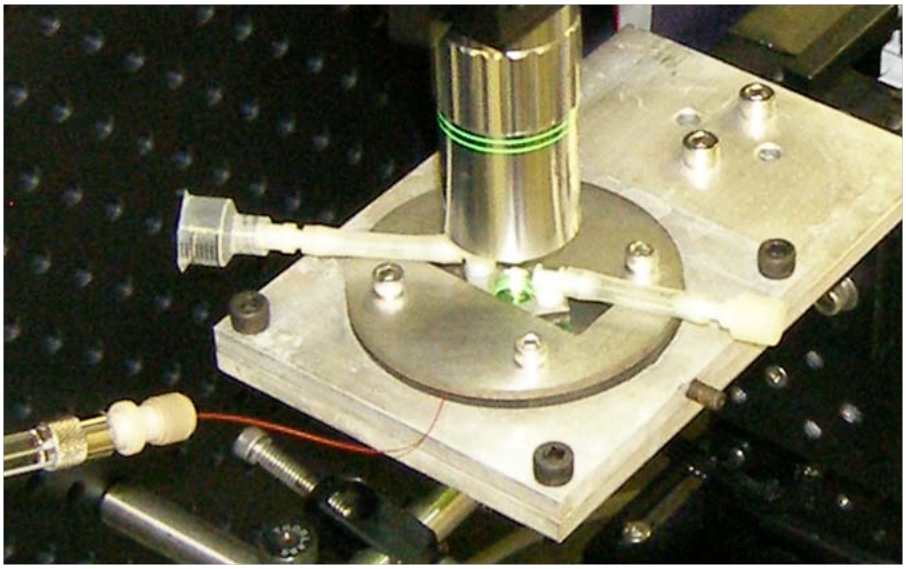

Figure 4.6: Stacked chamber fully assembled and mounted in the laser patterning system.

Patternscope Chamber

The patternscope design is based on a submersible laser passage window housed in a tubular structure which allows for rotation and height adjustment. Part of the patternscope component is a fiber guide which allows for the insertion and adjustable positioning of a microinjection fiber. The patternscope includes a 'skirt' which helps to stabilize the fluid beneath the chamber which is otherwise prone to sloshing. The sloshing is due to the incomplete filling of the chamber with media, in contrast with the stacked chamber design which was completely filled. In the patternscope chamber design (Figure 4.7) the substrate being patterned to should have a fluid containing wall (as in a Petri dish or the glass ring of a standard MEA). This wall is will be clamped tight to a PDMS laser attached to the underside of the top clamp. This PDMS layer seals the substrate dish as well as the pattern scope, creating an airtight seal. The importance of this design is that the seal is not wet as the previous seal was. The wicking action of this seal was hospitable to fungus. A dry seal is not. Furthermore, this allows for standard Petri dish or glass rings to be used. With the previous chamber, the PDMS wall was used as a culture dish. Because shallow chambers (<= 1mm) were best for patterning, they were also used for culturing, which presented a very low media volume which could evaporate quickly. It also allowed for thin layers of media to sit on top of the PDMS wall. We observed that the combination of fungal contamination during the patterning process by the wet seal and the following culture condition of thin media coverage of a porous PDMS wall was much too supportive of fungus in the presents of non-clean lab conditions. Finally, as an extra measure of contamination prevention, the patternscope chamber design employs an

airtight outer seal made of PDMS which creates one additional layer of protection from the un-clean laboratory conditions.

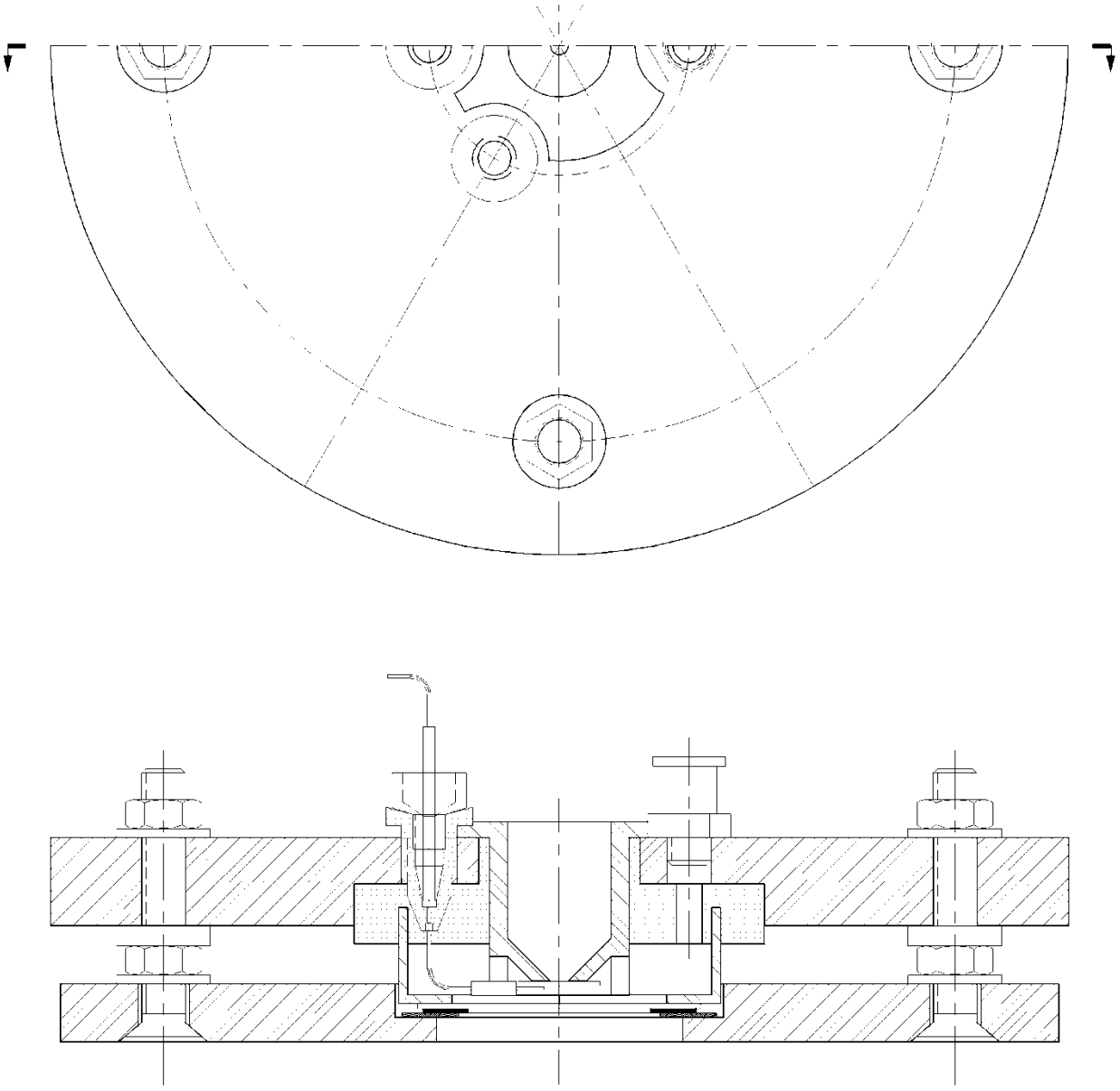

Figure 4.7: Patternscope chamber design. A standard Petri dish or mea is sandwiched between the two clams and a PDMS gasket which seals to the patternscope body and the top lip of the dish or mea.

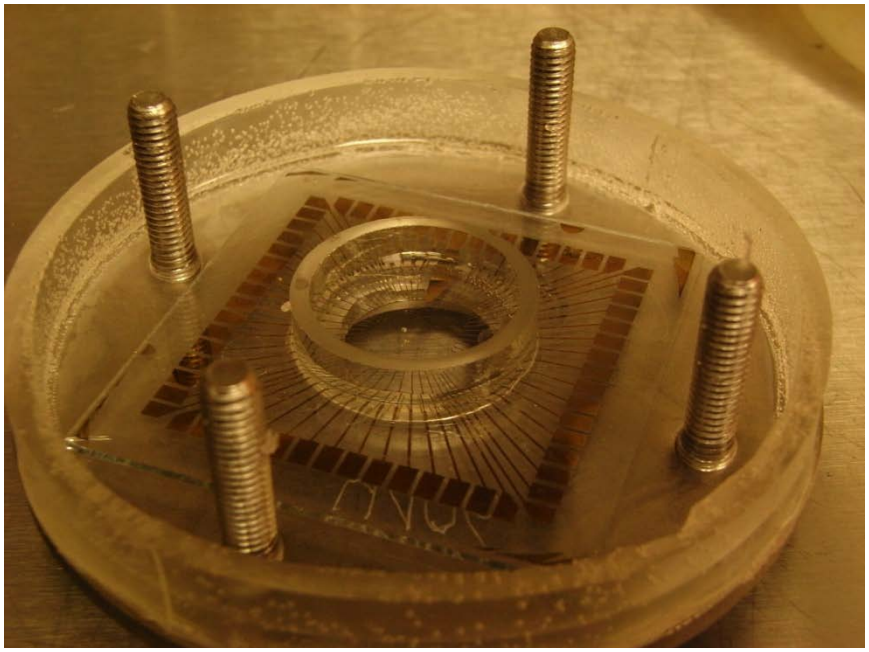

Figure 4.8: Bottom Clamp of Patternscope chamber. Bolts come up through for easy alignment of top clamp. PDMS wall creates second seal to outside environment.

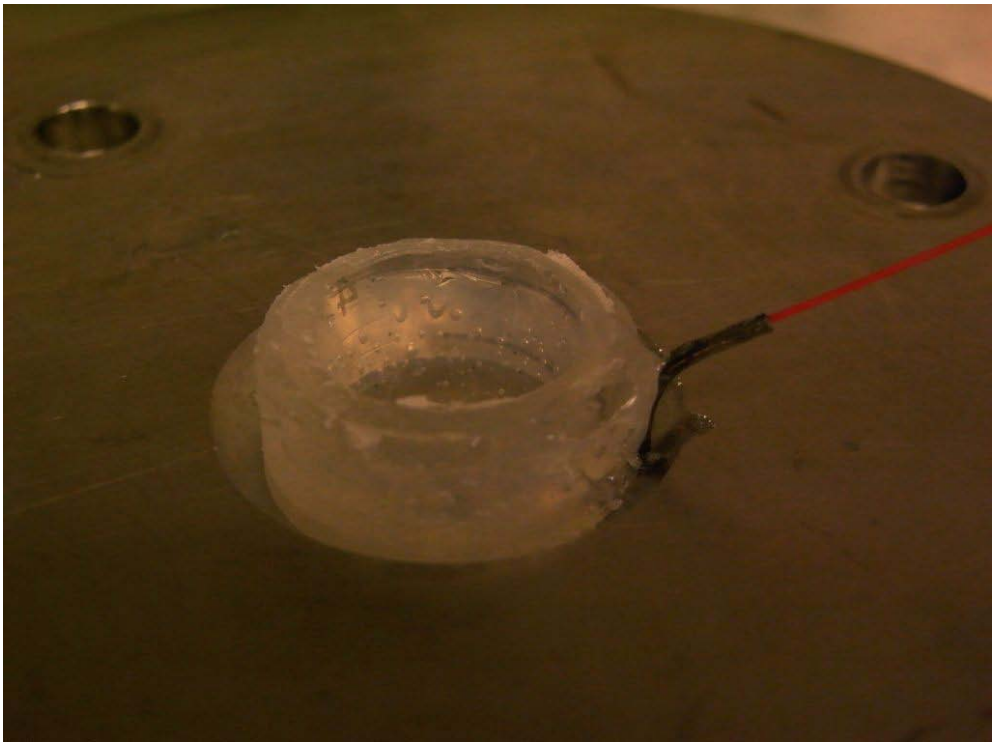

Figure 4.9: Top clamp of patternscope chamber. Patternscope is poking through the top. microinjection fiber feeds through the SS 21G conduit. In this prototype chamber the conduit does not lay flush with the patternscope tube so a notch was filed in the clamp top enable fit. This notch does not allow for rotation which an intended benefit of the patternscope design.

Figure 4.10: Bottom of patternscope. The prototype patternscope was constructed from a two 15mL tubes glued together. Then inner cone is cut and a 9mm x 9mm #2 coverglass was glued to the cone.

Figure 4.11: Upside down view of top clamp with PDMS seal and patternscope.

Laser Cell Patterning System - Microinjection

A microinjection system was implemented to introduce cells into the chamber with control over the number of cells and the time at which they were released into the chamber. The rotatable patternscope and fiber guide also enable control over where in the chamber the cells are injected. In early implementations of the laser patterning system before the inclusion of a microinjection system the chamber itself was filled with cell suspension, and the majority of those cells would fall randomly onto the substrate, disrupting the defined pattern. Under normal conditions cells eventually settle out of the suspension and come to rest on the substrate. While the laser guidance system can exert force in any direction within the horizontal plane, it can only push cells forward (downward). Therefore without the use of a cell feeding system, there is a limited amount of time (<15 minutes) during which the cells can be guided to points on the substrate before all have fallen onto the substrate. Furthermore, filling the entire chamber with cell suspension in this way inevitably leads to pattern disruption by unintended cells falling into the pattern area.

A cell suspension containing between $20x10^4$ and $50x10^4$ cells/ml was loaded into a 50µL glass luer-lock syringe (SGE). Microtight® fittings (Upchurch Scientific) were used to couple poly(etheretherketone) (PEEK) tubing with an inner diameter of 100µm and an outer diameter of 360µm to the luer-lock of the syringe. The tubing was then inserted into the cell deposition chamber during assembly. During patterning the syringe was loaded into an UltraMicroPumpII (World Precision Instruments Inc.) which was capable of injecting as little as 5nL of suspension at a time, allowing for a single cell to

be fed into the chamber if needed. Up to 4 of these micropumps may be controlled with the Micro4™ MicroSyringe Pump Controller, enabling multiple cell types to be patterned in a single session. The micropump controller was issued commands from the computer via an rs232 port.

Laser Cell Patterning System - Motorized stage

During the cell patterning process the chamber was secured in an aluminum mount attached to a 3 axis motorized stage (Aerotech FA90-25-25-25). The stage was driven by 3 Aerotech N-drive units which communicate with the computer via IEEE1394. The stage was capable of sub-micron resolution and accuracy and a 25mm travel for all three axis.

Laser Cell Patterning System - Incubator

An incubation system was built to maintain optimal culture temperatures during patterning to increase cell health as well as moderating the convection forces that can arise from the substrates absorbance of the laser radiation. The system consisted of thin Kapton coated heating elements and small resistance temperature detector (RTD), which were connected to an Omega CN9512 proportional-integral-derivative (PID) controller. However, patterning neurons at room-temperature was not detrimental to neurons survival. The convection forces were most noticeable on thick substrates (such as MEAs) with thick membranes, and larger deposition chamber volumes resulting from thicker >1.5mm PDMS gaskets. As the laser cell patterning and elastomeric membrane process was refined, both thinner membranes (<40µm) and PDMS gaskets (<500µm) were used,

minimizing the convection forces and making temperature control unnecessary. However, such convection forces were found to be minimal at room temperatures of 20ºC, and that maintaining this temperature was a far more effective way to mitigate convection forces than by the used of an incubation system. Use of the incubation system was discontinued.

Laser Cell Patterning System - Control System

A control system was needed to integrate the operation of the above components and to enable efficient and precise manipulation of cells.

Control System - Overview

The entire laser cell pattering system was controlled by an application written in LabVIEW 8.6 which allowed for tuning various parameters of the system. The application provides 3D-position memory mark and recall functions and an intuitive user interface and control system for navigating cells from the microinjection point to the deposition point on the substrate.

Cell manipulation and navigation were primarily controlled by a gamepad controller

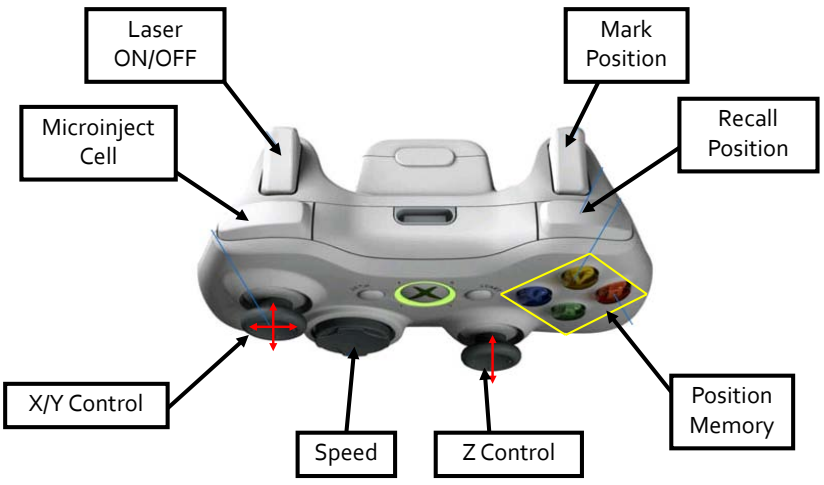

Figure 4.12: Gamepad Controller: The each button is labeled with its function

(Figure.4.12). The analog thumb-sticks were used to maneuver in X,Y, and Z. A mark and recall system allowed a user to mark way-points on the substrate, for example an electrode. Pressing another button triggered an injection of cells into the chamber, and commanded the motorized stage to bring those cells into the field of view (FOV) and laser guidance region. At that point the user would maneuver the cell into the center of the screen where the laser was focused and press a button to open the laser shutter, turning on laser guidance. Once the user captured the cell in the guidance beam, and it was held in the center of the FOV, an on screen direction indicator points toward the previously marked way-point. Following the indicator the user would navigate to the way point using the thumb sticks, carrying the cell along in the laser guidance region. A pattern of neurons could be created by repeating this sequence of events 1) Mark a way-point at the desired position to deposit the cell. 2) Inject cells for patterning. 3) Capture the cell with the laser. 4) Navigate the cell back to the way-point.

As previously stated, the primary user control input device was a gamepad controller (Microsoft Xbox 360) with 2 thumb sticks. The advantages of using this type of controller was that no hardware wiring was required, more inputs buttons were available than on the normal joystick controller available for most motorized stages, and it was considerably cheaper, readily available and easily replaced. Additionally, it is a device many users are already familiar with which decreased the learning curve.

The control system ran on an Intel Core 2 Quad computer (Dell Precision 390). Programming the control software in LabVIEW 8.6 allowed for the manual assignment of specific processes individual cores of the processor. The Aerotech stage used RTX

(Venturecom®) to communicate with the computer in Real-Time, allowing or fast and temporally accurate commands to be issued at a low-level outside the WindowsXP operating system through a firewire (IEEE1394) port. One processor core driver was replaced with an RTX enabled driver leaving 3 cores, two of which could be assigned exclusively. The program was comprised of 4 primary timed loops to handle 1) the user inputs from the front panel, keyboard and gamepad, 2)to capture process and display the patterning video with navigational overlays, 3)to read motion control data from the analog sticks and compute the movement vectors and 4)to issue motion commands to each of the three axis. Processes 3 and 4 were vital to the programs response time and were assigned to dedicated processor cores. These process ran in parallel, allowing for the shortest loop periods and smoothest control. Low priority tasks were executed using subprograms provided by Aerotech. However motion control commands were issued directly to .dlls.

The opening and closing of the shutter and intensity of the laser were controlled via serial port/rs232 access through VISA in LabVIEW. The injection command and parameters of volume and rate were also sent through rs232 to the microinjector.

Control System - Features

There are several system features which were integral to improving and adding to the patterning systems abilities. Here we will describe their function, application, and how they were implemented.

Features - Speed controls

There were several points to consider in controlling the speed of the laser pattering process. The ability to manipulate cells with the laser patterning system was dependent on the optical force. This force was only able to support a certain acceleration of the cells without 'dropping' the cell, leaving it behind as the stage moved on. Furthermore, the fluid filled chamber caused a drag force which limited the maximum speed a cell could be pulled by the optical force without similarly dropping the cell. While these values depended on the size and type of cell, they were typically on the order of 150μ/s in the X and Y axis. In Z axis the speed was not based on pulling but on keeping up with the forward motion of the cell due to the axial force. This downward velocity was typically 25μ/s.

During normal navigation through the chamber without a cell trapped in the guidance region, the maximum speeds used for moving a cell could be painfully slow. A more efficient speed for chamber navigation tasks such as scouting out the patterning area and marking specific points on the substrate was around 500-1000μ/s. The wide range in speeds needed made fine control difficult for inexperienced users. Poor control resulted in frequent dropping of the cell and inaccurate deposition to the substrate making the laser cell patterning process long, frustrating, and less effective.

In order to address these points several controls were created which enabled versatile and quick movements through the chamber while making it easy for even first time users to manipulate the cells skillfully. A master maximum speed control extended from 0-1000μ/s. This control could be changed by moving a slider on the GUI or by

pressing the D-pad on the gamepad controller. No matter what, the speed could not exceed this value. Within this range the speed was controlled by the extent of the thumbstick displacement from center. At full displacement the speed was equal to the master maximum speed. In between the speed followed a cubic curve allowing for greater precision while retaining top-end speed. Furthermore, the program automatically imposed a maximum acceleration which helped to make the controls smoother, reduced cell dropping, and reduced wear on the stage.

Finally a 'maximum guidance speed' could be set for both the horizontal (X and Y) and the vertical directions. When a user wanted to guide a cell a trigger on the gamepad was held down which in turn held the laser shutter open, enabling capture of the cell. If the maximum guidance speed had been set and enabled that speed (i.e. 100µ/s XY, 25µ/s Z) was imposed. This feature was the most effective at enabling novice users to use the laser cell patterning system successfully.

Features - Mark and Recall

The mark/recall functionality made use of the positional feedback of the Aerotech stage. The positional feedback was one of the crucial features of the Aerotech stage. Because the stage could report the current position of all 3 axis and later recall that point with sub-micron accuracy, it was trivial to record the current position to a table in the LabVIEW code with an assigned button or key-combination. However, the ability to recall a marked point was not a crucial function of the control application. The recall function was most usefully employed as part of the cell injection process, where the injection point was automatically recalled if the current position wasn't within the 'recall

area’ a user defined radius specified in microns. The positional feedback was most important to the navigation cue included in the GUI and to the auto-intensity function.

Features - Automatic Intensity Reduction

The electrodes of a standard MEA are made of Indium tin-oxide (ITO) coated with platinum. Even without the platinum coating the ITO electrodes absorb significantly more of the 800nm laser radiation than the glass substrate or silicon nitride insulation. This absorbed radiation creates sufficient heat to boil the media overlying the electrode, fouling or damaging it. Additionally, this amount of heat is likely to critically damage a cell besides forcefully expelling it from the electrode as the bubble is formed. To avoid this heating the laser intensity can be reduced from 100mW to 15mW. Reducing the intensity manual is difficult and prone to error. An auto-intensity reduction function, if enabled will reduce the laser to intensity to a set level when the stage/laser/cell is within a set distance from the marked deposition point in the horizontal plane (i.e. 50µm) and a set distance above (i.e. 150µm).

Features - Imaging

The GUI features a display of the cell deposition process. The control program included functions to record video or take snap shots of the laser patterning process. Additionally there were simple image processing abilities that could be enabled to increase contrast and to remove artifacts from dust on the imaging optics.

Control System Application - Programming
Program Design

The LabVIEW program design is most clearly explained by the flow chart in Figure x. Each program component (as represented by a block in the flow chart) was implemented in its own timed loop (or multiple loops). The timed loop structure is similar to a while loop, with the addition of control variables including the period, priority, processor, and overtime conditions (Figure 4.2). These variables were crucial to managing the many processes implemented in the application and synchronizing their execution. The period, specified in ms, was simply the amount of time allotted to the loop to execute. If the loop was finished executing before this time was up, it would wait before the next iteration. The overtime conditions specified what should happen if the loop did not finish executing in the allotted time.

The highest priority set of processes were those which received and interpreted user input from the control pad, calculated stage movement vectors, and issued movement commands to the motorized stage. These processes were of highest priority because of they were the primary function of the control application and because they required the highest frequency of execution in order to yield smooth and accurate control of the patterning process. Most of the control buttons from the GUI, keyboard, and control pad were handled by an event structure enclosed in a timed loop (shown in Figure 4.13 as the Operation Loop).

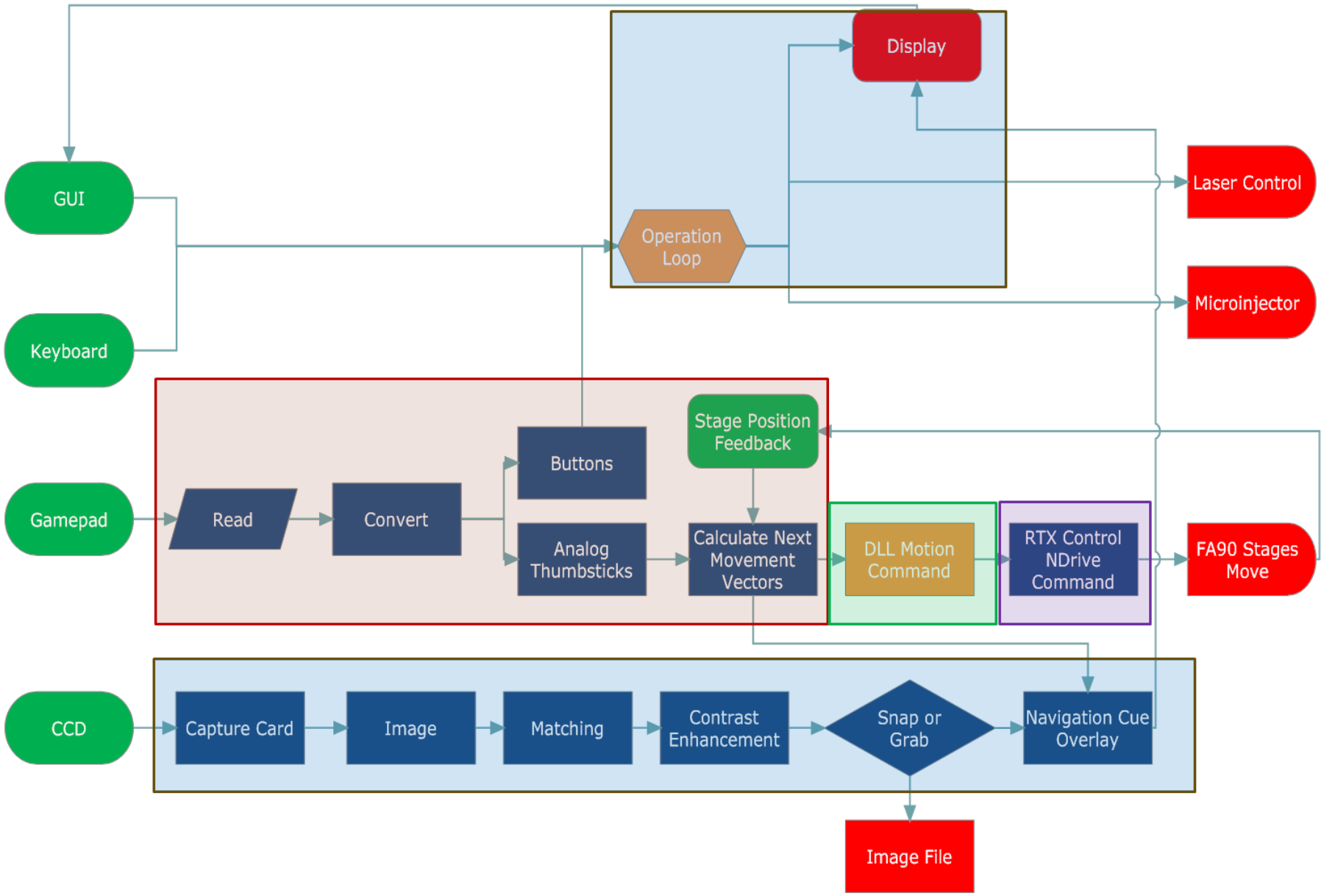

Figure 4.13: Laser cell patterning system control application flow chart. The shaded boxes surrounding operations depict a single processor core on which the operations are executed.

Programming - VISA for control of serial instruments

VISA is a standard I/O language for instrumentation programming. LabVIEW implements VISA for programming serial instruments (RS232). VISA is a simple object oriented language and the commands to the laser and the microinjector were easy to implement. However, improper programming, such as inappropriate opening and closing of the VISA instruments was found to be a major source of program instability and caused many communication errors with Aerotech NDrives. The instruments had to be set up in the NI Measurement and Automation explorer. The computer used in our setup had only one onboard serial port so a USB-serial port adapter was used to communicate with the microinjector. It was important to keep the USB-serial port adapter plugged into the same USB port at all times, otherwise the com port number would change and the instrument would have to be setup again in the Measurement and Automation Explorer to work with the control software.

Programming - Reading and interpreting game pad

Microsoft Windows® XP includes the winmm.dll file which can be used to query the state of any joystick or gamepad configured in Windows. Using the “joyGetPosEx” call of this dll would return a cluster of binary strings named dw*** for the relevant thumb stick or button data. This cluster was separated and the thumbstick data was normalized while button data was read into appropriately labeled Boolean variables. The thumbstick values which were now normalized between values of -1 and 1 for the X, Y and Z axis. This axis could be inverted by a GUI control in case the setup of the stages changed. Because the thumbsticks did not reliably come to rest to a specific point in the

center when released a ‘dead zone’ was implemented which was an area in the center for which all values remained zero. This was achieved with a simple ‘if’ or case statement. At the end of the dead zone to the furthest deflection of the thumbstick values increased in a cubic fashion so that finer control was available in the center and increased speed was available at the furthest deflections.

Programming - Navigation system

The navigation system drew input from a marked point deposition point, and the current position of the 3-axis stage. Using these coordinates a vector was computed, normalized and used to create a direction indicator line which was overlaid onto the chamber image before it was displayed in the GUI (Fig x). When the target deposition point was within 80µm in X and Y the line was replaced with a circle centered on the deposition point to avoid obscuring the view of the deposition point.

Programming - Image Capture

Image capture was performed with an NI1407 capture card which, because it was manufactured by National Instruments, was highly compatible with LabVIEW and easy to command with LabVIEW’s IMAQ functions and the Measurement and Automation Explorer. The NI1407 card was configured in NI Measurements and Automation explorer under Devices and Interfaces/IMAQ devices. This is where the interface name was set, which is how the card was referenced in the LabVIEW program. Additionally this is where the acquisition parameters were set including the acquisition window height and width, and the black and white reference levels. These attributes could not be set in the

LabVIEW workspace or the running application. If the image was too bright or dark the configuration of the capture card had to be reset to obtain the best image visibility.

In the LabVIEW program image capture started with the 'IMAQ Init.vi' using the NI1407 interface name (img0). A temporary memory location was created (IMAQ Create.vi) and a grab acquisition set up (IMAQ Grab Setup.vi) outside of the imaging timed loop structure, causing it to happen once at the program startup. These settings were run into a flat sequence structure with in the imaging timed loop structure where the first function was an image grab (IMAW Grab Acquire.vi) completing image capture. The image was further processed, overlaid with navigation cues, and recorded.

Programming - Image Processing

The image was processed in several ways to enhance the image for patterning and improve video quality. While the imaging optics were cleaned, the large number of filters in front of the CCD tended to make a perfectly dust free image unlikely and temporary. As such, to remove the image artifacts created by dust particles a matching algorithm was used. First an image was captured with the substrate far out of focus so the only visible things were dust particles. This image was saved as default file "baseline.bmp" which was loaded during the applications startup. This image was converted to an array, and the average value of elements was computed, then each element was subtracted from the average, this new array was then added to the incoming image converted to and array and then re-converted to an image. This removal of baseline artifacts could be switched on or off, and that option was carried through the rest of the image stream.

It was easier to recognize cells, which often appeared very faintly, by increasing the contrast of the image. Towards this end a BCG (brightness, contrast, and gamma) table could also be engaged. The values of the BCG table were configurable from the front panel (GUI). From here the image was sent to the recording functions.

Programming - Image Recording

Video footage of early experiments was captured on a different computer because of the processing requirements and lack of recording software. The entire patterning process had to be recorded, generating hours of footage and tens of gigabytes of data then needed to be sorted. With the introduction of multicore processors it became possible to perform this process to the patterning computer. We implemented an in-program recording facility which would allow for quick and on-demand capture of single frames/images (snap) or short lengths of video (grab). With the previously implemented image acquisition stream saving an image with IMAQ write.vi was simple. To record lengths of video an AVI had to be created, individual frames written and eventually closed, each as a separate step enclosed in a case structure as the entire sequence was part of a loop.

Stage Programming - Aerotech calls

There were two modes of speaking with the Aerotech stage, a queue mode or a queue free mode. The mode was set during the application and the stage initialization, and could be changed at any time. In the queue free mode every motion command was immediately issued to the stage and the previous commands were aborted in contrast to

queue mode in which successive commands were added to a stack and the stack dequeued from the bottom. In order to achieve smooth navigation with the controlpad the queue free mode was used. To recall specific points on the substrate automatically, the queue mode was used. There was another option of modes which was important in controlling the stage; Absolute or Relative modes when describing a movement and whether it should refer to an absolute position in space, or a movement relative to the current position. The Absolute mode was called with AerQueMoveAbs when a specific point needed to be recalled. Finally, the AerParamGetValue command was important for reading the current position of the stage.

Programming - Graphical User Interface

The graphic user interface (GUI) is shown in Figure 4.14. The 'front panel' as it is referred to in LabVIEW contains labeled controls and indicators linked to the features described earlier in this section.

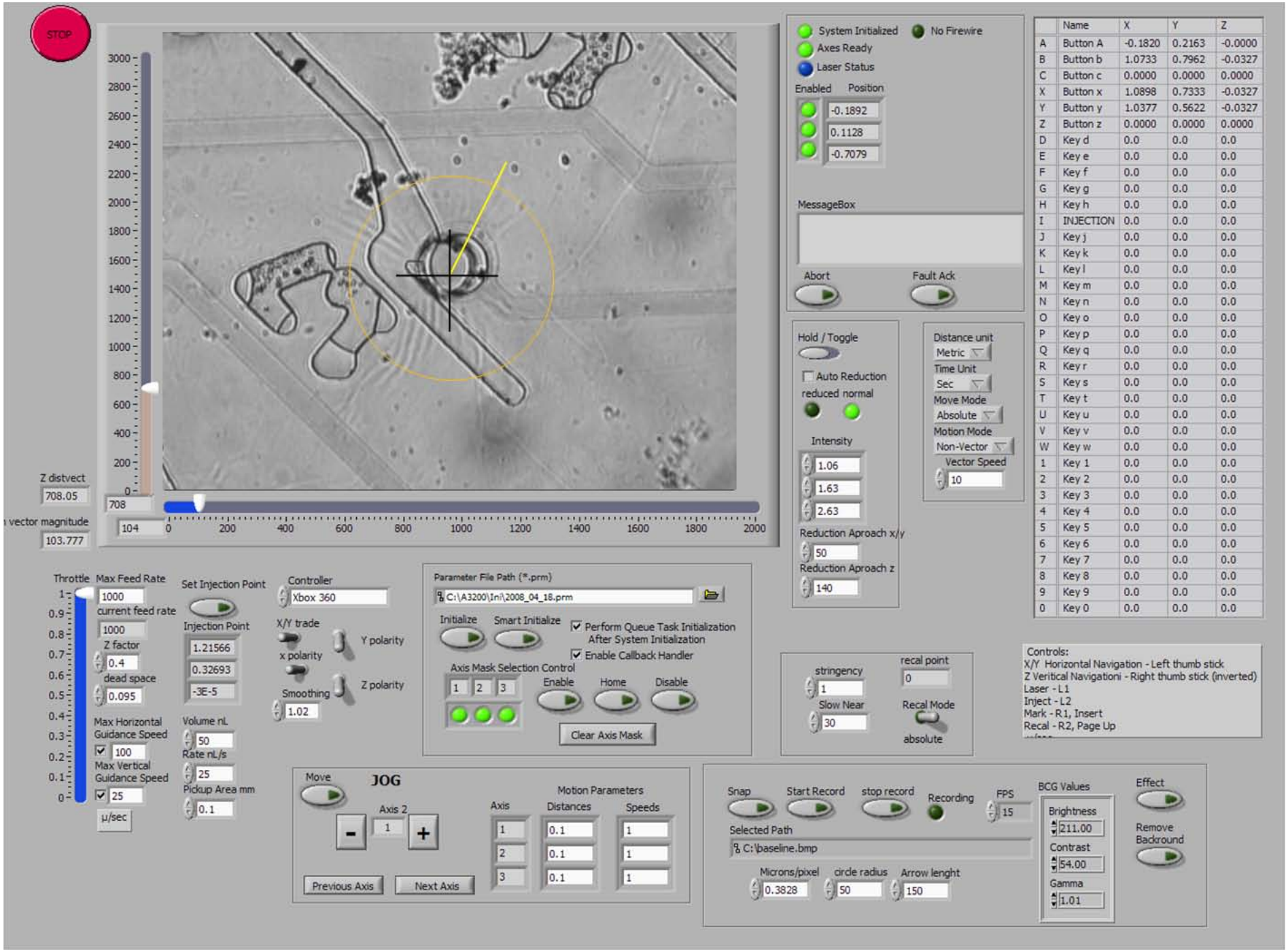

	Name	X	Y	Z
A	Button A	-0.1820	0.2163	-0.0000
B	Button b	1.0733	0.7962	-0.0327
C	Button c	0.0000	0.0000	0.0000
X	Button x	1.0898	0.7333	-0.0327
Y	Button y	1.0377	0.5622	-0.0327
Z	Button z	0.0000	0.0000	0.0000
D	Key d	0.0	0.0	0.0
E	Key e	0.0	0.0	0.0
F	Key f	0.0	0.0	0.0
G	Key g	0.0	0.0	0.0
H	Key h	0.0	0.0	0.0
I	INJECTION	0.0	0.0	0.0
J	Key j	0.0	0.0	0.0
K	Key k	0.0	0.0	0.0
L	Key l	0.0	0.0	0.0
M	Key m	0.0	0.0	0.0
N	Key n	0.0	0.0	0.0
O	Key o	0.0	0.0	0.0
P	Key p	0.0	0.0	0.0
Q	Key q	0.0	0.0	0.0
R	Key r	0.0	0.0	0.0
S	Key s	0.0	0.0	0.0
T	Key t	0.0	0.0	0.0
U	Key u	0.0	0.0	0.0
V	Key v	0.0	0.0	0.0
W	Key w	0.0	0.0	0.0
1	Key 1	0.0	0.0	0.0
2	Key 2	0.0	0.0	0.0
3	Key 3	0.0	0.0	0.0
4	Key 4	0.0	0.0	0.0
5	Key 5	0.0	0.0	0.0
6	Key 6	0.0	0.0	0.0
7	Key 7	0.0	0.0	0.0
8	Key 8	0.0	0.0	0.0
9	Key 9	0.0	0.0	0.0
0	Key 0	0.0	0.0	0.0

Figure 4.14: Graphical user interface of the laser cell patterning system's control application.

Control System - Automation

While the control application did automate some processes including automatic reduction of laser intensity and position recall, which was used to bring the injection point into view when a cell was injected, overall automation of the entire cell patterning process was never implemented. A semi-automatic patterning mode was attempted but ultimately abandoned. Though the patterning process was made to be very user friendly, it would be best if user control was not necessary to place each individual cell on every electrode.

We tried to implement a semi-automated cell deposition algorithm with some success. Under the semiautomatic mode, the control software used visual feedback to ensure that the cell was guided toward the destination point at maximum speed without moving the laser so quickly that the cell was dropped. During a normal recall operation without visual feedback when a cell was dropped the laser would continue on toward the destination point leaving the cell floating freely in the area where radial trap and axial guidance were lost. Visual feedback was used to keep the distance between the cell's centroid and the laser beam's center just less than the optimal distance, D. D was the distance from the

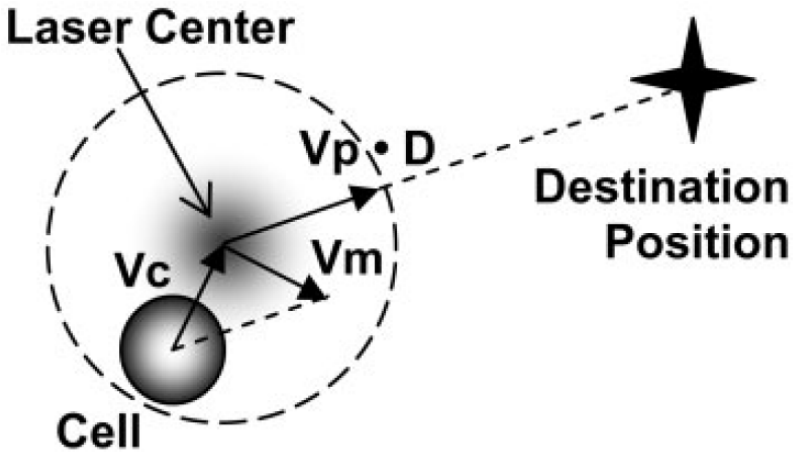

Figure 4.15: Illustration explaining the automation algorithm.

cross-sectional center of the laser beam (where the cell experienced a zero net radial force) to where the cell experienced a maximum net radial force. This value arose from the Gaussian profile of the laser beam and was determined experimentally, as discussed in optical traps [15]. The system computed a normalized vector Vp based on the real world coordinates of the stage from its current position to a marked destination position (Figure 4.15). The vector Vc extended from the cell center to the laser center and was based on the pixel coordinates. For ideal guidance, Vc multiplied by the micrometer/pixel ratio (0.46) should equal Vp. However, because Vc was always decreasing when there was no movement of the stage, and because of turbulence inside the chamber from thermal effects, the difference between Vc and Vp was computed and this vector, Vm, was issued in the stage's motion command, at a speed equal to the magnitude of the vector divided by the refresh rate of the entire process (about 200 ms). While this algorithm did not perfectly align the cell and laser in the direction of the destination point, it had the advantage of requiring much less processing than converting pixel coordinates to actual real world coordinates, and provided a smooth and efficient guidance motion. As the stage got nearer to the target position, a deceleration multiplier was used to reduce the magnitude of the motion vector, allowing the cell to catch up with the laser center as it becomes centered on the programmed deposition point.

The image recognition algorithm used to find the cell centroid began with a high-pass fast Fourier transform (FFT) to remove gradual variations in image brightness. Next in the processing sequence was an erode function followed by a circle finder function, both of which were available in the LabVIEW Vision Development Module. The circle

finder function was tuned find all the round objects between 7 and 12 um in diameter (the healthy size of chick forebrain neurons) though this could be changed for proper recognition of different cell types. Next the algorithm would select the round object which was nearest to the center of the field of view (where the laser guidance region was) and move the laser to that point.

Because of slight inconsistencies in the chamber mounting such as different chamber walls and slightly un-level chamber assemblies, the laser focus could vary for each patterning session by as much as 20 um. This required a rough mechanical adjustment of the CCD camera, and a finer calibration of the laser point. This fine calibration was performed by capturing the closest cell, and once trapped, marking that cell's centroid as the laser center. Using the image coordinates of the computed centroid of a currently patterned cell and the saved coordinates of the laser center a vector between them could be computed (Figure 4-15).

Because the patterning process was imaged perpendicular to the substrate plane (axis X and Y) the cells position in Z was not recognized and its guidance had to be manually controlled. Other options such as a set vertical guidance speed, or a focusing algorithm based on sharpness and or changes in circle size were not accurate enough to keep the cell in the guidance region.

Additionally, there were constant image irregularities (large bright or dark spots which occluded the image of the cell) present in the chamber arising from surface and suspended debris, accidental air bubbles, accumulated cells, and the refractive qualities of microstructures in the elastomeric membranes. These were so frequent, and in the case of

elastomeric membranes, unavoidable that a fully automated system was judged too intensive and outside the scope of this research. We believe a dedicated PhD project would be needed to develop the machine vision and image recognition technology to achieve full automation of the laser cell patterning process.

Cell Culture

Truly, one of the biggest concerns with any cell biology experiment is keeping the cells healthy and viable. Manipulations to cells such as laser patterning can reduce viability and increase the time before a cell is plated. Additionally a process such as laser pattering, live cell microscopy, or electrophysiology can increase the probability of contamination. Additionally, we aimed to culture neurons at a density well below the standard minimum density of 10,000 cells/cm^2. Finally, the substrates required modification to promote cell attachment, survival and neurite outgrowth. In this section we will discuss the cells used and their culture mediums. Because of its importance to culturing in elastomeric membranes, surface modification will be discussed in that section.

Cell Culture - Cell source

Aim one was focused only on creating the defined neuronal circuits and throughout this aim only chick neurons were used. This allowed for experiments to be performed on a daily basis.

Cell Culture - Primary Forebrain Neurons

Forebrain neurons were harvested from day 7 embryonic white leghorn chicks. Fertilized eggs were obtained from the poultry farm and kept at 4°C for up to 1 week before being placed in the incubator. Hovabators™ equipped with automatic egg turners and air circulation fans were used to keep the eggs between 37°C and 39°C. On day 7 eggs were wiped down with 70% ethanol, the top of the egg was removed with large forceps and the chick embryo removed. The chick was decapitated and the head was placed in a 35mm dish with a shallow later of sterile PBS. The neck was clipped of close to the skull and the head was flipped upright. Curved #7 forceps were used to pinch-clip the skin over the brain remove it. The forceps were then used to pinch and scoop the two frontal lobes. The lobes were then moved to a separate dish where the meninges was removed so that the remaining tissue was pure white. The tissue was then placed in a 1mL tube filled with .1% Trypsin EDTA, inverted twice and incubated for 5 minutes. After five minutes the Trypsin was removed and 1mL of media with 10% serum was added, the tube was closed and inverted twice and the media was removed and replaced with culture medium. The tissue was then triturated up to 10 times with a 21G needle and syringe with care not to create bubbles. The cells were then counted and used. Cultures were incubated at 37°C and 5% CO_2.

Cell Culture - Establishment of Astrocyte Cultures

The protocol for astrocyte cultures presented here is based upon [171]. Astrocyte cultures were derived from day 14 chick embryonic cerebral hemispheres (E15CH). Eggs were wiped down with 70% ethanol and the top was removed. The embryo was removed

from the egg and decapitated. The skull was opened with serrated scissors and the cerebral hemispheres were removed. The cerebral hemispheres from up to 3 chicks were broken into fine pieces with two pairs of forceps. Next these pieces were mechanically dissociated by sieving through a nylon mesh (73μm pore diameter) into Media 199 containing 10% fetal bovine serum (FBS). The cell suspension was plated in a T150 flask. Cultures were grown at 37°C and 5% CO_2. After 3 days the media was replaced with additional media changes every 3–4 days. Only a small fraction of the cells (<1/10) survived 24 hr after dissociation and were attached to the plastic substratum. Cultures reached confluency after 1-2 weeks at which time they were used to condition media for 3-4 days. After 3-4 days in of confluency the cells were passaged by dissociating with .25% Trypsin EDTA for 5minutes, neutralizing with normal glial media. They were then spun in a centrifuge at 1000rpm for 6 minutes. The supernatant was removed and the cells were re-suspended in 1ml of glial media. A fraction of these cells were re-plated in T-150 flasks while the rest were cryogenically frozen for later use. 1ml of a concentrated cells suspension in 50% FBS 10%DMSO were slowly frozen in a 2ml freezing vial and kept at -80°C for up to 3 months. Thawing and resuspension of cells was performed by quickly thawing the 2ml tube in a 37°C water bath just until liquid, but still cold. 1ml of glial media was added to this drop-wise. The 2ml was transferred to a 15ml conical tube and 8ml of glial media was added. This suspension was centrifuged at 1100rpm for 6 minutes, the supernatant removed, and 10ml of fresh glial media was added. After a gentle trituration this media was added to a T150 flask and placed in the incubator.

Astrocytes cultures were kept to condition media as well as with the intent for use in later heterotypic neuronal circuits. High purity astrocyte cultures were obtained by passage 3[172]. Astrocytes were discarded after passage 4 as their ability to produce astrocytic factors was questionable[173].

Cell Culture - Media

The media used for culturing and patterning neurons was conditioned by astrocytes. The preconditioned medium was comprised of Neurobasal™ (without l-glutamine or phenol red) supplemented with 1x GlutaMAX™ (Gibco) 1% antibiotic/antimycotic (10,000 units/mL penicillin G sodium, 10,000ug/mL streptomycin sulfate) 50µg/mL Gentamicin and 2.5µg/mL Amphotericin. When astrocyte cultures reached confluency they were switched to this serum free, preconditioned media for 3 days. 20mL of preconditioned medium was added to T150 flasks with confluent astrocyte cultures. The media was removed 24 hours later and added to a 250mL bottle of frozen conditioned media and returned to the freezer. When a bottle was filled it was thawed and filtered with .22µm filter and aliquotted into 50mL tubes and refrozen. As needed 50mL tubes were thawed and 2% B27 and 100ng/mL NGF 7s was added to create the a finished neuron culture media. The astrocyte conditioned media critically improved neuron survival at low densities (as low as 10cells/cm2)

Base media:

Media 199 without L-glutamine or phenol-red

5% fetal bovine serum

0.5 % (1x) GlutaMAX (L-glutamine substitute)

2% B27 neuronal supplement

100 ng/mL NGF

1% antibiotic/antimycotic

50ug/mL Gentamicin

2.5ug/mL Amphotericin

The other medium used in our experiments, referred to as glial media, was comprised of Media 199 (without l-glutamine or phenol red) with 10% fetal bovine serum with 1x GlutaMAX™ (Gibco) 1% antibiotic/antimycotic, 50µg/mL Gentamicin and 2.5µg/mL Amphotericin. This media was used to plate and grow astrocyte cultures to confluency, as well as to rinse brain tissue after digestion with Trypsin.

Serum free glial conditioned media:

Neurobasal without L-glutamine or phenol-red

0.5% antibiotic/antimycotic

0.5% Gentamicin

0.5 % (1x) GlutaMAX (L-glutamine substitute)

After 24 hours on confluent culture of glial cells

Freeze

Filter .2µm filter

Add 2% B27 neuronal supplement

100 ng/mL NGF

Laser Cell Patterning Process

The step-by-step process of assembling the laser deposition chamber and patterning cells using the laser cell patterning software control application is described in Appendix A and B respectively. Generally, 25-100nL volumes of cell suspension were injected into the chamber by the microinjection system to an area near (Z<1000µm, XY<2000µm) but not directly above the desired deposition point. Some clumping could occur while cells were sitting in the syringe and injection fiber and these clumps should not fall into the desired deposition area. Single, round, dark cells were selected from the injected suspension and manipulated at about 150µm/s horizontally and 25 µs vertically toward electrodes and/or microwells of the substrate. Rows were patterned at once, from the closest to the farthest from the injection point. The microinjection fiber was inserted or withdrawn from the chamber every 2 to 3 rows in order to keep minimize the distance (and time) between the microinjection point and the target positions on the substrate. Each cell took between 30 and 45seconds to guide to a point on a substrate. However, injection and finding healthy looking, single cells added to the overall pattern time. The overall average time to pattern a cell was closer to 90 seconds.

Laser Cell Patterning Process - Post patterning

After patterning the chamber was sprayed with 70% ethanol or Enivrocide™ and wiped down. The microwells of the membrane protect the cells from being washed out by movement, so the patterned substrate may be immediately removed from the chamber. After removal form chamber membrane bound coverslips were placed in 35 mm dishes (if not already in a dish) prefilled with 2mL of culture media. MEAs were placed in MEA

boxes and media was topped off. Patterned substrates were then incubated at 37°C and 5% CO_2. Cells were kept inside custom made boxes with FEP film tops which allowed for the exchange of gasses ($C0_2$ and 0_2) but retained water. A small container of water with AquaClean (Wak-Chemie®) was kept inside these boxes. This was especially important because some of the MEA cultures had very low volumes of media which were otherwise prone to dehydration. Furthermore, it allows for increased isolation, and more sterile transport between the incubator and the bio-hood or microscope.

Results

Accuracy of Laser Cell Deposition System

To calculate the accuracy of the laser deposition system, we patterned rows of 8-µm diameter polymer microspheres rather than cells because they had a more uniform shape and size which allowed for more accurately pinpointed centroids. The beads where

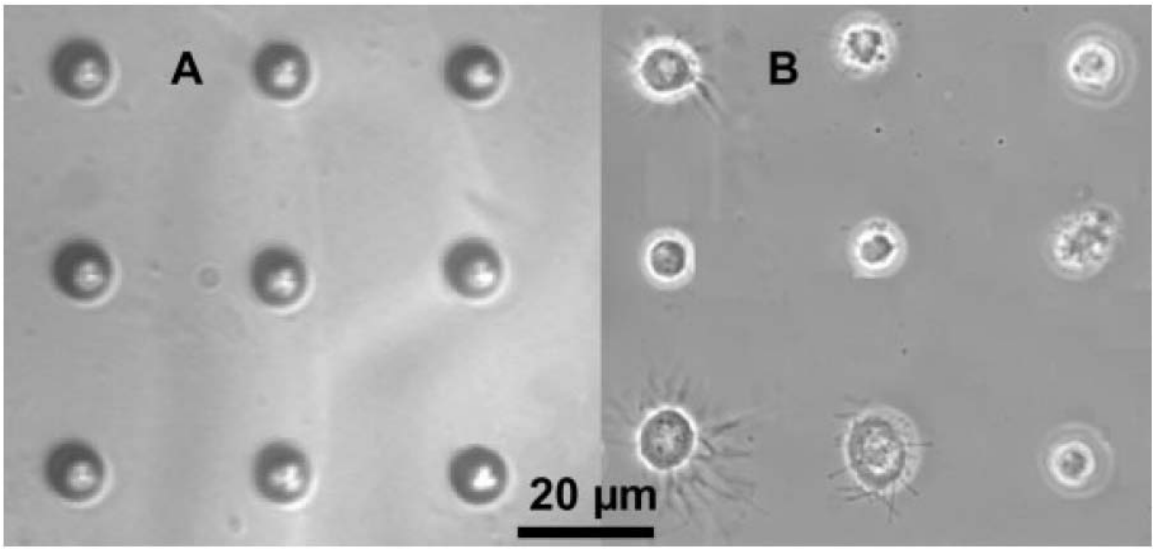

Figure 4.16: Examples of patterning accuracy. A) 8µm polymer microspheres patterned with the laser cell patterning system in a square array. B) Chick forebrain neurons patterned with the laser cell patterning system with the same square pattern.

patterned every 100μm and the resulting 10-bead pattern was imaged and analyzed. The average distance between spheres, from centroid to centroid was 100.0 ± 0.9μm, yielding an accuracy of less than 1μm. By repeatedly depositing beads into the same location, we obtained that the spatial accuracy for a single guidance was better than 1/10 pixel (0.46 μm/pixel for that setup). This accuracy and precision is far beyond the error imposed by cell irregularities and cell migration. Furthermore, the substrate features which are the target of our pattering process in this research were 30μm diameter electrodes.

Results - Viability of Laser Patterned Neurons

During early development and testing the laser pattering system judgment of viability was briefly assessed to ensure the method was suitable and warranted continued development. The viability of neurons patterned with similar IR and near IR lasers had been demonstrated by other groups[109] as discussed in chapter 2. Observing cells within four hours of patterning was used to demonstrate not only the accuracy of the system but also the viability of patterned cells. We deemed the extension of neurite outgrowth by phase microscopy sufficient to show the viability of neurons. Long term viability was difficult to address because of the nearly guaranteed migration of the cells. Until a means of confinement or tracking was developed further assessment was not possible. Additionally, viability of the laser patterned neurons and DNA damage were assessed by a co-worker, Tabitha Rosenbalm, and presented in her master's thesis. She exposed neurons trapped in agarose gels the laser radiation normally used for patterning and assessed outgrowth and DNA damage using COMET assay.

Results - Cell types and cell patterns

The laser cell pattern system was used to pattern multiple cell types and created various cell patterns; it was also used to patter growth factor encapsulated microspheres.

Results - Astrocyte Culture Purity

In order to ensure a high probability of patterning a true astrocyte during the single cell heterotypic neuronal circuit experiments the astrocyte cultures were evaluated for purity. This was done by re-plating a small fraction of astrocytes in a standard 35mm polystyrene dish with at a density that allowed individual cells to be easily identified. These cells were allowed to attach for 4 hours and then fixed with 4% formaldehyde and 1% glutaraldehyde in 0.1 M Phosphate Buffer (PB) (pH 7.4) for at least 2 hours at room temperature or overnight. This plate was then immunocytochemically stained with a primary antibody for Glial Fibrillary Acidic Protein (GFAP)(MAB360, Millipore), and Alexa Fluor 488 Donkey anti-mouse

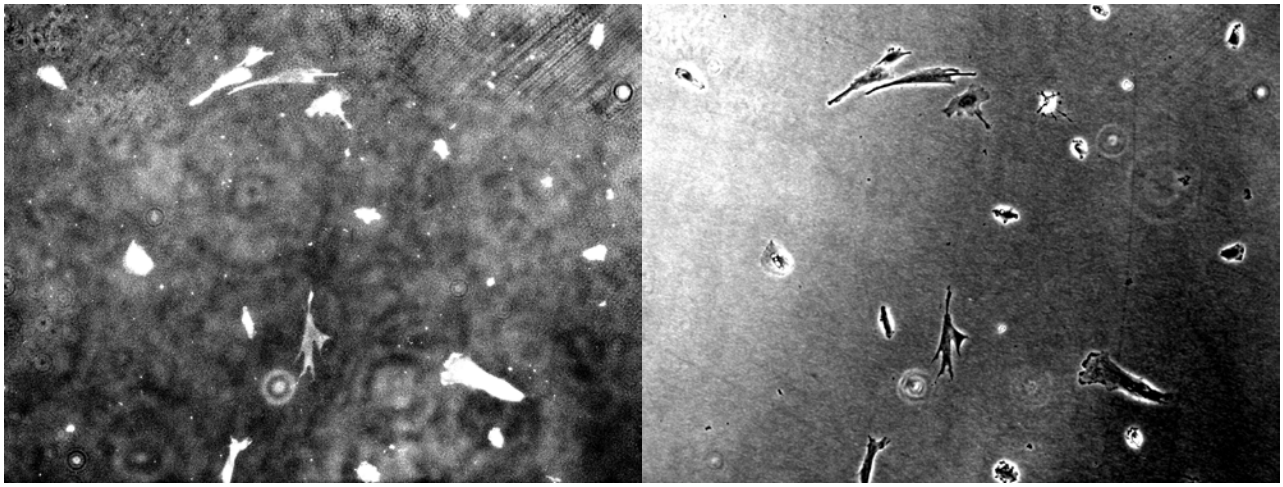

Figure 4.17: 10x micrographs of first passage astrocytes stained for GFAP. a) fluorescent image showing GFAP positive cells b) Phase image showing all cells.

secondary (Molecular Probes A21202). A 10x micrograph with a field of view covering a 600µm x 1200µm area of the culture was taken under phase microscopy and fluorescent microcopy. Approximately 100 cells were imaged in this area and the fraction of GFAP positive cells over phase contrast identified cells was recorded. After the first passage cells were nearly 100% pure astrocytes (Figure 4.17).

Results - Laser Patterned Fibroblast Bridge

As the Laser Cell Patterning System was developed it was continually applied to various research projects which were also used to test its ability and aid in developing a widely applicable research tool. One example was its use in building a bridge of fibroblasts between two 'islands' of cardiomyocytes. This was done to test the distance

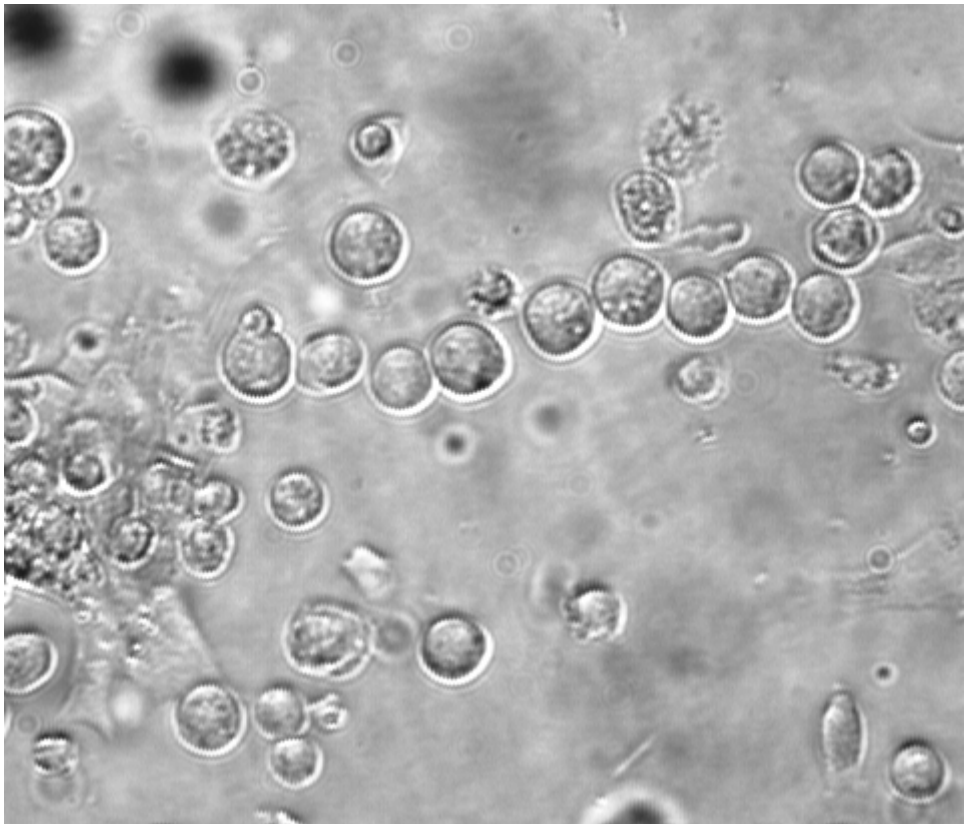

Figure4.18: Fibroblast bridge between two cardiomyocyte 'islands'.

over which fibroblasts could synchronize the beating of the two groups of cardiomyocytes by electrical signal conduction. This application is illustrated in Figure 4.18. The application illustrates the ability of the system to deposit cells to areas specific, but not predetermined points on the substrate with high resolution. It also demonstrated the temporal precision of the system, and how it can be employed in cell biology research.

Results - Laser Patterned Line of Pectoral Myoblasts on MEA

In early attempts to create a simple but fully closed neuronal circuit we attempted to build an on-chip reflex arc. For these experiments pectoral myoblasts were harvested from day 12 embryonic chicks and patterned in a line between two electrodes (Figure

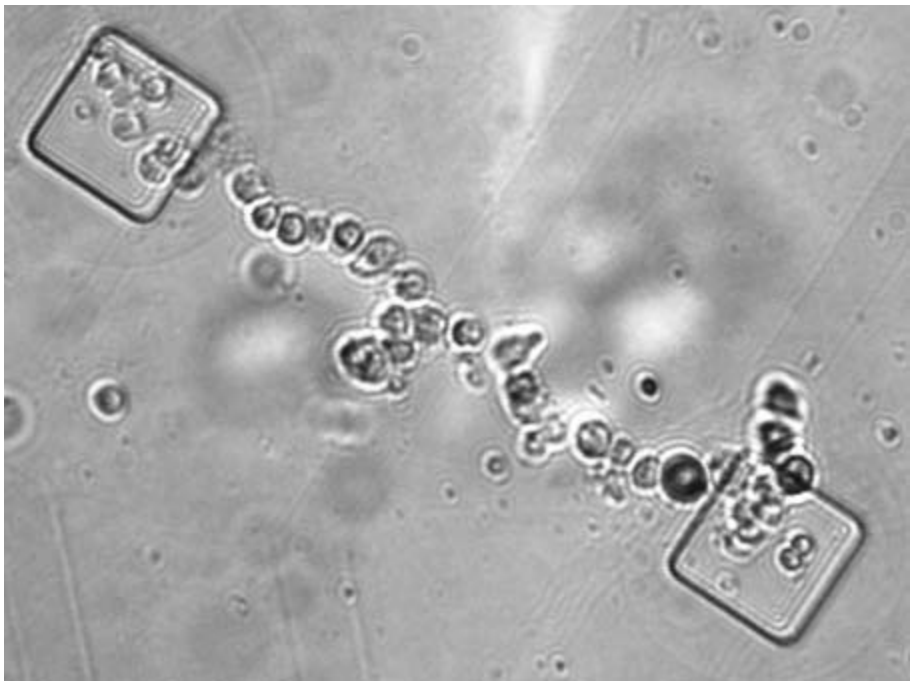

Figure 1-1: A line of Pectoral Myoblast cells patterned across two electrodes of an MEA.

4.19). This early application demonstrated the additional need for some form of restriction (i.e. elastomeric membranes) as the cells would clump into an island rather than fusing to form a myotube.

Results - Laser Aligned Adult Cardiomyocytes

Another unique application of the laser patterning system was for patterning and aligning rod-shaped adult cardio myocytes. Adult cardiomyocytes are rod-like cells about 150µm in length and 30-50µm in diameter. In vivo these cells have a very organized structure, one that is difficult to recreate after dissociation. The laser cell patterning system because of the weakly focused laser's axially elongated (200µm) guidance and

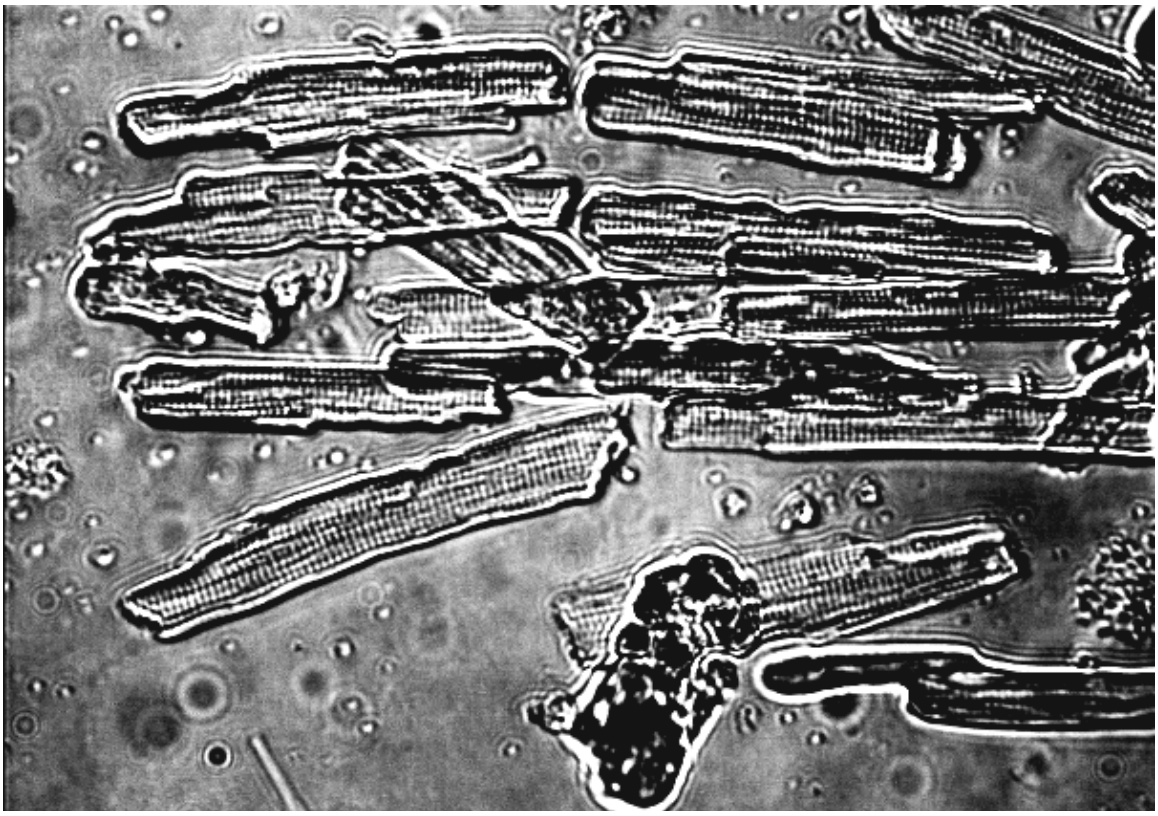

Figure 4.20: Adult cardiomyocytes aligned side by side.

trapping region could be used to manipulate the cells into a vertical column and guide them to the substrate. Once the bottom end of the cell made contact with the substrate the laser was used to pull the cell in a specific direction as it was pushed flat onto the substrate. In this manner the rod-like adult cardiomyocytes could be aligned side by side (Figure 4.20**)** and end to end (Figure 4.21).

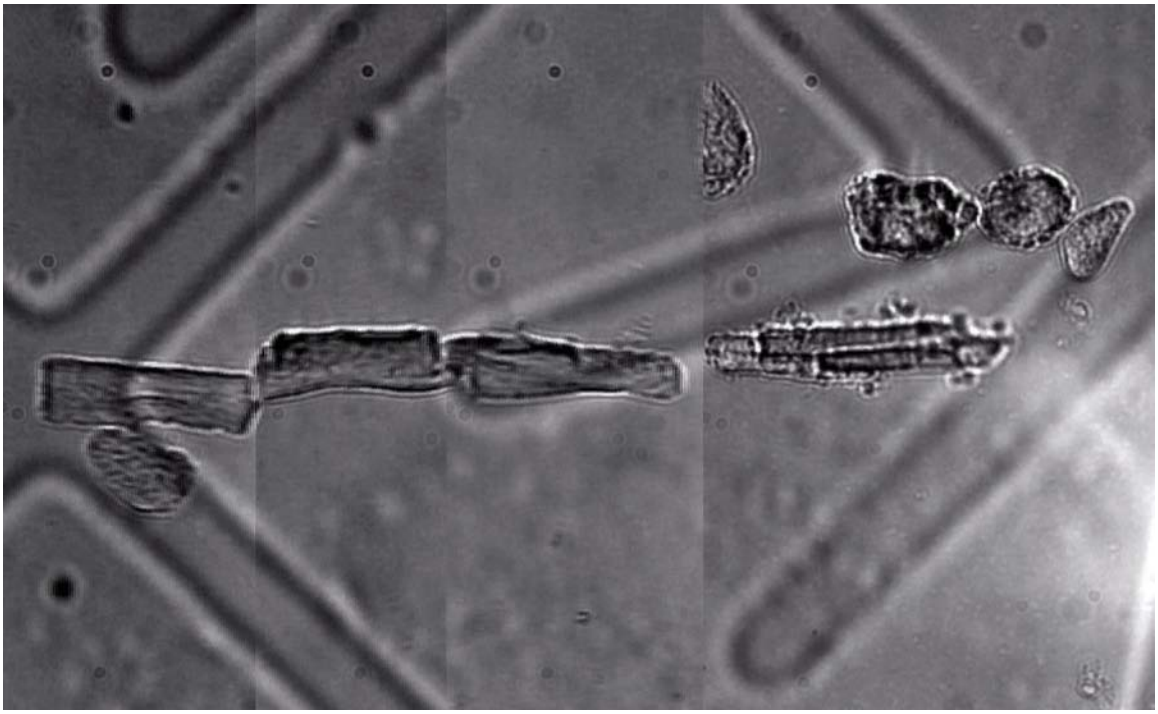

Figure 4.21: Adult cardiomyocytes aligned end to end.

CHAPTER V
MICROFABRICATION FOR CIRCUIT DEFINITION

Introduction

Physical confinement and restrictive guidance imposed by a 3D construct is a simple and highly effective method for patterning cells and controlling axon outgrowth[105, 174, 175]. The only example of single-cell-resolution neuronal circuits to date employed channels and microwells etched in agar[21] to confine and direct neurite outgrowth. We have chosen to use PDMS elastomeric membranes with microwells and microtunnels for this purpose. PDMS is biocompatible, reusable, transparent, and increases the signal to noise ratio of electrodes[20]. The elastomeric membranes are very similar to and fabricated using the same techniques as microfluidic devices.

Materials and Methods

Microfabrication - Design

Design of the elastomeric membranes was based on a simple system of microwells connected by microtunnels. The microwells would keep neurons patterned to the electrodes of an MEA from migrating off the electrode. The microtunnels would restrict neurite outgrowth from neurons along a specific path to adjacent neuron/microwell/electrode targets. The microwells and microtunnels were created when an elastomeric membrane with clear-through holes and shallow channels was aligned and a attached to an MEA. As long as the elastomeric membrane is firmly sealed to the MEA all neurite extension will be restricted to the tunnels defining interneuron connectivity. Based on publications dealing with geometric guidance of neurite outgrowth[174, 175],

two different designs were proposed which were intended to influence neurite polarity as well imposing direction. These designs were created with the goal of overcoming the resolution and feature size limitation of our photolithography process, which could only produce channels as narrow as 8 microns across. Such a wide channel width could not be used as a barrier to cell migration. Instead, the tunnel height was made shallow enough (<3μm) to keep the neurons from moving from the microwell into the microtunnel (Figure 5.1). The “directed” design is composed of rows of clear through holes connected by tapered channels as seen in Figure 5.2. In the “snag” design (Figure 5.3) the tapered channels end in a sharp turn, which may reduce the probability of a neuron extending its axon in the wrong direction. With higher resolution features, the tapering could be more drastic and probably more effective. Finally, once some experiments were carried out and we began to understand more about the limitations of the microfabrication system a final microstructure design intended to influence polarity was developed. This "hook" design is shown in Figure 5.4.

Microfluidic channels in the elastomeric membranes were used to flow surface modification solutions, culture media and experimental factors into the microwells and guidance channels. This allows for neuronal survival at the very low culture density required to achieve a one-to-one neuron-electrode ratio and completely identified connections.

Figure 5.1: Elastomeric membrane. The Microwells confine the neurons the short microtunnels allow only the neurites to pass through.

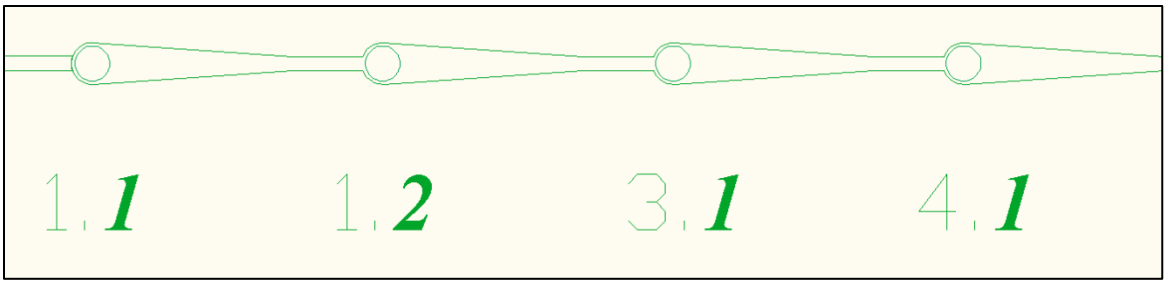

Figure 5.2: Original "Directed" microstructure design. At the narrowest point the channels are 8-10µm in diameter.

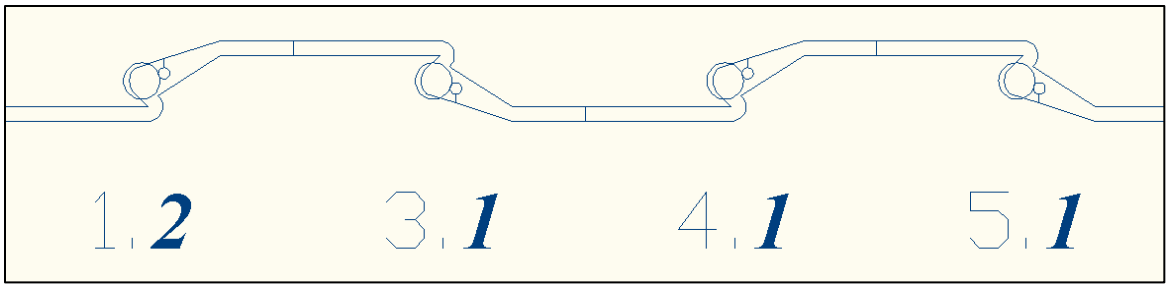

Figure 5.3: "Snag" microstructure design intended to induce polarity by hindering neurite outgrowth in the backward direction via a sharp angled turn. However, misalignment of the circular micro wells could easily overwrite the sharp angles of the first layer.

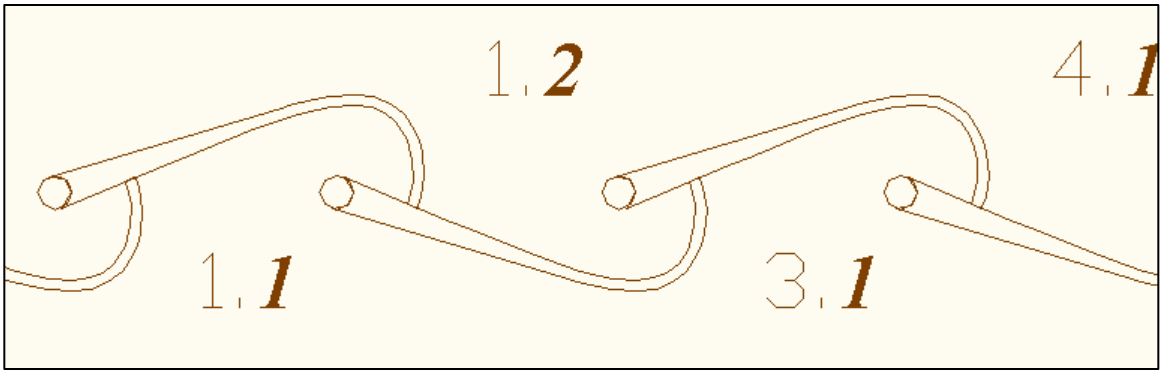

Figure5.4: "Hook" microstructure design. In this design the microwell is distanced from the sharp angled meeting of microtunnels, eliminating the chance of overwriting. However, the path of the presynaptic neuron 1.1 takes when it converges with the microtunnel of 1.2 is uncertain. This is the type of scenario that can be studied with the microstructure and laser cell patterning systems.

Microfabrication - Photolithography

The elastomeric membranes were made by curing PDMS on rigid silicon molds. The silicon molds were created using standard photolithography techniques with 2" mechanical grade polished silicon wafers, SU-8 (2000.5,2005,2025,2050) negative photoresist, a Laurell WS-400B-6NPP/LITE spin coater and a Suss MJB-3 microaligner with 200W lamp house. With these materials it was possible to create molds with short (<2 μm) channel features and strong 30-60 μm tall posts.

Microfabrication - Photolithography Masks

The masks which were used to selectively block the UV radiation from the mask aligner and UV lamp were designed in AutoCAD™ and laser photo-plotted by CAD/Art Services, Inc. Laser photoplots were much cheaper than traditional chromium masks allowing for frequent modifications of elastomeric membrane designs. The drawback was that the resolution of the masks was limited to 8-10μm for the smallest feature. When using photoplots the emulsion side was placed downward in immediate contact with the photoresist coated wafer to obtain the best resolution. If a design was intended to align to a certain layout, as was the case with membranes aligned to the electrodes of the MEA, it was important to make sure that the layout correctly oriented and that the desired emulsion side be specified to enable proper alignment. For the multilayer molds needed to form shallow channels and deep holes an alignment guide was added around the outside of every mask design (Figure 5.5). The alignment pattern included an outline matching the shape of the 2" wafer which was helpful in quickly making a rough alignment. The masks were cut out from the photoplot sheet and attached to 4"x4"x ¼"

soda-lime glass with small dabs of superglue in 4 corners. The masks were cut larger than the 2" wafers to ensure that full coverage was achieved. If a mask only partially covered a wafer it could cause poor leveling leading to poor resolution, or it could scratch the photoresist surface and become stuck, making alignment difficult. Care was taken to avoid contamination of the transparent areas with glue, and to use as little glue as possible to minimize the distance between the mask and the glass. The features which were meant to match the MEA were enlarged by 4.3% in the AutoCAD™ drawing (but not the alignment marks) to account for shrinkage of the PDMS molds during curing.

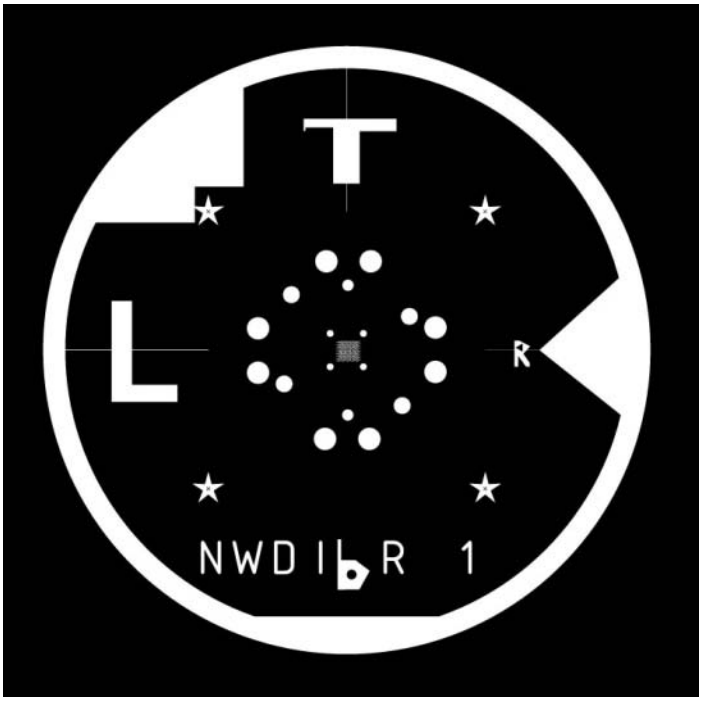

Figure 5.5: Image of a photolithography mask. The actual microstructure design is in the very center with four corner dots surrounding it. The outer circles are holes to vent bubble when attaching the membrane. The larger shapes including stars, letters and lines are the alignment guides.

Microfabrication - Layers Spinning

The protocol for creating a multi-layered silicon mold had many steps necessitated by the limitations in visualizing the exposed features in the photoresist and

by defects in the photoresist. Small air bubbles, dust, scratches, or an 'edge-bead'(an artifact of the spinning process) could case surface inconsistencies which hindered full contact of the photomask or alignment of the photomask. These cause poor resolution, or poor alignment respectively. The first layer created on the silicon wafer was the layer containing the 2-3µm tall features which served as molds for the microtunnels. With the Karl Suss MJB3 aligner it is nearly impossible to discern these features through a second coat of photoresist more than 10µm thick. We experimented with creating a blank alignment layer before the first layer of features, but the inconsistencies present in a thicker (>30µm) layer adversely affected the wafer-mask contact and critically reduced resolution. Table 5.1 shows the multiple layers of a typical mold, their thicknesses and details about their construction including UV exposure, baking and development times.. The procedure for aligning a mask to the previously exposed layers of a wafer is detailed in Appendix C.

Layer	Thickness (µm)	Resist (SU8-)	Spin Speeds (RPM)	Spinner Program
1	2	2002	800/2800	I
2	6	2005	500/1500	C
3	7	2005	500/1000	B
4	20	2025	500/1000	B
5	50	2050	500/2800	I

Table 5.1; Microfabrication Parameters A

Layer	Soft Bake Times (s)	Exposure Time (s)	Post Exposure Bake Times(m)	Develop
1	2/2	23	2/2	Yes
2	2/3	30	3/4	No
3	2/3	25	3/4	Yes
4	2/3	35	3/4	Yes
5	4/9	50	4/10	Yes

Table 5.2; Microfabrication Parameters B

Microfabrication - Exposure

Negative resists such as SU-8 are crosslinked by exposure to UV radiation. The energy required to fully crosslink the resist is related to the thickness of the resist. The specification sheet provided by Microchem for their SU-8 photoresists lists a table of exposure energies (mJ/cm^2) for different resist thicknesses. The power supply/controller for the UV lamp on the MJB3 aligner will keep the output of the lamp at a constant intensity (mW/cm^2). Exposure times are simply computed by dividing the suggested energy by the lamps set output. For best results an overexposure of 10%-50% was normally used. Over exposure ensures full crosslinking and penetration to the bottom of the resist, but can reduce resolution.

Microfabrication - Development

When a layer or several layers were finished, the uncross-linked photoresist was removed by submerging the wafer in developer. Many different chemicals could be used as a developer, we chose MicroChem® SU-8 developer. In the instruction documentation

provided by MicroChem there was a table of layer thickness vs. development time. In our experience we found these times to be much longer than needed. If the mold is exposed to developer for too long (at times listed in the table) there was a tendency for features to separate from the silicon mold and flake off. As such, molds were developed just long enough that no resist is visible on the wafer. At this point the wafer was removed and rinsed one last time with fresh developer, and then both sides were rinsed with isopropyl alcohol. Care was taken to not spray the center features directly as even the force from this rinsing could damage the features. If the isopropanol created a milky residue on the wafer, the wafer required further development. No harm came from rinsing the mold too early, so it was better to observe the milky residue than to develop for too long which could cause flaking of the photoresist from the wafer. Often, an additional 10-30 seconds of development was sufficient to finish development. After rinsing with isopropanol both sides of the wafer were rinsed with DI water. The wafer was then placed back on the 65degree hotplate to evaporate the DI water. This final step was optional unless more layers were to be added. In the case of additional layers, full drying of the mold on the hotplate before adding photoresist was crucial.

Microfabrication - Hard Baking

Though it was not required for SU-8 resists, a hard-bake may increase the strength of a molds features as well as insuring release of any solvents. Molds were hard baked at 137°C in a vacuum oven for at least 4 hours.

Microfabrication - Soft lithography

Soft lithography refers to processes which use lithography via elastomeric (soft) transfer of a pattern. We used the same techniques used for creating the soft lithography stamps to create our elastomeric membranes.

Softlithography - Silanization of Rigid Mold

To aid in the removal of elastomeric membranes from the silicon molds the surface was first silanized. The thin elastomeric membranes were not strong enough to withstand removal without this step. Hard-baked molds were placed in a vacuum desiccator face up. 3-7 drops of 1H,1H,2H,2H-Perfluorooctyltrichlorosilane (PFOTS) was placed in the desiccator and it was placed under vacuum. Once a maximum vacuum (~25 inches) was attained, the desiccator valve was shut and the molds were evaporation coated over night. Usually the vacuum desiccator would lose its vacuum seal by the next day, if not care was taken to slowly bring the desiccator back up to atmospheric pressure as a sudden influx of air would whisk and shatter the silicon wafer inside the desiccator.

Softlithography - Polymer Spinning

Polydimethylsiloxane (PDMS) was obtained as a two-part elastomer, Sylgard™ 184, from World Precision Instruments. The base was mixed with the curing agent in 9:1 (rather than the recommended 10:1) as a higher curing agent content has been shown to be more biocompatible to in vitro cell cultures[100]. To this mixture we added 10% xylene to decrease viscosity allowing more uniform breakthrough clear-through-hole-forming pillars. The uncured PDMS solution was spin-coated onto the silicon molds at speeds sufficient to reduce the PDMS thickness to just below the 40µm posts. The posts were fabricated at this height in accordance with the desired membrane thickness. To

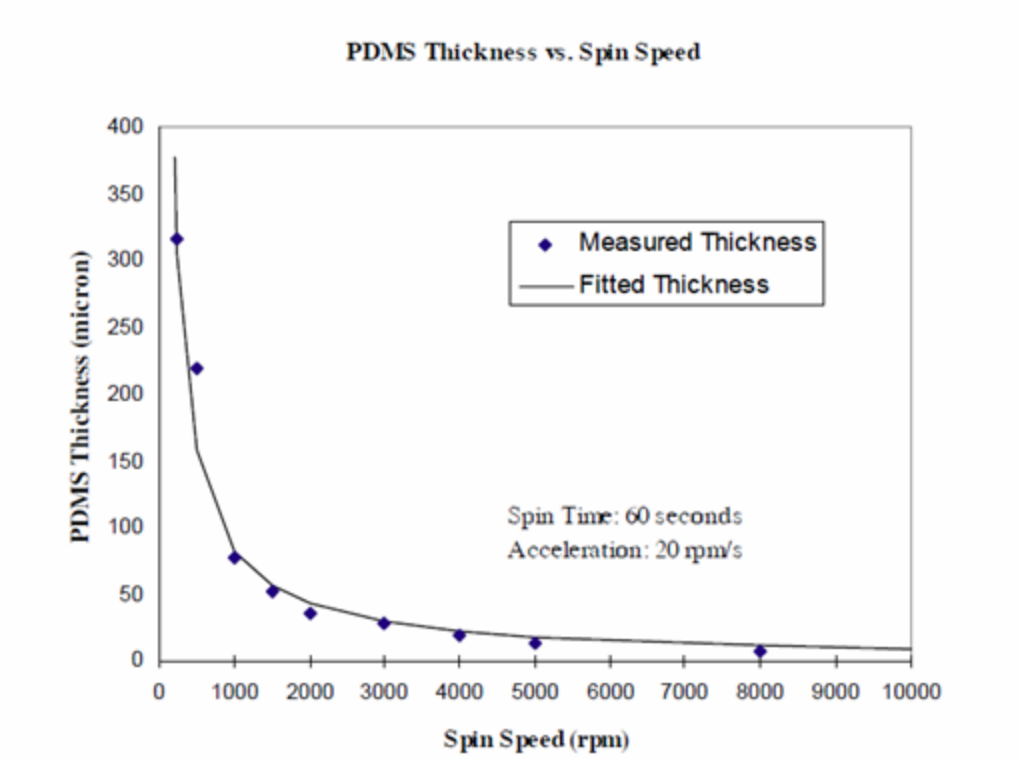

Figure 5.6: Graph (published by Zhang [4]) used to estimate spin speed for a desired PDMS film thickness.

minimize optical aberrations and thermal absorption the thickness of the elastomeric membranes was minimized. However, to retain a sufficient amount of mechanical strength and durability a balanced thickness was found to be 35µm. There are several journal publications which plot PDMS spin speed versus PDMS film thickness [4, 176, 177]. While it did not account for PDMS mixed with xylene, we chose to use the chart published by Zhang[4] (Figure 5.6) which served as a good guide while we experimentally determined the appropriate speed to spin PDMS. To obtain clear through holes with minimal microwell aberrations a PDMS mixture with 10% xylene additive was spun at 4000rpm.

Softlithography - Polymer Baking

The PDMS was then cured by baking the wafer on a hotplate at 125ºC for 1-3 minutes. An entire membrane of this thickness is virtually impossible to peel off the mold or align to the MEA, therefore additional annular layers were spun on top the 35µm layer excepting the central features. Next a syringe was used to deposit a thicker annular of PDMS (without xylene) around the feature area and then spun flat to about 100 µm and baked again. A second annular layer was added exactly as the first. The annular provided mechanical support for the delicate center area. The elastomeric membranes could then be gently peeled from the mold and the process is repeated. A single silicon mold could be used to produce over 20 elastomeric membranes before losing integrity (features breaking off).

After all 3 layers were cured in this manner, a collection of membranes was baked in a vacuum oven at 137ºC for at least 2 hours. This was done to ensure maximum cross-

linking and equivalent cross-linking between membranes. In work by Millet and colleagues it was found that an improvement in biocompatibility of PDMS microfluidic neuronal culture systems resulted from both autoclaving and short chain oligomer extraction[66]. They posited that the autoclave process increases the amount of cross-linking, reducing the number of short chain oligomers which are presumed to be a cytotoxic. We therefore baked the membranes before the oligomer extraction process.

Elastomeric Membrane - Oligomer Extraction

The cured PDMS membranes were then leached of oligomers in a three solvent process derived from one published by Millet and coworkers[66]. They found that the extraction of oligomers improves cell survival inside PDMS microfluidic devices. PDMS membranes were sonicated twice for 1hour in each of 3 solvents, triethylamine, ethyl acetate, and acetone, listed in decreasing solvency. The membranes were then vacuum baked for at least 2 hours to make sure solvents were removed. Next the membranes were attached to the substrate (coverglass or MEA).

Alignment and Attachment of Membranes to MEA

The membranes were aligned to the MEA under a dissection microscope in a dissection hood. Both the MEA and the elastomeric membrane were treated with oxygen plasma at 150 mTorr for 5 minutes on medium (longer times and higher power rendered the PDMS surface too glassy and lead to cracking and greater shrinkage). After plasma treatment the MEA was lightly sprayed with 70% ethanol which acted as a quickly evaporating lubricant to aid in sliding the membrane. As the ethanol-water mixture dried,

the movement of the membrane became slower. Using two sets of forceps the membrane was aligned so that all microholes were arranged over the electrodes. Once proper alignment was achieved the substrate was allowed to dry under the microscope illumination, temporarily fixing it in place. Next any air bubbles were pressed out toward the edges with a gloved finger and alignment was rechecked. If alignment was preserved the MEA was then heated at 50°C for 2 hours, creating a permanent bond.

Results

Elastomeric Membrane Microstructures

Figure 5.7 shows a finished 'snag' membrane aligned to an MEA. The features are well resolved and the membrane features align very closely to the electrodes of the MEA. While the features are well resolved and align well to the MEA, the position of the microwell within the membrane may be slightly misaligned relative to the microtunnels as seen in Figure 5.8. This is a result of the small misalignments in successive layers of the mold during the many layered photolithography process. Several molds must be microfabricated to obtain a perfectly aligned set of layers even with meticulous alignment by a skilled person. For this reason the 'hook' design was created which is more forgiving of slightly misaligned microwells.

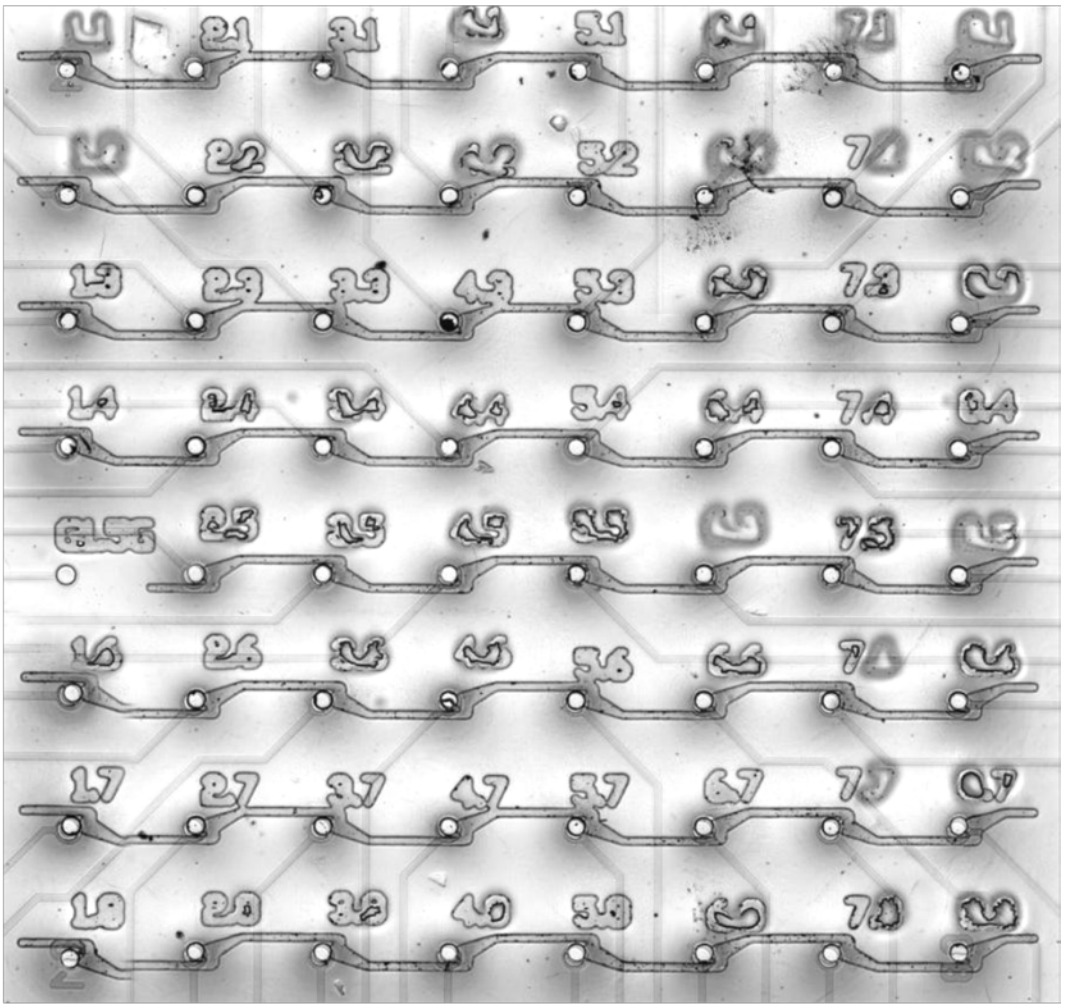

Figure 5.7: Elastomeric membrane with 'snag' microstructure. The microwells are aligned to the electrodes of an MEA.

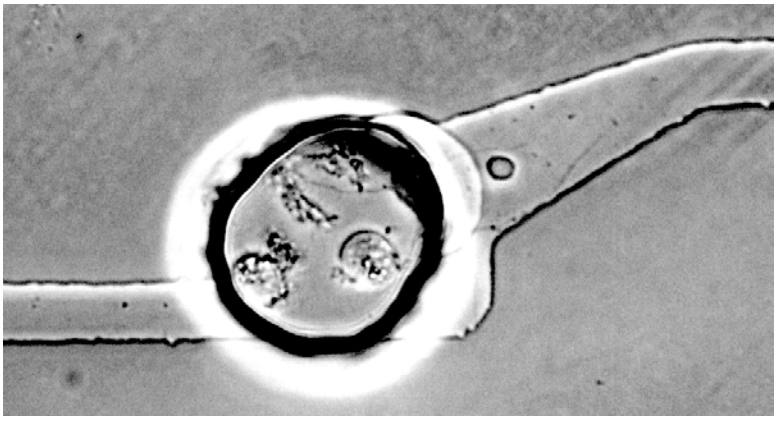

Figure 5.8: Example of off target microwell resulting from misalignment of masks with the bottom layer during the photolithography step of microfabrication. The microwell's position eliminated the intended sharp angle in the backward microtunnel.

CHAPTER VI
CREATING DEFINED CIRCUITRY

Materials and Methods

Defined circuitry was achieved by using the laser patterning system in conjunction with the elastomeric membranes. Implementation of these methods was the same as described in the previous section. New or altered methods include the surface modification techniques and other substrate preparation measures to culture cells in the elastomeric membranes and on MEAs.

Substrate Methods - Surface Modification for Cell Culture

The unaltered surfaces of the MEA and the overlying PDMS membrane were not natively supportive of cell attachment, spreading or neurite outgrowth. Therefore we developed/adapted a series of surface modification treatments to improve the biocompatibility of the substrate materials. The surface modification techniques were used to transform the silicon nitride (MEA insulating layer) indium tin oxide (ITO, electrode material) and PDMS (elastomeric membrane) substrate into a cytophilic surface which promoted neuron attachment and neurite outgrowth. All three of these materials were able to be activated by treatment with oxygen plasma. Such treatment burns off organic residues and gives the surface a negative charge by adding 0^- and $0H^-$ groups. The charged surface increases hydrophilicity, helps bind cationic polymers, and can be used to irreversibly bind PDMS to silicon nitride or glass.

Substrates were treated with oxygen plasma (or ashed[20]) for 10 minutes at 150 mTorr using the high setting on a Harrick Plasma PDC-32G cleaner/sterilizer.

Immediately following plasma treatment the substrates were immersed in a cationic polymer suspended in borate buffer with pH of 8.4. The two cationic polymers tested were polyethylimine (PEI) and Poly-D-Lysine (PDL). PDL (500-550 kD BD™ #354210) was diluted to 100µg/mL as reported by Dworak[20]. PEI was diluted to 0.05% w/v in 8.5pH borate buffer.

Methods - MEA reuse

While culturing random monolayers on MEA we used several MEAs, some new and some older, some over 5 years old with an unknown number of uses. Cell attachment was not consistent across MEAs even with the same cleaning and surface modification procedures. This is to be expected as Multi Channel Systems (MCS GmbH) lists the MEA lifespan at 30 uses, and some groups use[20] their MEAs (not MCS) as few as 5 times before replacement. We also observed that over time the MEA surfaces become unsuitable for cell attachment. Two primary modes of failure were observed with cell attachment to MEAs. In the first mode, the majority of cells simply fail to attach and spread, remaining round and clear, eventually dying. In the second mode, cells do attach spread and form a network, but the network detaches from the center of the mea and recedes towards the walls of the MEA or even of a polystyrene culture dish. The second mode of failure occurred with cell seeding densities above $2x10^5$cells/cm).

Furthermore, to test the hypothesis that MEAs could ‘go bad’, as cells were cultured on MEAs, the cell attachment status was recorded and tracked over several cleaning, coating, culturing trials to determine if poor attachment was a characteristic of specific MEAs. This was found to be true, and use of these MEAs was discontinued. One

final attempt at growing cells on the MEAs was to grow glial cells on the MEAs, which are more robust and attach to untreated surfaces relatively well. If even astrocytes cannot attach and survive on the surface there is not hope for neurons to do so. Furthermore, culturing astrocytes on the surface could condition the surface and improve attachment of neurons later.

Methods - Substrate Cleaning

The substrates including membranes were reused. Irreversible bonding of elastomeric membranes to the MEAs which are expensive required reuse. Cell debris in microwells and microchannels had to be cleaned out to allow new cells to be patterned into the microwells and to clear any debris blocking the microtunnels for neurite outgrowth. If the substrate has been contaminated by fungus or bacteria it was first cleaned and soaked in Envirocide™. After a 24 hour soak in Envirocide™ the substrates were rinsed for 2 days and boiled in DI water for 1 hour before they were treated with the normal cleaning process. Normally, the cleaning process began by rinsing the substrate with DI water to kill cells and remove media. Next the substrate was soaked in DI water with 5% Tergazyme™ for 1-2 days, until cell debris was fully dissolved by the enzymatic action of the cleaner. Substrates are rinsed 5 times with DI water, and soaked in DI water for 1 day before boiling for 1 hour in DI water. Next the membranes were placed in a sterile bio-safety hood and allowed to dry, and then exposed to UV radiation for at least 15 minutes. The final sterilization step was the use of oxygen plasma in the surface modification procedure.

Methods - Patterning Cells Into Circuit Defining Microstructures

The elastomeric membranes contained 63 microwells (64 - 1 for the electrode lead used for the internal reference) despite the MEA only having 59 electrodes. The corner microwells were included to increase the array elements because the same elastomeric membranes were used on plain coverglasses. Single neurons were patterned to each well. In the rare case where a random neuron had fallen into a well, that was indicated with an R and a neuron was not patterned to that well. In some cases debris covered the well and a pattern was not possible, this was marked with a D. Some membranes had a blocked microwell resulting from a failure of the pillar to break through the PDMS layer during the membrane fabrication process; this was marked with a S. The final case which required notation was when single cells could not be found to pattern to a well and more than one was patterned. This was noted with the number patterned to the well (1 cell was with no problems was marked as a 1). This scenario occurred when the cell supply was running low, or if the cell suspension had been inadequately dissociated. At the end of a patterning session the pattern was reviewed to make sure no cells had floated away, if they had a replacement cell was deposited. For every patterning session a 8x8 tablet was filled out denoting the session's cell pattern. The substrates were transferred to a 35mm Petri dish and immersed in astrocyte conditioned media. Every day half the media was changed. 48 hours post patterning the substrate/ cell patterns were evaluated via phase microscopy using a LD 40x (or 63x using the 1.6x optovar) objective. Each cell was counted for presence and whether or not it exhibited neurite outgrowth. These results were compared with the initial pattern to evaluate viability and neurite outgrowth.

Methods - Antibody Staining

To verify astrocyte purity we stained astrocyte cultures after the first passage for Glial Fibrillary Acidic Protein (GFAP)(MAB360, Millipore). To identify axons we stained with an antibody for neurofilaments (MAB1621, Millipore). To identify dendrites we will use an Anti-Microtubule-Associated Protein 2 (MAP2) (IHCR1004-6, Millipore). Alexa Fluor 488 anti-mouse and Alex Fluor 594 anti-rabbit were used as secondary antibody fluorescent markers.

Viability and Time in the Microsyringe

During the course of some laser cell patterning sessions we had to refill the microsyringe with cell suspension in the middle of the patterning process. Later, when reviewing the neurite outgrowth of the patterned neurons an abrupt spike in the occurrence of neurite outgrowth coincided with the cells patterned immediately after reloading the microsyringe. Further review pointed to a correlation between the time cells resided in the microsyringe and a decrease in the probability that they would extend neurite outgrowths.

The replacement cells came from the same dissection and were prepared the same way and left at the same cell density. The only difference was whether they had been sitting in the microsyringe, and whether they had been kept at 37ºC. While sitting in the syringe there was also no atmospheric buffer. Typically 3ml Cell suspension was kept in the incubator in a 15mL conical tube, leaving over 12mL of atmospheric air. Furthermore, a relatively large volume of cells should be available in the 50µL syringe as the typical injected volume is around 50nL injections. However the supply of cells

normally ran out long before the 50µL of cell suspension were fully ejected. Between 30 minutes to one hour into the patterning process the ratio of large round cells to smaller cells and cell debris decreased until no cells could be found. The decline in viability correlated with the time the cell suspension resided in the microsyringe may result from the decreased atmospheric buffer allowing the cells enough O_2 to survive or CO_2 to keep a compatible pH. An alternative but unlikely cause may be the difference in temperature between the two cell suspensions. We believed this was unlikely because cells patterned to the substrate but sitting in the chamber at room temperature (20ºC) show no decrease in survival. Finally, the glass syringes, though well cleaned and rinsed, may cause some harm to the cells.

Temperature and Atmospheric Buffer

The first experiment performed to investigate the cause of decreased viability focused on temperature and atmospheric buffer. This was achieved by using a $C0_2$ independent media (Hibernate E) and leaving extra cell suspension in a conical tube beside the laser cell patterning system for the time of patterning.

Freshly dissociated chick forebrain neurons were suspended in Hibernate-E without $CaCl_2$ with Gentamicin, Amphotericin, and Penicillin/Streptomycin at previously stated concentrations. Again, both the cells suspension and chamber medias must be perfectly matched to avoid media density flows which hinder the pattering process. The cells were suspended at a density of 333,333 cells/mL following normal patterning procedure. Before patterning (t=0) three 35mm polystyrene culture dishes were coated with Laminin for 10 minutes and then seeded with 2mL of cell suspension each. An

additional 6mL of cell suspension was placed in a 15mL conical tube and placed with by the chamber during the patterning process. The cells were patterned for 1 hour and the typical decrease in viability and cell count was witnessed. The chamber was returned to the hood, and the substrate media was changed to astrocyte conditioned Neurobasal media with the standard supplements. After patterning (t=1hour) 2mL of cell suspension

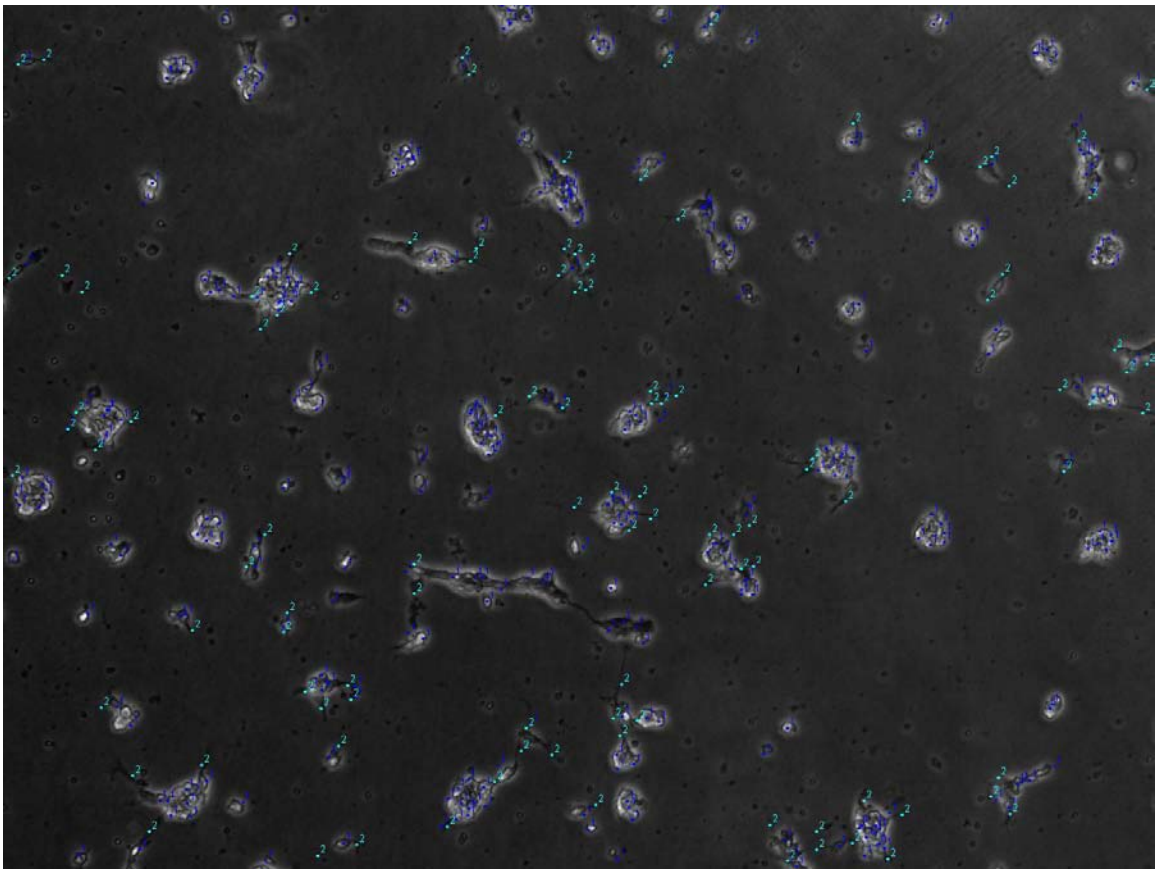

Figure 6.1: A 10x micrograph of cells plated for the $C0^2$/ temperature viability experiment. The ImageJ Cell Counter markers are overlaid. Blue type 1 markers are for cells. Green type 2 makers are for neurite outgrowth

from the 15mL conical tube was plated to each of three more Petri dishes prepared identically to the first three.

The dishes were fixed after 24hours in culture. 5 different micrographs with the same 10x size field-of-view were taken of each dish. Using ImageJ application with the Cell Counter plug-in every cell or cell sized particle was counted (6.1). Clumps of cells were counted for the number of cells that it seemed made the clump up or for the number of cells required to cover each cell. This was a very imprecise way of estimating the number actual number of cells but was consistent across the different samples. Next the number of neurite outgrowths was counted. If a cell had more than one outgrowth it each was counted. If a cell connected to another cell the interconnecting neurite was counted only once. The total number neurite outgrowths was counted and divided by the total number of neuron sized (6-12µm) round bodies.

Results - $C0^2$/Temperature Viability

The average ratio neurites to neurons for each set of samples was taken and results from each set showed that there was little difference in the fraction of cells exhibiting neurite extension at each time point. Using a two-sided Student's T-test no significant difference in the ratio of neurite outgrowth was found ($t=-0.30$, $DF = 27.89$, $P = 0.77$). From this we concluded that it was neither a deficiency of CO_2 buffer nor the lowered temperature that had caused the reduced viability of the cells in the microsyringe. We suspected two possible causes related to cells residing in the microsyringe; 1) the continual movement of the cells through the microsyringe as it was

depressed every minute agitated the cells and caused them to apoptosize. 2) Residing in the small space of the microsyringe induced cell death.

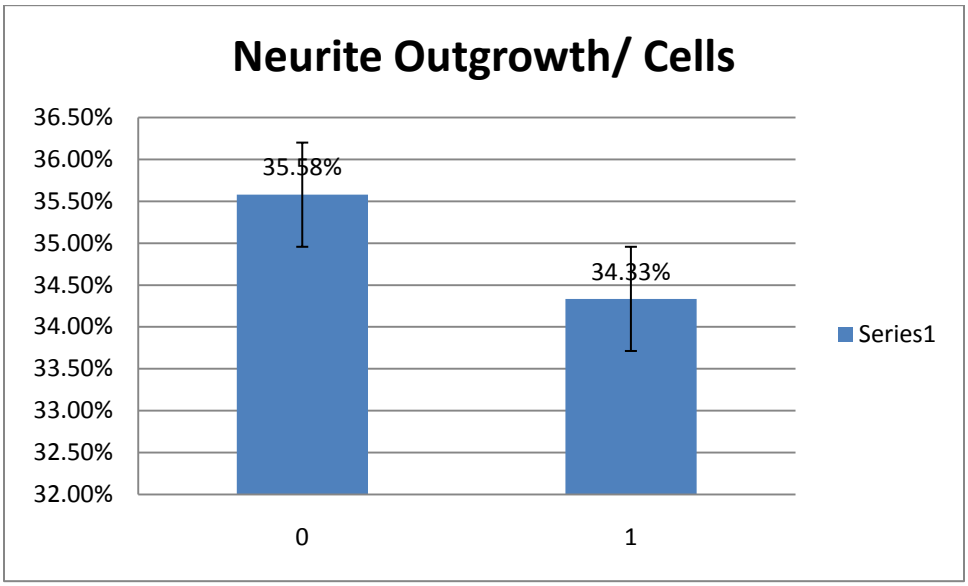

Figure 6.2: The ratio (as a percentage) of neurite outgrowth to cell number for the CO^2/Temperature viability experiment. Error bars represent standard error. There is no statistically significant difference between in neurite outgrowth between cells seeded at 0 hours after dissociation and re-suspension and cells seeded after 1 hour left at room temperature.

Microsyringe Movement Experiment

To test the hypothesis that the continual movement of the cells along the micro syringe stressed the cells to the point of apoptosis a microsyringe movement experiment was performed. Fresh cell suspension was prepared as previously described and loaded into two microsyringes which were laid flat in a culture hood (Figure 6.3). One microsyringe was depressed at a rate of 14nl/second for 1 hour to eject the entire 50µL of cell suspension. The other microsyringe received no depression of the plunger until the 1 hour time point, and then was fully depressed in 2 seconds. The output of each syringe was routed through the Microtight fittings and peek tubing used for laser patterning. The fibers were fed through small holes in a cover into single wells of a 48 well plate. The wells were coated with PDL and Laminin and filled with 500uL of Hibernate E medium with previously listed supplements. The dish was incubated at 37°C for 48 hours before being micrographed.

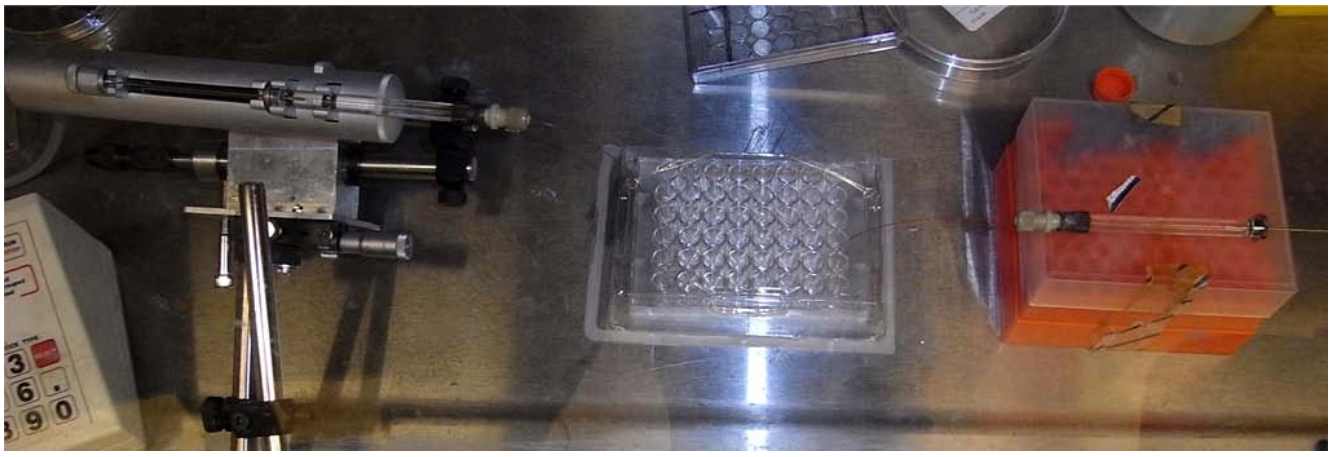

Figure 6.3: Syringe movement experimental setup.

Results

Results - Syringe Movement Experiment

Micrographs from each sample type (continuous and single ejection) are shown in Figures 6.4 through 6.7. We did not attempt to count the cells because the spreading of the cells through the well bottom was not evenly distributed. However, there were a significantly larger number of cells and cells with outgrowth in the well that was filled by a single ejection than the well that was filled by continuous ejection.

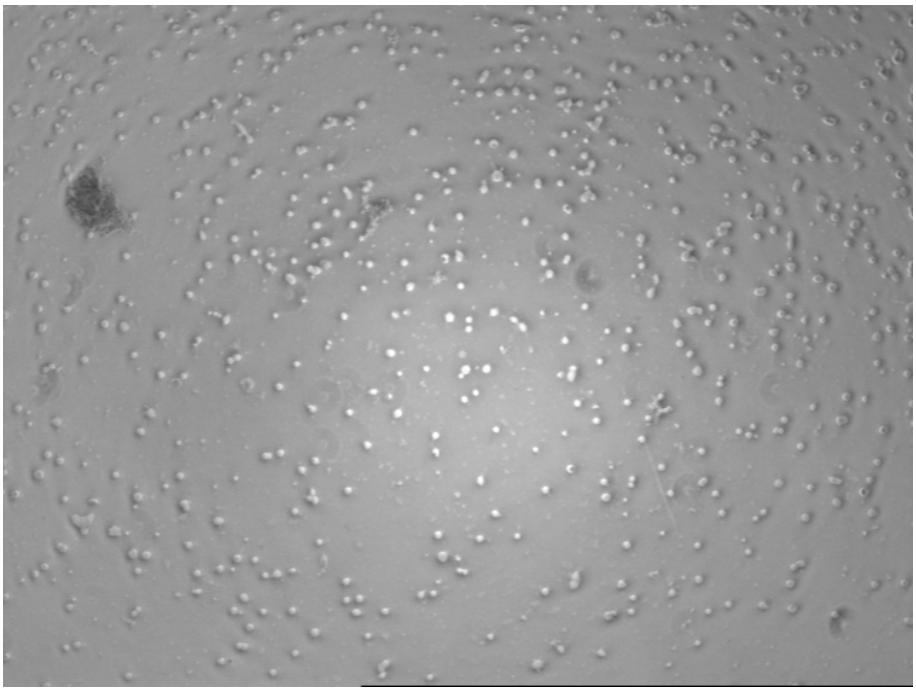

Figure6.4: 4x micrograph of 50µL of cells ejected in a single pulse of 25µL/s once cells had come to rest on the surface following ejection.

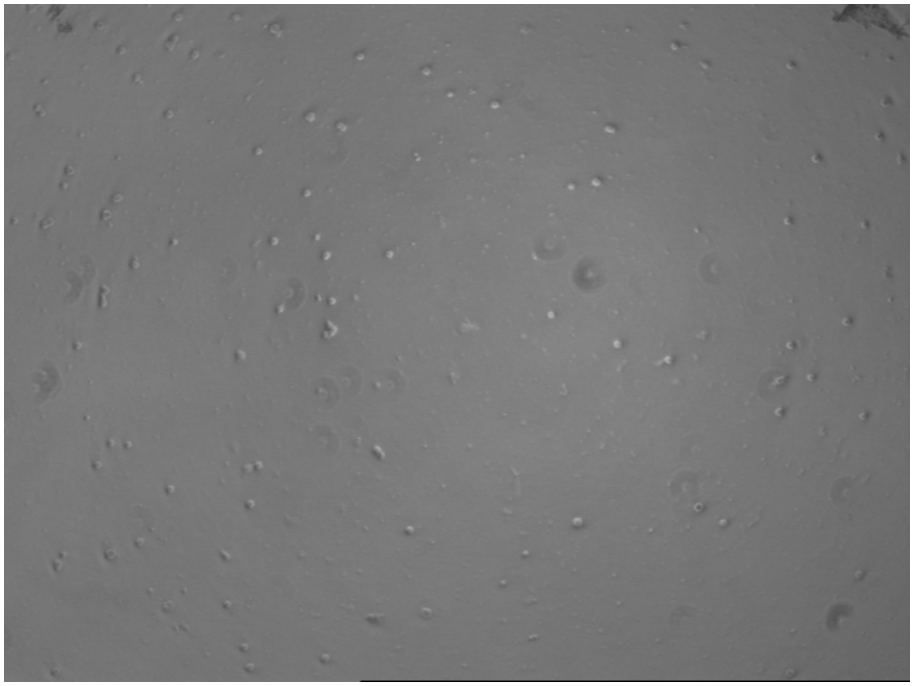

Figure 6.5: 4x micrograph of 50µL of cell ejected at a continuous rate of 14nL/s. immediately following completion of ejection.

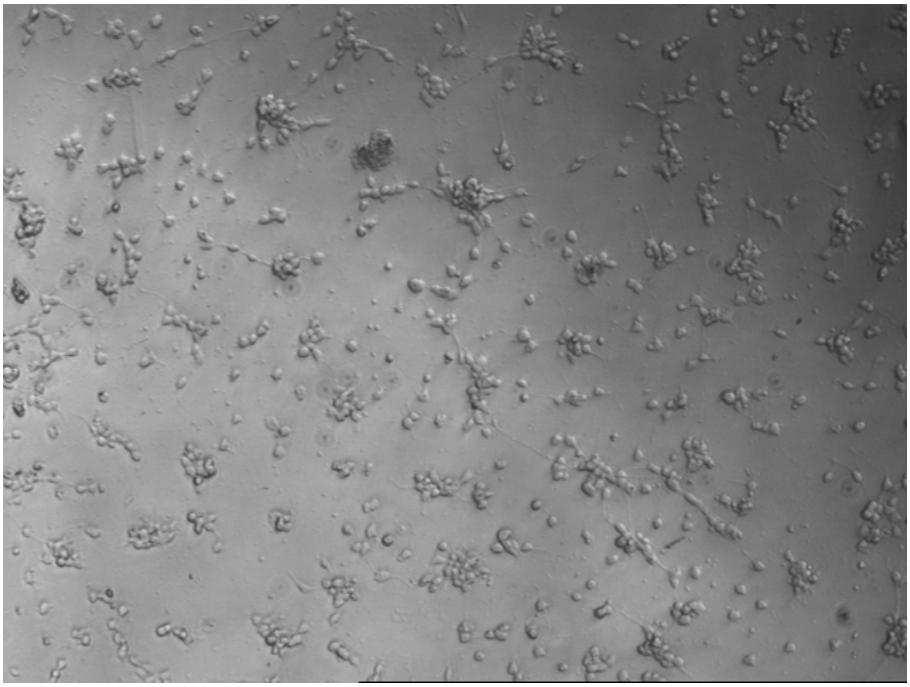

Figure 6.6: 4x micrograph of 50µL of cells ejected in a single pulse of 25µL/s once cells had come to rest on the surface following ejection.

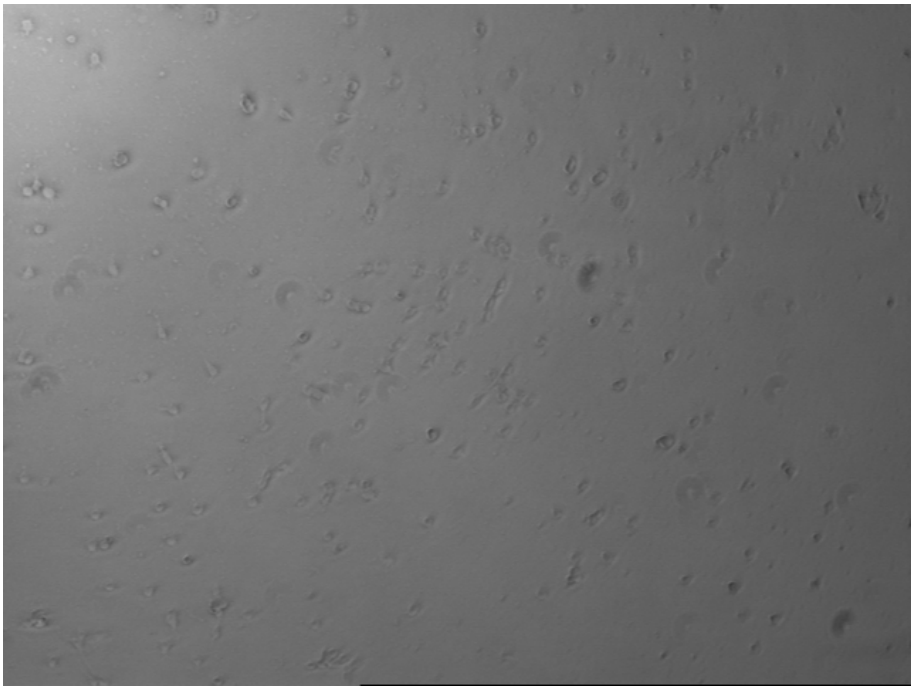

Figure 6.7: 4x micrograph of 50µL of cell ejected at a continuous rate of 14nL/s 48 hours after ejection.

Results - Viability Patterned Neuron Cultures.

To obtain a basis for comparison of patterned neuron viability and neurite outgrowth we used the same data from the CO^2/temperature viability experiment. That neurite to cell ratio expressed as a percent was 35.58% with a standard error of 0.03%. This is relatively close than the published results of Heidemann[49] which was the basis for our chick forebrain neuron culturing protocol. Heidemann and colleagues found very little to no neurite outgrowth from chick forebrain neurons plated below $5x10^3$ cells/cm^2. This was in contrast to rat hippocampal neurons which more readily survive and extend neurites at low densities. Furthermore, they found that at $10x10^3$ cells/cm^2 only about 50% of the plated cells survived.

Discovery of the link between the time cells spent in the microsyringe and the rate of survival and neurite outgrowth was toward the end of this research project. Assessing the viability and outgrowth of all cells patterned before this discovery is unrepresentative of the true rates of viability and neurite extension of neurons patterned to microwells of elastomeric membrane microstructures. For this reason these results are based on a single patterning session in which the microsyringe was refilled with from an undisturbed aliquot of cell suspension for each or 8 rows of cells patterned. A total of 33 cells were deposited with the laser patterning system into clear through unobstructed microwells. After 24 hours in culture 28 of these 33 cells survived (retained a round, un-blebbed structure) and 14 had extended neurites. The percentage of patterned cells that survived and extended neurites was 48%. Which is better than our measured neurite/cell ratio for normally plated cells and about equal to the results reported by Heidemann[49].

Results - Viability and Surface Modification

Following the surface modification protocol published by Dworak and colleagues[20] we found an abrupt increase in the viability and neurite outgrowth of neurons we patterned into elastomeric membrane microstructures. Their protocol differed from ours in several ways. They used PDL as a cationic polymer film instead of the PEI that we used. The suspended their PDL in a borate buffer with pH 8.5 and finally they rinsed their microtunnels for 24 hours in comparison to our 4 - 8 hour rinses. To determine what factors were responsible we did several experiments changing only a single parameter at a time and found that the use of borate buffer was most important. Without suspending the cationic polymer in borate buffer we had zero surviving neurons. When using a borate buffer we witnessed survival and outgrowth from neurons even when using PEI with a minimal 4 hour rinse.

Results - Circuit Connectivity

Patterned cells took longer to extend neurites than non-patterned neurons randomly seeded in glass bottom Petri dishes prepared with the same surface modification procedures. Typically 5 to 6 days were required for a neuron to extend its neurite the full 200μm length of a microtunnel from one microwell to the next. In normal cultures such an extension took 2 to 3 days. Figures 6.8 through 6.10 show typical circuit connectivity.

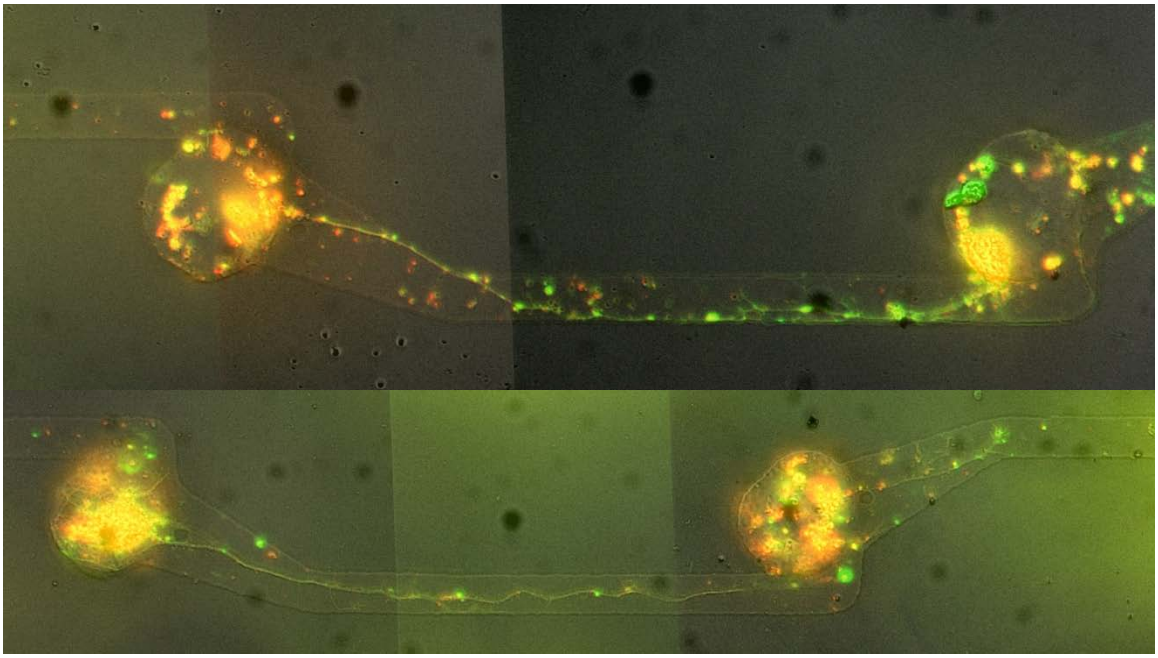

Figure 6.8: Laser patterned neurons extending neurites towards adjacent wells to form circuits. Green indicates the presence of MAP2 and Red indicates the presence of neurofilaments.

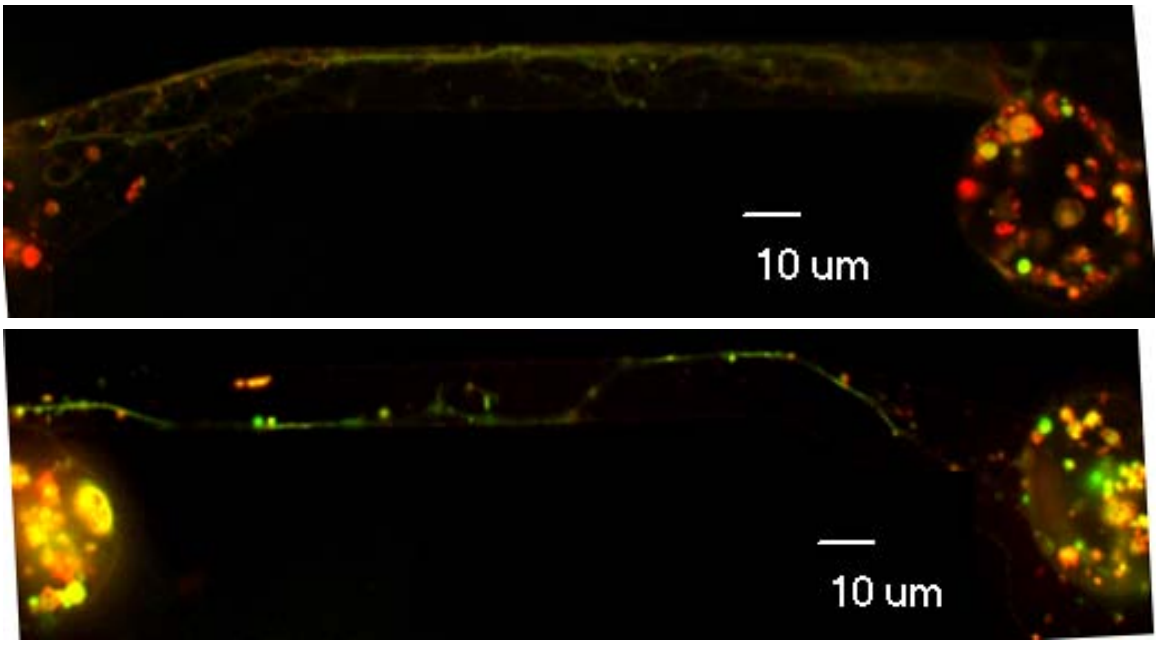

Figure 6.9: Confocal images of laser patterned neurons extending neurites toward adjacent wells to form circuits. Green indicates the presence of MAP2 and Red indicates the presence of neurofilaments.

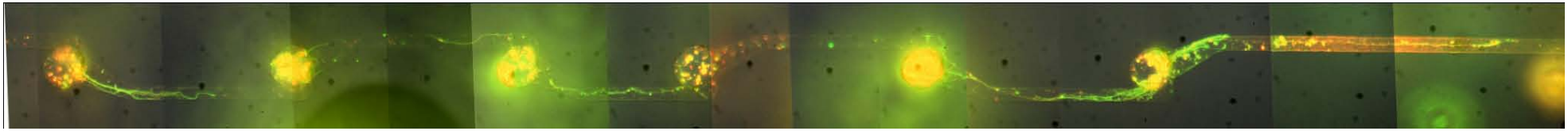

Figure 6.10: Fluorescent micrograph spliced to show a typical row of neurons.

Results - Polarity and Microstructure Design

Polarity could not be discerned from the antibody markers of the IHC stained circuits (though some polarity info could be gleaned from circuits that did not fully connect such as in Figure 6.11). Instead of identifying polarity by axon and dendrite specific markers we used live cell phase microscopy of cells as the neurites developed but before they fully connected. There were four possible scenarios that could be witnessed by a neuron. It either extended a primary neurite in the direction intended by the microstructure geometry (+), in the opposing direction (-), into the channels in both directions (Both), and it extended neurite(s) but not into either microtunnel (Neither). As previously mentioned, some microstructures had misaligned microwells which nullified the geometry of the microtunnels (Figure 6.12). Membranes of this type were not considered. Only the elastomeric membranes with the 'snag' microstructures were considered as preliminary data suggested the simple tapered channels of the 'directed' microstructures had no influence. Table 6.1shows the compiled results for 87 neurons with visible neurite outgrowth present in 8 different laser cell patterned microstructures. Figures 6-13 through 6-16 depict typical results for each scenario.

	Observed	% of Total
Neurite +	43	49.4
Neurite -	13	14.9
Neurites Both	9	10.3
Neurites Neither	22	25.3
Total	87	100

Table 6.1: Occurrence of Neurite Extension Types

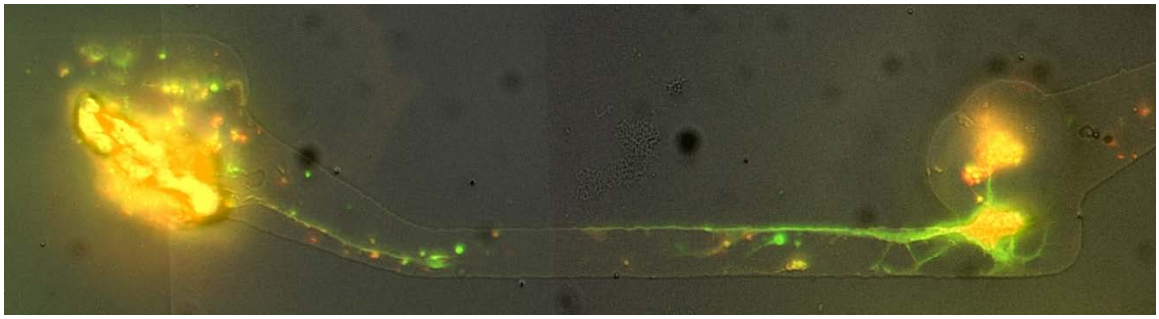

Figure 6.11: Fluorescent micrograph of patterned neurons showing both forward and backward extending neurites. Stains for MAP2 appear as green and stains for neurofilaments appear as red.

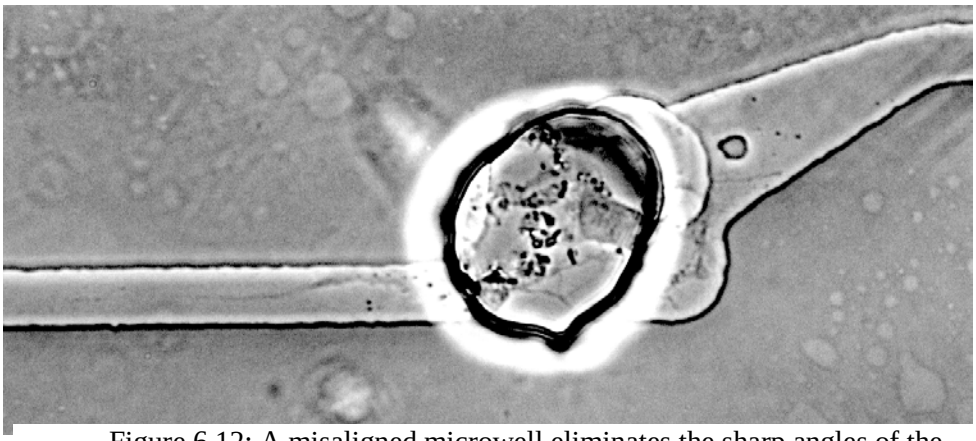

Figure 6.12: A misaligned microwell eliminates the sharp angles of the microtunnels. Neurites are extended in both directions.

Figure 6.13: A well formed microstructure with a neuron extending neurites in both directions.

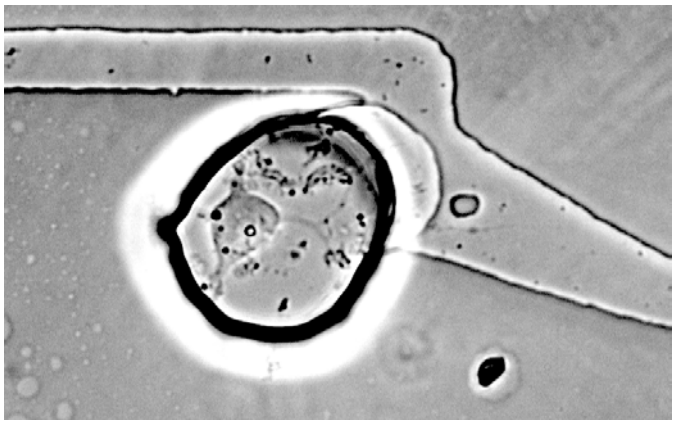

Figure 6.14: A neuron exhibiting neurite extension which does not clearly extend into either microtunnel.

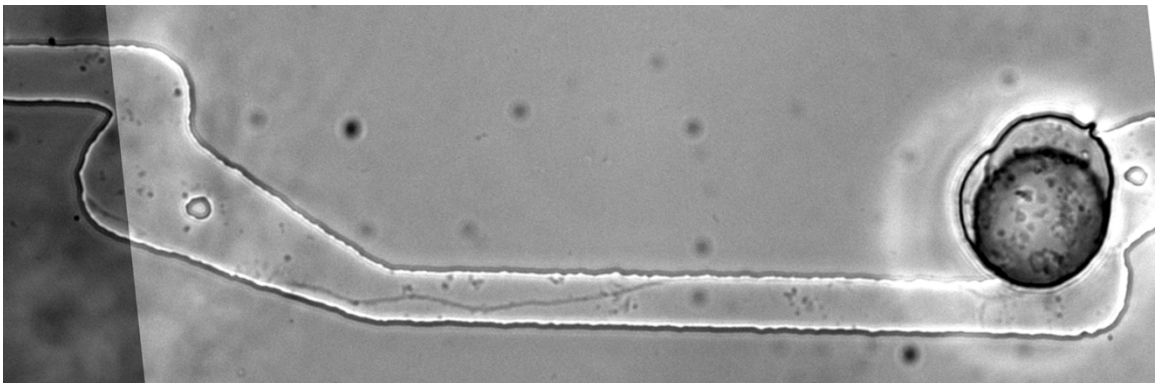

Figure 6.15: A neuron exhibiting neurite extension in the unintended direction.

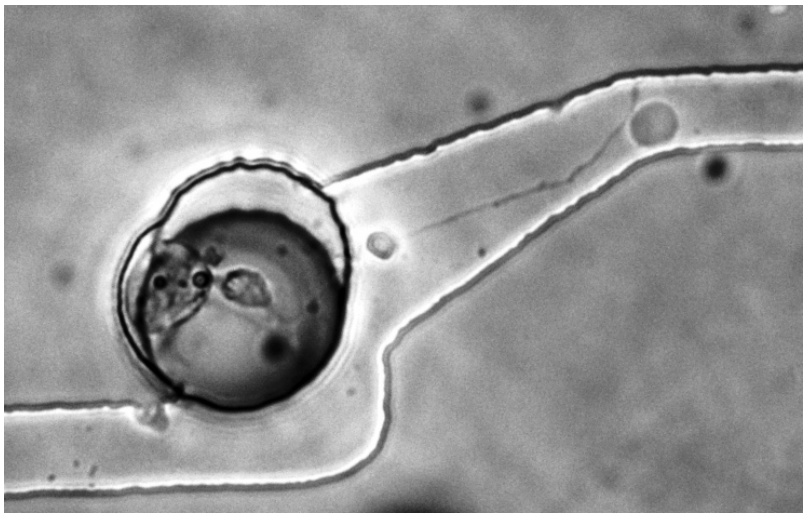

Figure 6.16: A neuron exhibiting neurite extension in the intended direction.

Results - Heterotypic Patterns

A typical heterotypic pattern created by patterning Neurons (0 hours) and astrocytes 24 hours later has the following results shown in Table 3. Micrographs were taken of every microwell which had a cell body present. It was easy to identify a single neuron or a single astrocyte if they were extending neurites or spreading. However, sometimes there were only round blobs. If there were 2 such blobs and it was known that one of each type was patterned there, than one was attributed to each cell type. Where only a single round cell was present with no spreading or outgrowth it was marked as unidentified. Finally, not all neurons may have been counted as the astrocytes often spread very wide and it were much thicker making it difficult to recognize a neurite outgrowth if one was present. From the data in Table 6.2 we can see that after 24 hours 61 % of neurons survived. Yet only of 45 % of surviving neurons showed neurite outgrowth. The rate of survival of patterned astrocytes is nearly 100 % at 72 hours after patterning (96hours). 24 hours after they patterning only 5/23 were identifiable as astrocytes by their spread morphology. Some typical results are shown through the different time points in Figures 6.17 through 6.26

	0 hours (Neuron Patterning)	24 hours (Astrocyte Pattering)	48 hours	96 hours
Neurons alive	39	24	16	12
Neurite extensions	0	11	10	9
Astrocytes Alive	0	23	10	23
Astrocyte spreading	0	1	5	19
Unidentifiable Cells	0	6	16	7
Total Cells	39	53	42	42

Table 6.2: Heterotypic Pattern Behavior

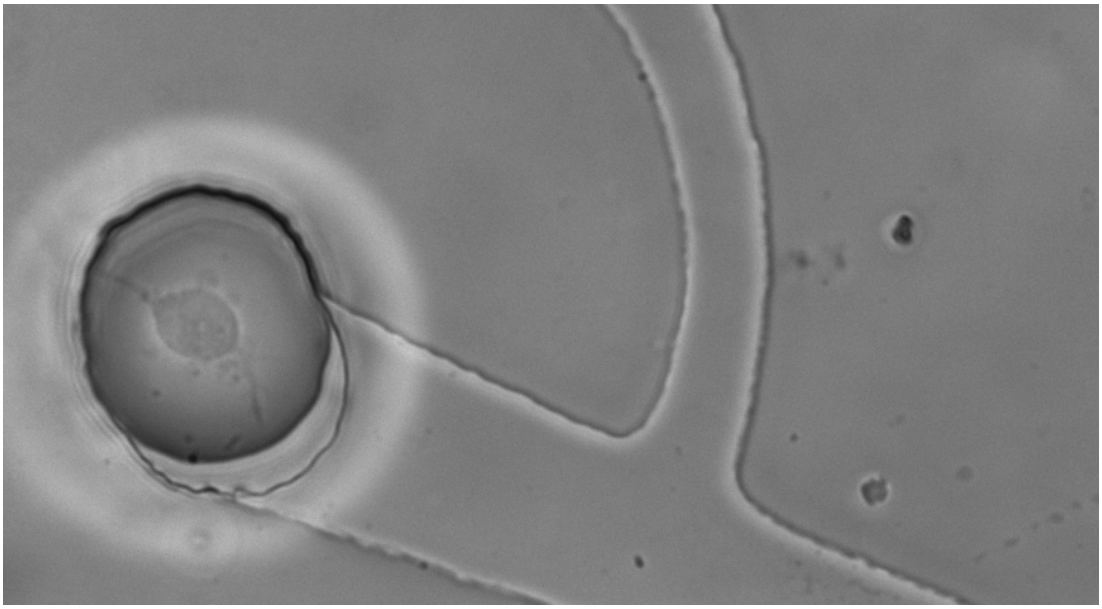

Figure 6.17: Neuron A 24 hours after deposition with laser cell patterning system.

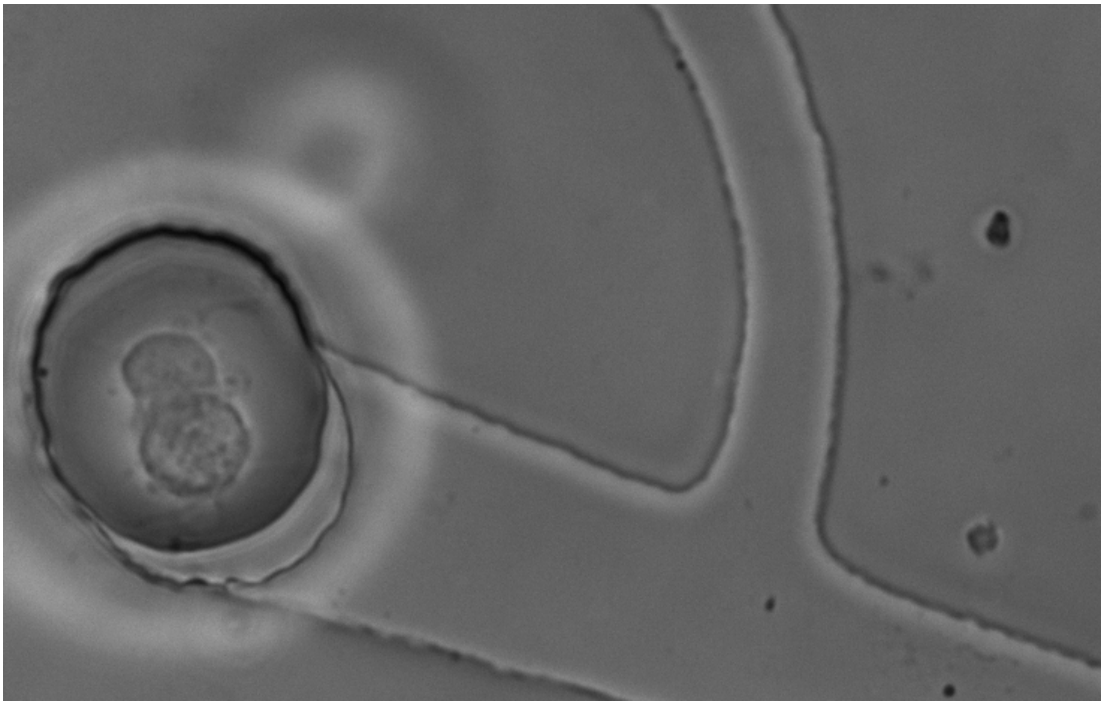

Figure 6.18: Neuron A and astrocyte A 1 hour after astrocyte deposition with laser patterning system (1 day after neuron deposition).

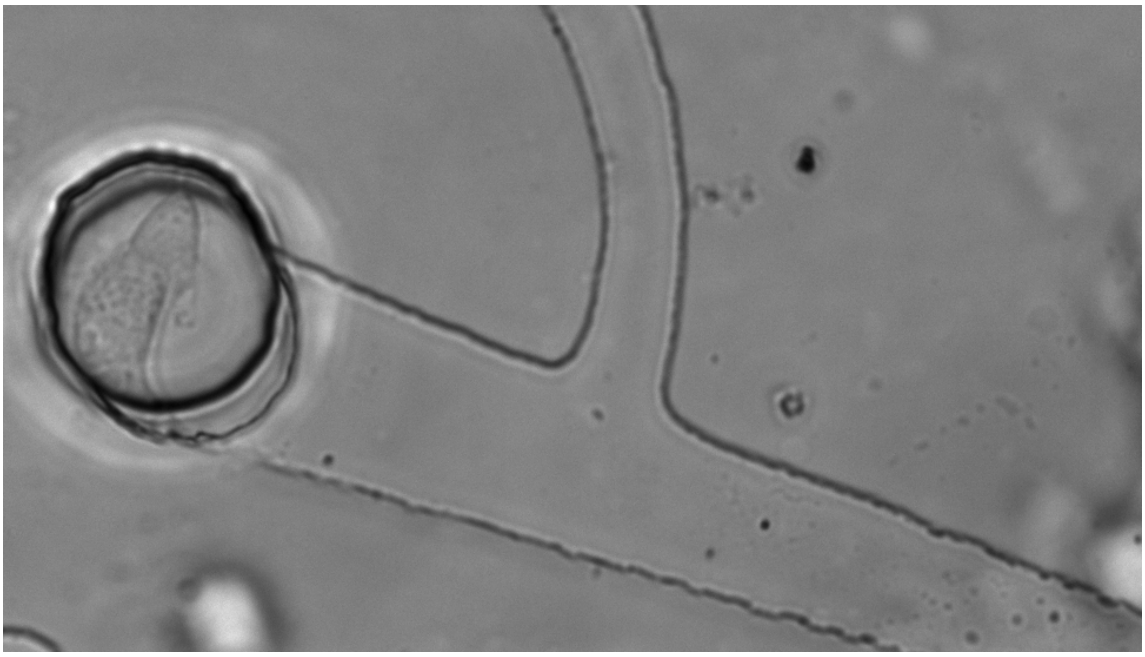

Figure 6.19: Neuron A and astrocyte A 24 hours after astrocyte deposition (48 hours after neuron deposition)

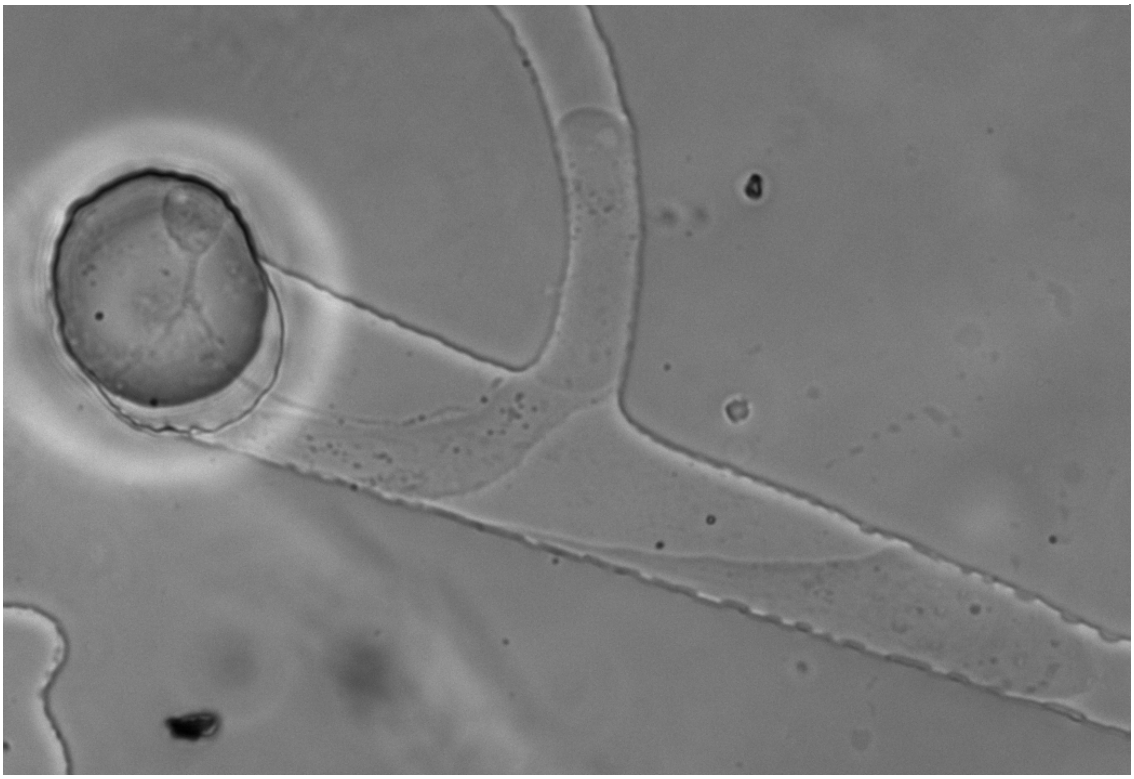

Figure 6.20: Neuron A and astrocyte A 72 hours after astrocyte deposition (96 hours after neuron deposition)

Figure 6.21: Neuron B 24 hours after deposition with laser cell patterning system.

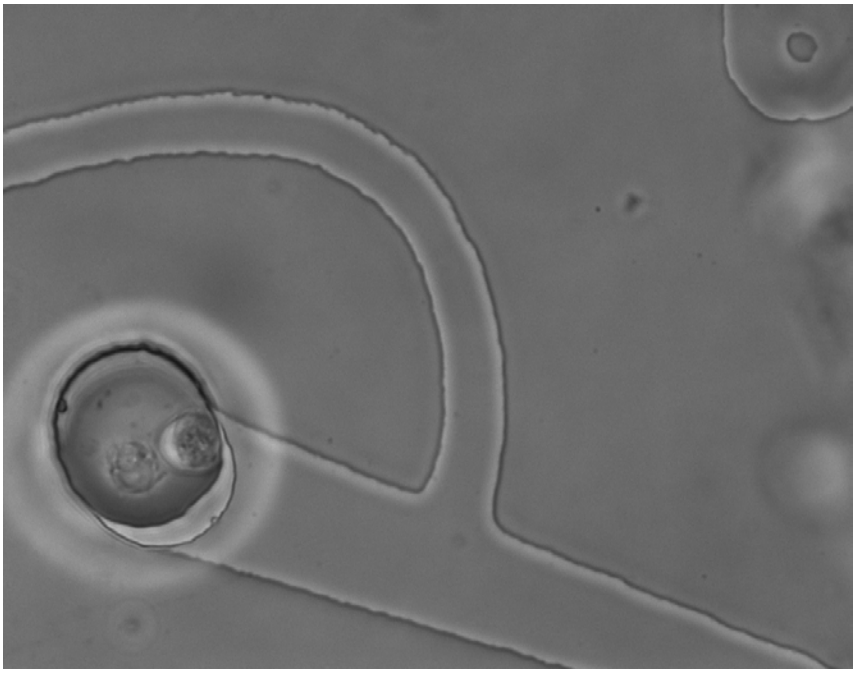

Figure 6.22: Neuron B and astrocyte B 1 hour after astrocyte deposition with laser patterning system (1 day after neuron deposition).

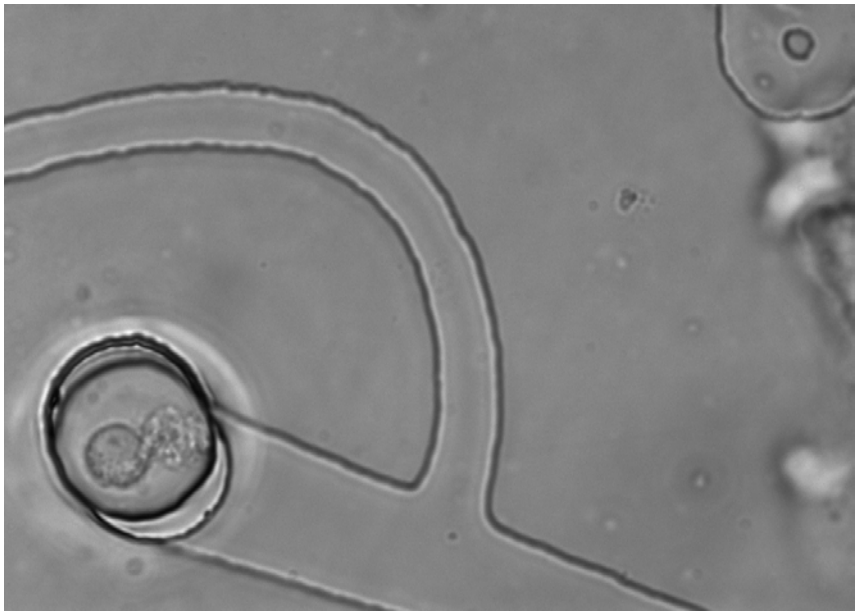

Figure 6.23: Neuron B and astrocyte B 24 hours after astrocyte deposition with laser patterning system (48 day after neuron deposition).

Figure 6.24: Neuron B and astrocyte B 72 hours after astrocyte deposition (96 hours after neuron deposition)

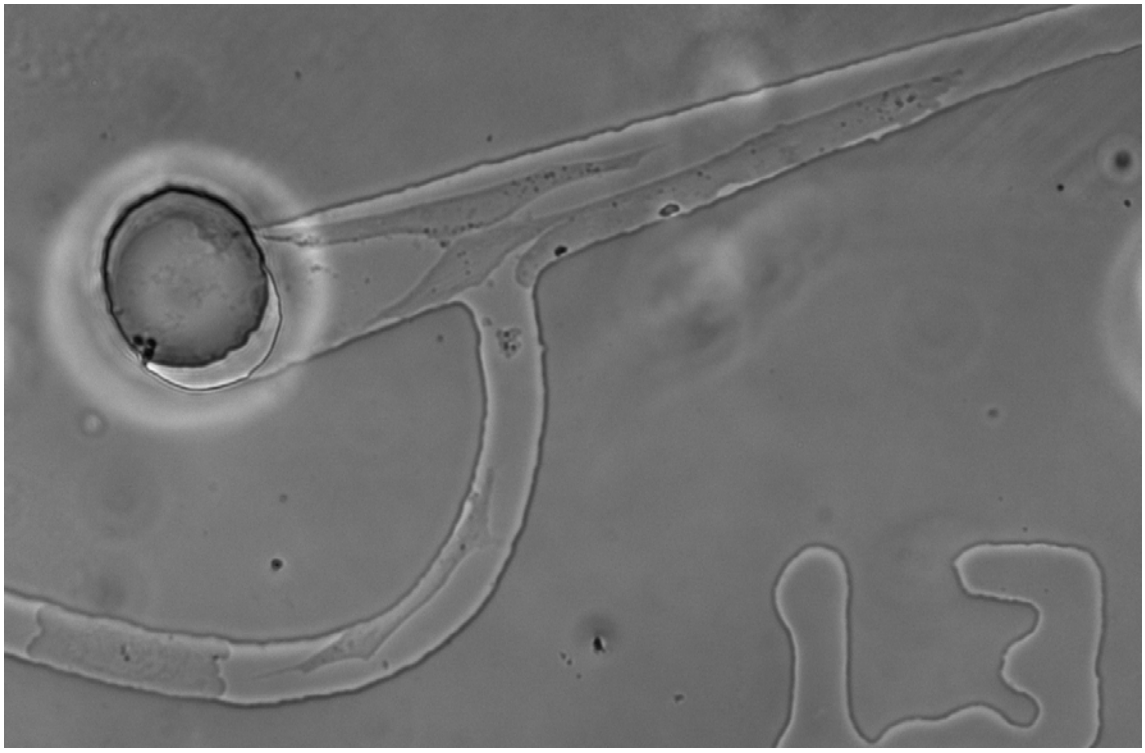

Figure 6.25: A single astrocyte 72 hours after laser deposition has multiplied and migrated

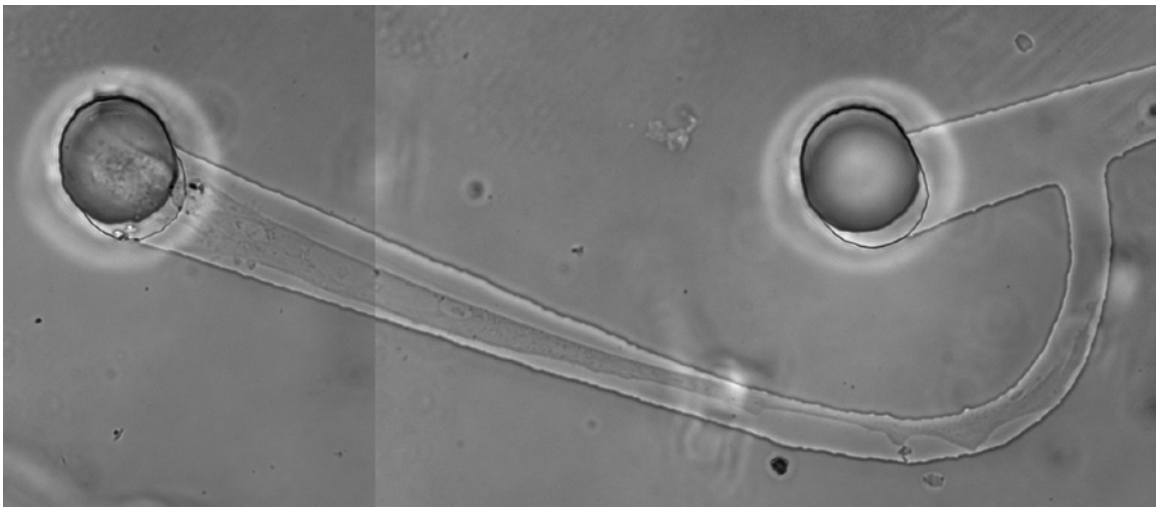

Figure 6.26: A single astrocyte 72 hours after laser deposition has elongated through almost the entire microtunnel.

Results - Circuits on MEA

Finally, using the laser cell patterning system we were able to deposit single neurons into microwells aligned to the electrodes of an MEA. The microtunnels of the elastomeric membrane guided the neurites which extend toward adjacent microwells (Figure 6.27) and connect and to neurons patterned on adjacent electrodes (Figure 6.28).

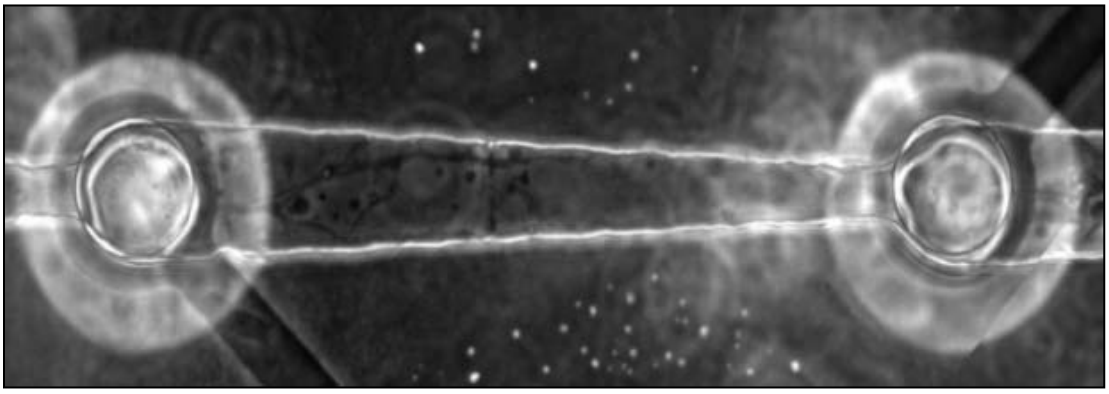

Figure 6.27: A neuron deposited to an electrode with the laser cell patterning system and confined there by the overlaid elastomeric membrane microstructure extends a neurite which is guided by the tapered microtunnel.

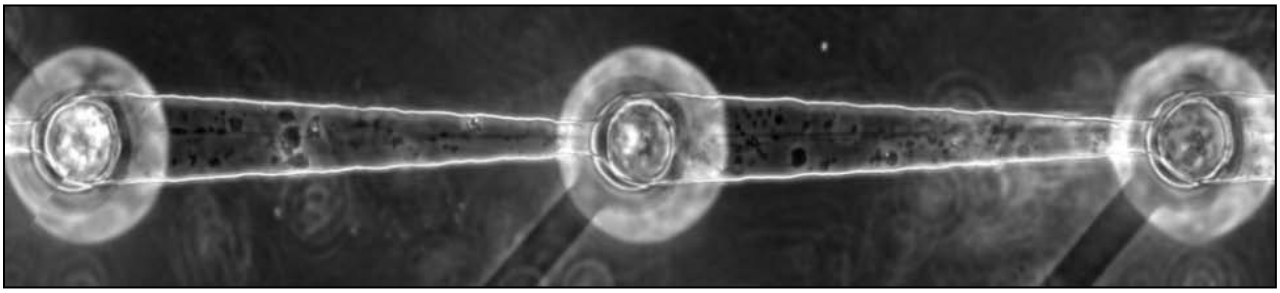

Figure 6.27: A row of neurons deposited with the laser cell pattering system creating a defined linear circuit across 3 electrodes. Once connected the axons tensioned into a straight line.

Discussion

Syringe Viability

The introduction of the new patternscope chamber design enabled easier refilling and reintroduction of the microinjection system because the microinjection fiber was not pressed tightly between the PDMS wall and the ventblock but instead was threaded through a hollow stainless steel conduit. During a refill using the earlier chamber a problem that frequently occurred during removal and reattachment of the microsyringe from the Microtight™ fitting (which coupled it to the injection fiber) was the introduction of air bubbles into the microinjection system. The patternscope chamber, by facilitating removal and re-insertion of the injection fiber, allowed for the injection system to be primed after reloading the syringe, removing air bubbles and making reloading of the syringe much more practical. The patternscope chamber was only implemented toward the very end of this research progress as a measure to overcome a period of challenging laboratory conditions. While the viability experiments performed prior to implementation of the patternscope chamber are likely invalid because a standard refill protocol was not followed and the time of each cells deposition/time-in-the-microsyringe was not documented important questions were introduced by this period of research which ultimately have lead to improvements in the laser cell patterning system,. It was determined that the continual movement of cells in the microsyringe lead to cell death and decreased viability of cells deposited with the laser cell pattering system.

Analysis of Polarity

Previous research in controlling neuron polarization[178, 179] has been evaluated by immunocytochemical staining of neurofilaments (abundant in the axon but not the dendrites) and MAP2 (abundant in the dendrites but not the axon). Our fluorescent microscopy photos of immunocytochemically stained neurofilaments and dendrites were not indicative of neuronal polarity. Unlike the previously mentioned research, where axons and dendrites occupied mutually exclusive areas of the substrate, our hypothesized method of defining polarity allowed both axons and dendrites to occupy the same space and there was large overlap of each within the microtunnels so that once fully connected the direction could not be discerned.

By using live-cell phase microscopy before complete connection between neurons was achieved a better analysis of polarity could be determined. One shortcoming of the 'snag' microstructure design was that the turning points of the microtunnels where much too close to the microwells. This was a problem because of the multi-layered fabrication process, in which small misalignments which would normally be tolerable, where overlaid on each other and sometimes eliminated the sharp angular turns of the microtunnels thereby nullifying our proposed mode of polarity induction. However among the subset of microstructures which were properly formed 49% of neurons exhibiting neurite outgrowth extend those outgrowths in the desired direction compared with only 15% directed in the opposing direction This equates to over 3 times as many neurites being guided in the intended direction than in the wrong direction. Furthermore only 10% of cells exhibiting neurites extended those neurites in both directions. The 25%

of cells whose neurites did not fully extend into either microtunnel may, with improved culture techniques be promoted to extend their neurites, and would likely split directions along the 49%-15%-10% ratio. Still, for fully defined circuits with control over polarity the odds of getting 4 cells connected with the intended polarity would be less than just over 5%. In order to address both the design flaw of the 'snag' membrane and it's successful but less than ideal control over polarity a new 'hook' microstructure was designed. No experiments were performed on the polarity control of this membrane. However, besides showing that neurite polarity can be influenced by geometric guidance these polarity experiments demonstrate the ability of the laser cell patterning system and the microfabrication system to set up and test the development of single neurons in a controlled microenvironment. In the case of the 'hook' microstructure, the developed systems will allow us to investigate how an axon is guided, up or down the postsynaptic cells axon, when it is incident at 90°.

Analysis of Heterotypic Patterning

Heterotypic patterning of neurons and astrocytes into a single elastomeric membrane microstructure was successfully demonstrated. As could be seen in the micrographs there are several different outcomes that may results from such heterotypic cell-cell interactions. The laser cell pattering system is a unique and powerful tool for investigate these heterotypic cell-cell interactions. Specifically it can be used to set up and study developmental scenarios between neurons and astrocytes and by patterning to an MEA the contribution of astrocytes to the electrical activity of neuronal circuits.

.

CHAPTER VII
ELECTROPHYSIOLOGY

Introduction

The primary objective of the electrophysiology experiments was to show the health and functionality of the defined neuronal circuits and demonstrate the ability of the biochip to record and stimulate the defined circuits. As a final validation of the biochips use in neuronal network research, we aimed to show a difference in neuronal network activity in relation to an imposed parameter of the neuronal circuits. Possible experimental comparison included neuron type (chick vs. rat), neuron number per node, and contact with astrocytes.

Because our group had only limited experience with neuron electrophysiology using microelectrode arrays part of the electrophysiology aim included culturing random monolayer cultures on MEAs to verify neuronal network activity by conventional culture methods.

Materials and Methods

Circuit Creation

Neuronal circuits tested for electrophysiology were created with the exact same procedures used in the circuit definition experiments. The only difference was the use of an MEA as a substrate, and that PDMS walls were permanently bound to the substrate in order to for it to stay sealed to the MEA while it is placed inside the amplifier during electrophysiological experiments. Of note, rat neurons have a darker color and a slightly larger size (~10-12μm in diameter) than chick neurons. These visible differences as well

as other undetected differences resulted in a faster guidance speed of 30-35μm/s. This difference was an advantage in pattern time, and illustrates the phenomenon which our lab is exploring for cell sorting and identification.

Cell culture

Chick neurons were cultured as previously described and plated on PDL coated MEAs at a density of x cells/cm^2 which is around $1.5x10^6$ cells per glass ring MEA and $1x10^6$ cells per PDMS gasket bound MEA. These are also the densities used for rat cells.

Rat Cortical Neurons were purchased from BrainBits LLC (Springfield, IL). Brain bits cells are available in the form of fresh brain tissue or as frozen cells. Initially vials of 1million frozen cells were ordered, but cell survival was poor. The stress of freezing necessitates immediate plating of neurons for survival. Even with immediate plating, the fraction of cells that remain viable is much less than can be achieved when using fresh tissue. Considering the 1 hour delay before cell-substrate contact imparted by the laser patterning process and the already tenuous culture conditions of the single cell resolution circuits we chose to use only fresh cells.

BrainBits LLC supplies neurons from embryonic day 18 Sprague/Dawley or Fischer 344 rats. Fresh tissue comes as a pair of cortex halves packaged in a 2ml tube containing B27/ Hibernate® (with calcium) media. Under refrigeration (4-8^oC) Hibernate® media can preserve neural tissue for weeks[180], though the recommended period is 1 week. To maximize the experiment opportunities per tissue order the cortical halves were separated the day of delivery. One half was used that day, and the other within 2 days. The Hibernate® media can also be used for C02 independent culture

situations such as live cell microscopy, or in our case, electrophysiology experiments. During electrophysiology experiments we used Hibernate®-E (for embryonic tissue) without calcium. During normal culture the cells were cultured in Neurobasal media supplemented with B27, 0.5 mM glutamine, 25 uM GlutaMAX, and NGF.

Results

Early experiments with random monolayer cultures of chick forebrain neurons on MEA yielded very little activity. On one occasion of nearly 50 experiments activity was observed from two electrodes (Figure 7.1). This was from a 5 Day old culture of chick neurons. This activity was never reproduced. Because of these difficulties we moved on to using Rat cortical neurons which are widely used in MEA experiments. There was a distinct difference in morphology and in the tendency of the neurons not to adhere to the center of the MEA where the electrodes were present. Because of this difficulty, and the clear disadvantage of chick neuronal network arrangement, and the lack of published work using chick neurons on MEA, the use of chick neurons on MEA was abandoned.

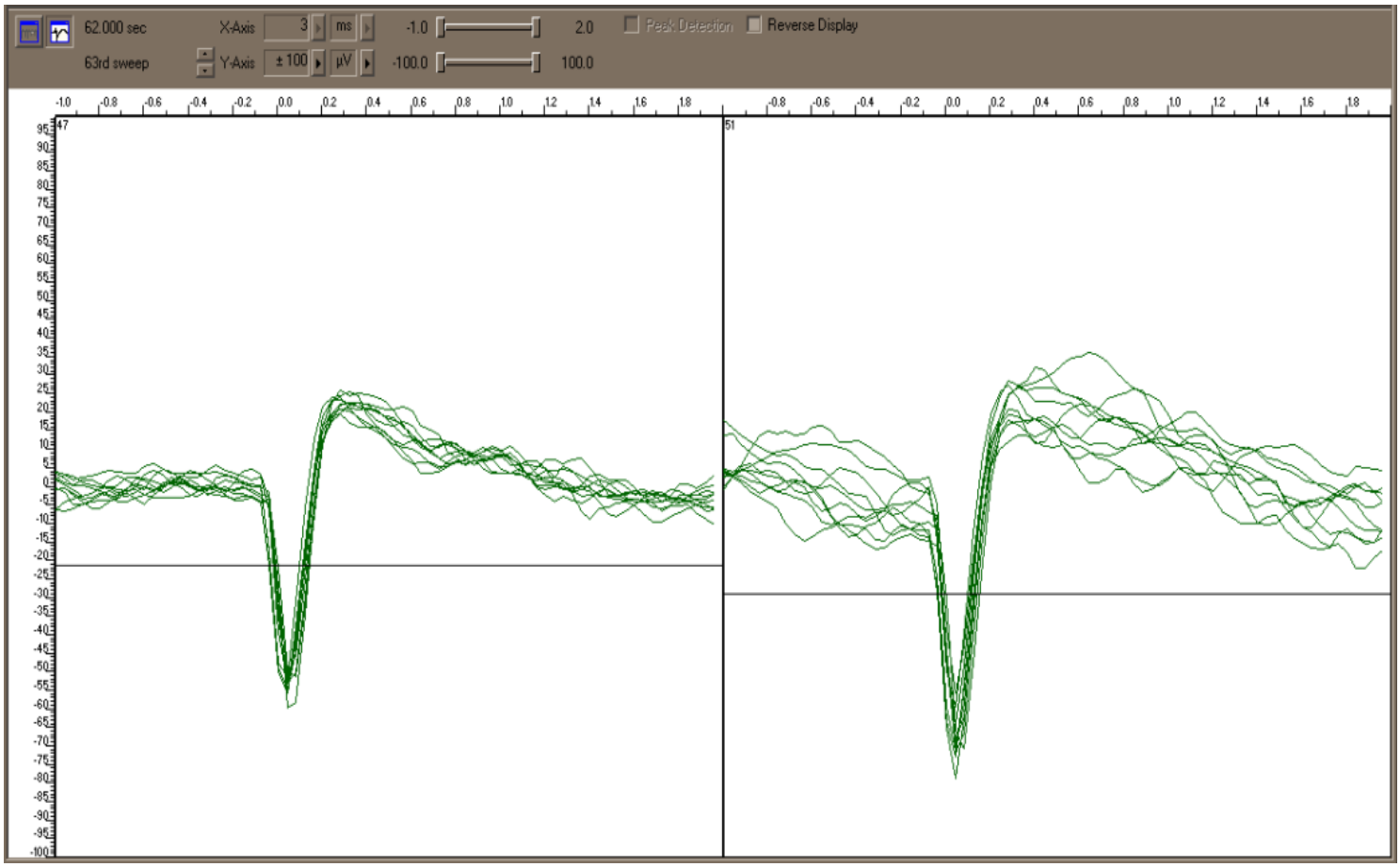

Figure 7.1: Activity from 5 day old chick neurons randomly cultured on an MEA. The screen capture from the MCS MCRack software shows waveforms are from two electrodes. Each electrode was sorted for spikes and the last 10 spikes are overlaid on each other. The frequency of spiking for each electrode is 77.40hz and 51.98hz. The spike threshold was set at 3 standard deviations of the signal. Spike amplitudes were -55µV and -65µV.

Results - Astrocyte Culture on MEA

Astrocytes were cultured on MEA which would not support neuron attachment or neurite outgrowth to determine if the surface could support a different, more robust cell

type. Astrocytes did not adhere well to the MEAs or multiply to confluency. Typical cultures are shown in Figures 7.2, 7.3, and 7.4.

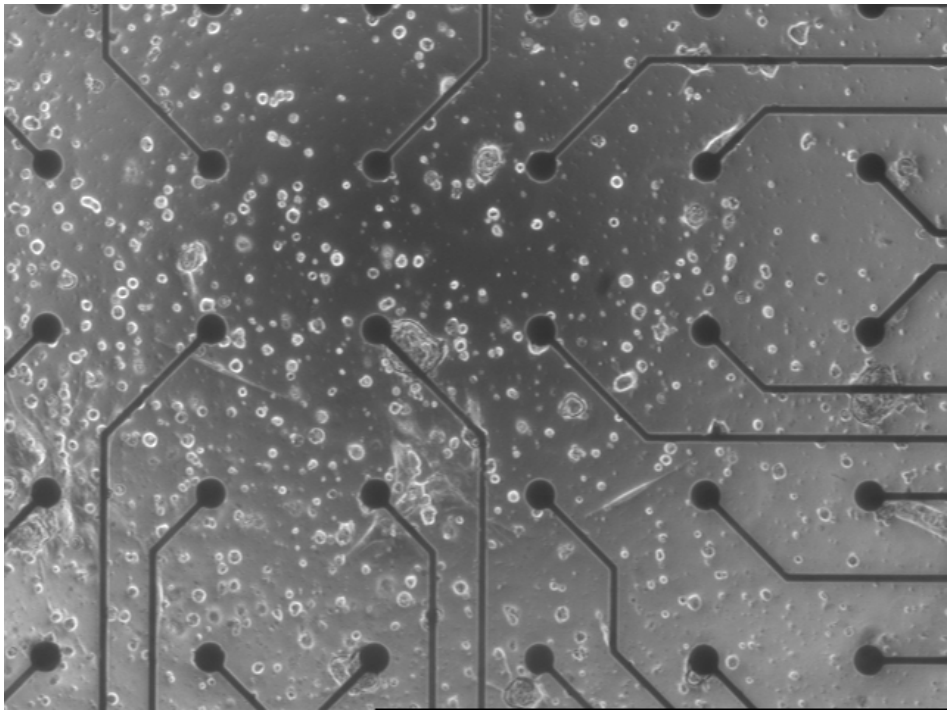

Figure 7.2: An MEA seeded with astrocytes at 1 week. Very few cells were attached to the surface of the electrode area. Cells that did exhibit a spread morphology did not multiply.

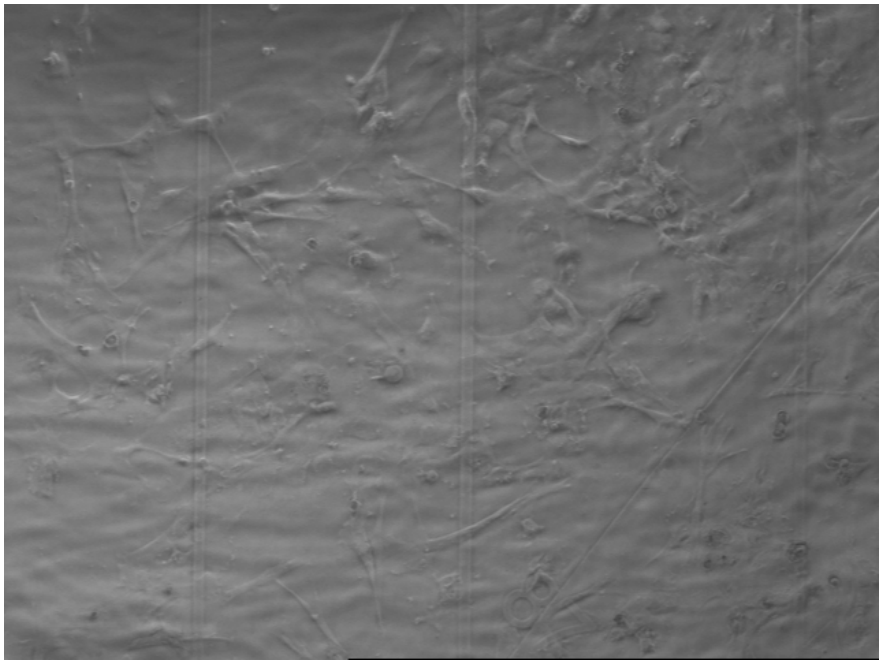

Figure 7.3: An MEA seeded with astrocytes at 1 week. More cells attached around the outside of the MEA surface away from the electrodes.

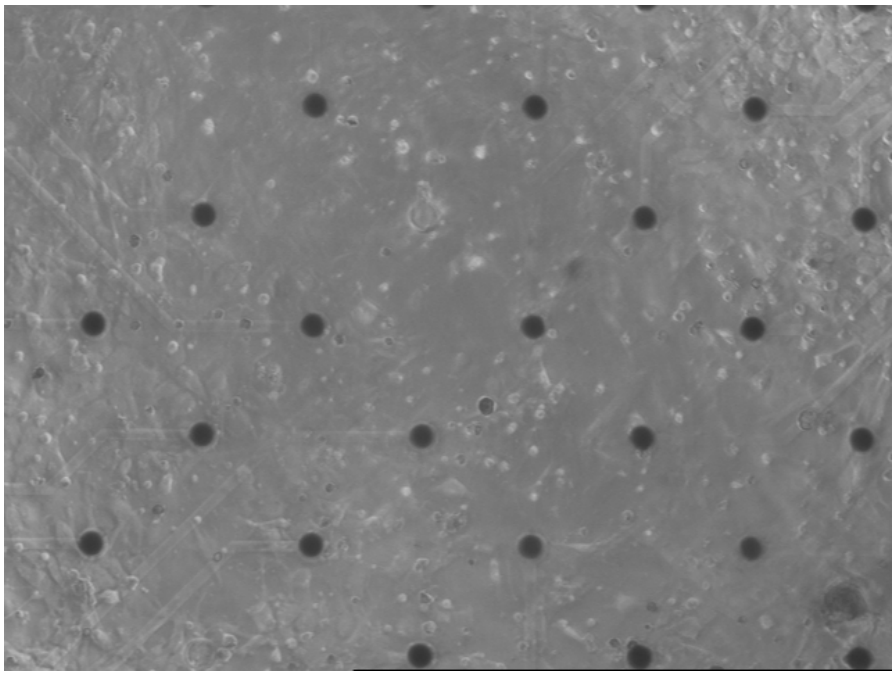

Figure 7.4: An MEA seeded with astrocytes at 1 week. Astrocytes attach on the perimeter but do not adhere to the center area where the electrodes are located.

Discussion

The surfaces of MEAs degrade with use. Multichannel Systems sets an upper limit of the times an MEA can be reused at about 30. Wheeler's group which studies the electrophysiology of large groups of neurons cultured on MEAs report reusing MEAs a maximum of 5 times[20]. During the course of this research our group performed many experiments culturing neurons on MEAs in order to developed successful protocols for culture, stimulation, and recording. The high cost of MEAs limited the number of MEAs available for our research to 10-15 MEAs. This necessitated a high reuse rate. Problems with contamination which required more aggressive cleaning measures may also have shortened the life of the MEAs. Astrocytes are hardy cells which attach very well to substrates and will grow to confluency on most culture surfaces. The results from the astrocyte culture experiments suggest that the MEAs we were using were degraded to a critical point unsupportive of cell attachment and spreading. Early in the experimental process electrophysiological recordings were obtained from chick neurons cultured on an MEA, an achievement which has not been previously reported (on MEA).

CHAPTER VIII
CONCLUSIONS AND RECOMMENDATIONS

Significance

This research is significant because it provides a tool that can create single cell resolution heterotypic neuronal circuits with defined connections on microelectrode arrays. This accomplishment cannot be achieved by other contemporary research methodologies. The tools and protocols developed to achieve this research objective are applicable and advantageous to the field of neuronal network research as well as cell biology research in general.

Moreover, while the singular achievements of the laser cell pattering and microfabrication systems can be combined to meet the intended goal of creating defined single cell resolution heterotypic circuits with one-to-one neuron electrode coupling, the singular achievements demonstrate other valuable applications of the system. Specifically, the laser cell patterning system can be used to orient cells such as adult cardiomyocytes to study cell-cell interactions of polar cells. The laser cell patterning system can place cells with high spatial and temporal resolution which was demonstrated in building a fibroblast bridge between myocyte islands. The laser cell pattering system is well complimented by the microfabrication system in order to study how single cells develop in novel microenvironments as demonstrated by the experiments testing the geometric control of neuronal polarity. It was shown that geometric microstructures are effective at influencing neuron polarity and such microstructures can be use as a tool in defining the polarity of circuits. Finally, the laser cell pattering system and the

microfabrication system can be used to place two cells of different types in close contact with in a closed, marked environment so that the cell-cell interactions can easily be tracked over time.

The patterning and confinement systems we have chosen give us the ability to use multiple cell types and to control the direction of neurite outgrowth. These abilities open up the potential to create more complex circuits such as the reflex arc, or a single-cell resolution hippocampal loop. Furthermore, our use of microfluidic type structures introduces the possibility for microfluidic delivery of acetylcholine or dopamine, which may be used in models of memory and neurodegenerative diseases.

One potential application is the study of Amyotrophic Lateral Sclerosis (ALS). This disease of the motor neurons could be modeled with an on chip neuromuscular junction (motor neuron, muscle fiber and glia). The electrophysiological and microscopic analysis could be easily performed on circuits where single cell components were replaced with cells from a transgenic mouse model of ALS.

Another application that could advance from this research is to model the circuit that is suspect in the development of Alzheimer ’s disease. Here a circuit of cells from the entorhinal cortex (EC), dentate gyrus (DG), CA3, and CA1 could be created on a biochip. These cells have been shown to be highly affected in AD and their respective brain regions contain many markers associated with the disease such as NFT and loss of cholinergic input. It is not clear what the exact causes are, or how the disease progresses in its ordered fashion. The proposed model would allow us to look at individual cells in

relation to the rest of the network, and analyze their electrical activity and signal transmission in the presence or absence of certain factors.

Microfabrication has been previously demonstrated as a useful tool for cell biology research. The laser cell patterning system is a unique and powerful tool developed in this research project. However the whole of these two systems is surely more than sum of the parts.

Recommendations

Optics

The optics configuration of the laser pattering system was very effective. Only one improvement is suggested. The current system uses a large, expensive, and sensitive tunable laser. The laser cell patterning system does not require a tunable laser, such a high power laser, or one with such a pure mode. A diode laser has the advantage of being cheaper, smaller, and more durable. The laser of the laser cell patterning system should be replaced with a diode laser to reduce cost, maintenance, and make the system smaller and possibly portable.

Control Application

The control system has been made very user friendly and was very effective. The only improvement we can recommend would be to revisit image recognition based automation, however this does not seem like a good allocation of resources at the present time.

Microfabrication

The microfabricated membranes were effective at controlling cell outgrowth and polarity. However, microstructure design for inducing polarity and for controlling astrocyte migration has not been optimized. This is less a recommendation and more of an avenue for future work as constant redesign of the microstructures was the reason for using laser photoplotted photomasks.

Electrophysiology

The electrophysiology component of this research is the most in need of development. Commercial MEAs are expensive and do not last very long. Wheelers group has in the last few years begun fabricating their own MEAs. The elastomeric membranes used for microstructures may also be used as an insulator over MEA electrode leads. Without the need for an extra insulation layer the fabrication of an MEA is on step simpler. Additionally, the irreversible attachment of elastomeric membrane microstructures is required to keep neurons from extending neurites underneath the non-microtunnel areas of the microstructure. This irreversible binding also limits the number of times the MEAs can be reused. A silicon dissolving product is available which will not harm metal or glass (Dynasolve218 from Dynaloy). This product may be used to remove worn out or clogged elastomeric membranes so that an MEA may be reused more times.

APPENDICES

Appendix A

Chamber Loading Process

Before chamber assembly all chamber parts and accessories should be cleaned and sterilized. Parts should be cleaned in a Tergazyme® solution which removes cell debris which may otherwise clog microinjection fibers and Microtight fittings. Except for the microinjection syringe all parts may be autoclaved. The microinjection syringe is sterilized by filling with and soaking in 2% bleach and then thoroughly rinsed with DI water. Next it is rinsed ethanol and allowed to dry fully for at least one day (to remove traces of ethanol toxic to cells). For best results, all chamber parts are exposed to UV radiation for 15 minutes just before use.

First the bottom clamp is placed with the beveled side down on a flat surface with the four threaded holes making a square as shown in Figure x. The substrate, which was either a coverslip with membrane or MEA with membrane, either of which are square, was placed in a diagonal/diamond configuration with the corners pointing between screw holes. If a PDMS chamber wall has been bound to the substrate, the microinjection fiber channel should be oriented to one side. If one has not been applied it should be carefully aligned to the substrate in a similar fashion. If a PDMS wall is not permanently bound, it may be difficult to obtain a tight seal, especially if the surface has been coated with slippery gel. Additionally, after culture, if an MEA is not using a permanently bound PDMS wall, the wall will leak fluid through the spaces of an unclamped PDMS wall setting on the substrate. One should also consider the height of

the PDMS wall. For patterning a 500µm height may be desirable to reduce the Z travel distance and overall patterning time; however this height provides very little space for an adequate media volume to cover the culture. With these considerations in mind, it was best to apply a thin, but full covering silicon grease to the underside of the PDMS wall before attachment to ensure a water-tight seal improve PDMS wall immobilization.

Before the microinjection fiber is inserted it should be checked to ensure proper fluid flow to avoid assembling the chamber with a clogged fiber. To check fluid flow, loosely assemble the three-piece Microtight fitting and insert one end of a microinjection fiber in the fitting. Make sure the fiber is fully seated in the fitting and then secure the fitting with moderate torque. To loose of a fastening will come undone or leak, to tight can damage the fitting and reduce the flow aperture. Next attach a 3ml luer-locking syringe filled with media or sterile water (no air bubbles). Depress the plunger and observe fluid flow from the microinjection fiber tip. Once fluid flow is confirmed, rest the fiber in the fiber-channel of the PDMS wall so that the fiber tip is ½ to ¾ of the way into the chamber. Rest the syringe on the table so that the fiber stays in this position.

Next, insert 10-32/barbed nylon elbow fittings into the ventblock and tighten them as far as they will go while remaining pointing out. Make sure that the glass is clean, if it is not, clean it with ethanol, and/or scrape it with a razorblade. Now place the ventblock directly over the PDMS wall, with the inlet and outlet ports pointing up/down, towards/away from you so that they align with the inlet and outlet cutouts in the PDMS walls. At this point, the microinjection fiber may be placing some pressure on the vent block to move. If so, hold the vent block down with one hand. With the other hand pick

up the top clamp so that your index and middle finger go through the rectangular opening. Use these fingers to press downward on the nylon fittings of the vent block, holding it in place, and freeing the first hand. Orient the top clamp so the holes align with those of the bottom clamp and drop all four thumb screws into the holes. Insert and tighten 1-2 turns at a time 2 opposing screws at a time until the clamp is lightly secured. Do not over tighten the screws; this will crack the glass substrate or ventblock window.

Now the 50µL syringe should be loaded with cell suspension. Optimal cell density is between 200,000 and 500,000 cells/mL If cells are plentiful, 1 million cells may be added to 3mL of media in a 15mL conical tube. This allows room to insert the 50uL syringe into the tube and be adequately submerged in media. Place the syringe with fully depressed plunger into a tilted tube and tap it against the tube to release air bubbles from the luer lock. Next, slowly withdraw the plunger almost completely. Notice the air bubble near the whit Teflon plunger tip. Slowly depress the plunger 80% of the way. Now quickly tap the plunger with a finger to depress it fully and expel air bubbles, tap the plunger to release air bubbles and repeat this process until no air bubbles are seen in the microsyringe. If cells are limited, perform this last step with blank media. With 20% volume remaining in the syringe, invert it and slowly depress the rest of the way. With a pipette aid, dispense the patterning cell suspension with appropriate cell density drop-wise onto the microsyringe tip. Slowly withdraw the syringe to decrease the size of the drop resting on the tip. Do not suck in all of the drop. Add another drop of suspension and repeat until the syringe is fully loaded.

Set the micro syringe aside, on its side) and pick up the 3mL syringe attached to the microinjection fiber. Carefully unscrew it from the Microtight fitting. Dispense drop-wise media into the top of the Microtight fitting until filled. There will be bubbles on top, remove bubbles by suctioning them off with the 3mL syringe. Refill the Microtight fitting until it is full and there are no bubbles on top. Holding the Microtight upright in one hand, grab the 50µL syringe with the other, plunger sticking up. Depress the plunger slightly so that a drop of cell suspension is visible at the tip of the syringe. Place the syringe into the Microtight fitting and screw them together tightly. Depress the plunger 10% just to ensure any air bubbles in the line are expelled.

Attach the tubes with nylon barb/luer-lock fittings onto the barbed ventblock fittings, (they need not be fully inserted, just securely). Attach the previous 3mL syringe full of media to the tube nearest you. From here on every step of the way be careful not to pull out the micro injection fiber. Now tilt the chamber toward you so that you can see inside the chamber including the micro injection fiber. Slowly inject media into the chamber, clearing all bubbles from inside the chamber. When the media begins to flow into the exit tube, pause and watch the media level. If it is stationary then you have a good chamber seal, if it is slowly receding, the chamber is not sealed properly and you must restart the process. If the chamber is not leaking, affix a cap to the end of the outlet tube.

Place a chamber in a sealed box for transport to the laser patterning system. The potential for contamination of your culture while travelling through the hallway and different rooms high. Turn on the nitrogen supply to the stage counter balance and the

power to the laser patterning system components. Remove the chamber from the box and place the bottom camp into the mount so that the microinjection fiber is leading towards the micro injector. Raise the stage with your hand so that the substrate comes into focus on the imaging screen. Place the 50uL syringe next to the microinjector, note the disparity between the plunger holder and the plunger position. On the UltraMicroPumpII controller use the cursor keys to select the “I” for inject, press select to change the “I” to “W” for withdraw. Use the cursor and number keys to change the injection volumes and rates to 900µL and 925µL/S, this will speed up this step. Press the “run” button repeatedly until the plunger holder is aligned with the plunger end. Now press the syringe clamp button on the microinjector and push the syringe inside. Secure the plunger by tightening the plunger clamp.

Make sure that the Xbox360 controller is turned on, press the x button until the battery status is displayed on screen, then press it again to remove the status display. You may now start the laser patterning control software.

Appendix B

Using the Laser Cell Patterning Control Application

Before starting the application make sure the power to the stage and microinjector are turned on and that the Xbox360 controller is on and recognized.

Start Application

Initialize

Click each axis indicator once to turn it green, adding it to the axis mask which will receive commands

Enable axis

If automatic intensity reduction is desired, check the box next to it and input the desired values for X and Y closeness and for Z distance above when you want the intensity to be reduced.

Use the thumbsticks to navigate through the chamber and find the area of the substrate where the cells should be deposited. Mark the first deposition point

Navigate back through the chamber (toward the bottom of the screen) while sweeping left to right until you see the long shadow of the microinjection fiber.

Navigate to the tip of the microinjection fiber and press the 'set injection point' button on the control program's front panel.

Press the top left shoulder button on the game pad to inject cells.

Select a cell that looks healthy, maneuver it to the center of the screen, and pull the left trigger to open the laser shutter and grab the cell.

Hold the laser trigger and follow the onscreen navigation arrow to guide the cell to the deposition point.

Push the cell to the surface until it will not slide. The cell has been patterned. Release the laser trigger

Find the next deposition point and mark it.

Repeat from step 9 (the chamber will automatically move to bring the microinjection fiber into the field of view.)

When all cells are patterned, press the STOP button (do not hit the top right X).

Appendix C

Alignment of Masks

Operation of the Karl Suss MJB-3 Mask aligner was described in the machines manual. Practically however, alignment of the pattern in the exposed layers of photoresist on the wafer with the un exposed mask attached to the mask holder was not described, and must be worked out on one's own, taught in the photolithography lab. Here we will briefly describe a method for aligning the mask and the wafer so as to provide a third or supplementary means of learning the process. A set of alignment guides or marks (as shown in Figure 5.5) must be present in all layers to make alignment possible. A rough alignment is helpful because it saves time spent searching over a wide area for the alignment markings. Additionally, X, Y and rotational travel of the chuck stage was limited and may be insufficient to bring the wafer into alignment without a good rough alignment. Using the large outer marking for rough alignment to the 2" wafer shape was very helpful. Once the wafer was placed on the chuck and moved beneath the mask, the chuck was raised, but without coming into contact with the mask. The mask and the wafer could both be visualized in this manner, though not as clearly as in contact mode or defined separation. The first stage of alignment was performed at this point by finding and perfectly aligning the top markings, then moving to the bottom markings and aligning half the difference with the X translation and half with the rotational adjustment. Once the alignment was close, the chuck was brought into full contact and then separated by 350μm with the separation lever. At this stage, surface defects could cause sticking

between the wafer and the mask, and separation may be increased to 450μm if needed. For best visualization the illumination iris was closed to its smallest position and the intensity turned to its max. Again the wafer was aligned by adjusting the top and bottom markers using the 'half difference' method, and then the left and right markers using the 'half difference' method. Finally, the horizontal (X) alignment was confirmed using the top and bottom markers, and then never touched again. The vertical(Y) alignment was finalized by looking at the right arrow shaped marker (Figure 5.5) which could give a good indication of alignment without changing the X translation. Next the separation lever was withdrawn and vacuum contact engaged. A good contact sufficient for obtaining good resolution was affirmed by a vacuum reading of at least -4.5 mTorr.

REFERENCES

1. Ashkin, A., *Acceleration and trapping of particles by radiation pressure.* . Phys Rev Lett 1970. **24**(4): p. 156–159.
2. Carlson, N.R., *Physiology of behavior*. 9th ed. 2007, Boston: Pearson/Allyn & Bacon. xviii, 734 p.
3. Ashkin, A., *Observationof a single-beam gradient force optical trap for dielectric particles.* Opt. Lett., 1986. **11**: p. 288 – 290.
4. W.Y. Zhang, G.S.F., S. Tatic-Lucic, *Elastomer-Supported Cold Welding for Room Temperature Wafer-Level Bonding.* **IEEE**, 2004(MEMS 2004 Technical Digest).
5. Haydon, P.G., *Glia: listening and talking to the synapse.* Nat Rev Neurosci, 2001. **2**(3): p. 185-193.
6. Kandel, E.R. and C. Pittenger, *The past, the future and the biology of memory storage.* Philos Trans R Soc Lond B Biol Sci, 1999. **354**(1392): p. 2027-52.
7. Livet, J., et al., *Transgenic strategies for combinatorial expression of fluorescent proteins in the nervous system.* Nature, 2007. **450**(7166): p. 56-62.
8. Zador, A.M., *The basic unit of computation.* Nat Neurosci, 2000. **3 Suppl**: p. 1167.
9. Lubke, J., et al., *Frequency and dendritic distribution of autapses established by layer 5 pyramidal neurons in the developing rat neocortex: comparison with synaptic innervation of adjacent neurons of the same class.* J Neurosci, 1996. **16**(10): p. 3209-18.
10. Brewer, G.J., et al., *Neuron network activity scales exponentially with synapse density.* Journal of Neural Engineering, 2009(1): p. 014001.
11. Lin, C.-H., et al., *Protection of ischemic brain cells is dependent on astrocyte-derived growth factors and their receptors.* Experimental Neurology, 2006. **201**(1): p. 225-233.
12. Vernadakis, A., *GLIA-NEURON INTERCOMMUNICATIONS AND SYNAPTIC PLASTICITY.* Progress in Neurobiology, 1996. **49**(3): p. 185-214.
13. Magistretti, P.J., et al., *Regulation of astrocyte energy metabolism by neurotransmitters.* Ren Physiol Biochem, 1994. **17**(3-4): p. 168-71.
14. Murphy, T.H., et al., *Rapid communication between neurons and astrocytes in primary cortical cultures.* J Neurosci, 1993. **13**(6): p. 2672-9.
15. Kandel, E.R., J.H. Schwartz, and T.M. Jessell, *Principles of neural science*. 4th ed. 2000, New York: McGraw-Hill, Health Professions Division. xli, 1414 p.
16. Rao, A., E.M. Cha, and A.M. Craig, *Mismatched appositions of presynaptic and postsynaptic components in isolated hippocampal neurons.* J Neurosci, 2000. **20**(22): p. 8344-53.
17. Chang, J.C., G.J. Brewer, and B.C. Wheeler, *Microelectrode Array Recordings of Patterned Hippocampal Neurons for Four Weeks.* Biomedical Microdevices, 2000. **2**(4): p. 245-253.

18. Wheeler, B.C., et al., *Microcontact printing for precise control of nerve cell growth in culture.* J Biomech Eng, 1999. **121**(1): p. 73-8.
19. Chang, J. and B. Wheeler, *Pattern Technologies for Structuring Neuronal Networks on MEAs,* in *Advances in Network Electrophysiology*. 2006. p. 153-189.
20. Dworak, B.J. and B.C. Wheeler, *Novel MEA platform with PDMS microtunnels enables the detection of action potential propagation from isolated axons in culture.* Lab Chip, 2009. **9**(3): p. 404-10.
21. Suzuki, I., et al., *Stepwise pattern modification of neuronal network in photo-thermally-etched agarose architecture on multi-electrode array chip for individual-cell-based electrophysiological measurement.* Lab Chip, 2005. **5**(3): p. 241-7.
22. Claverol-Tinture, E., et al., *Multielectrode arrays with elastomeric microstructured overlays for extracellular recordings from patterned neurons.* J Neural Eng, 2005. **2**(2): p. L1-7.
23. Magee, J.C. and D. Johnston, *A synaptically controlled, associative signal for Hebbian plasticity in hippocampal neurons.* Science, 1997. **275**(5297): p. 209-13.
24. Guettier-Sigrist, S., et al., *Cell Types Required to Efficiently Innervate Human Muscle Cells in Vitro.* Experimental Cell Research, 2000. **259**(1): p. 204-212.
25. Gaughwin, P.M., et al., *Astrocytes promote neurogenesis from oligodendrocyte precursor cells.* European Journal of Neuroscience, 2006. **23**(4): p. 945-956.
26. Sylvie Poluch, S.L.J., *A normal radial glial scaffold is necessary for migration of interneurons during neocortical development.* Glia, 2007. **55**(8): p. 822-830.
27. Dennis A. Steindler, E.D.L., *Astrocytes as stem cells: Nomenclature, phenotype, and translation.* Glia, 2003. **43**(1): p. 62-69.
28. Wilson, J.X., *Antioxidant defense of the brain: a role for astrocytes.* Can J Physiol Pharmacol, 1997. **75**(10-11): p. 1149-63.
29. Desagher, S., J. Glowinski, and J. Premont, *Astrocytes protect neurons from hydrogen peroxide toxicity.* J. Neurosci., 1996. **16**(8): p. 2553-2562.
30. Dringen, R., J.M. Gutterer, and J. Hirrlinger, *Glutathione metabolism in brain. Metabolic interaction between astrocytes and neurons in the defense against reactive oxygen species.* European Journal of Biochemistry, 2000. **267**(16): p. 4912-4916.
31. Dringen, R., et al., *The Pivotal Role of Astrocytes in the Metabolism of Iron in the Brain.* Neurochemical Research, 2007. **32**(11): p. 1884-1890.
32. Xu, H.-L. and D.A. Pelligrino, *ATP release and hydrolysis contribute to rat pial arteriolar dilatation elicited by neuronal activation.* Exp Physiol, 2007. **92**(4): p. 647-651.
33. Pellerin, L., et al., *Activity-dependent regulation of energy metabolism by astrocytes: an update.* Glia, 2007. **55**(12): p. 1251-62.
34. Nicholls, D. and D. Attwell, *The release and uptake of excitatory amino acids.* Trends in Pharmacological Sciences, 1990. **11**(11): p. 462-468.

35. Magistretti, P.J. and L. Pellerin, *Cellular Mechanisms of Brain Energy Metabolism. Relevance to Functional Brain Imaging and to Neurodegenerative Disordersa.* Annals of the New York Academy of Sciences, 1996. **777**(1): p. 380-387.
36. Perea, G. and A. Araque, *Synaptic information processing by astrocytes.* Journal of Physiology-Paris, 2006. **99**(2-3): p. 92-97.
37. Allen, N.J. and B.A. Barres, *Signaling between glia and neurons: focus on synaptic plasticity.* Curr Opin Neurobiol, 2005. **15**(5): p. 542-8.
38. Porter, J.T. and K.D. McCarthy, *ASTROCYTIC NEUROTRANSMITTER RECEPTORS IN SITU AND IN VIVO.* Progress in Neurobiology, 1997. **51**(4): p. 439-455.
39. Ventura, R. and K.M. Harris, *Three-Dimensional Relationships between Hippocampal Synapses and Astrocytes.* J. Neurosci., 1999. **19**(16): p. 6897-6906.
40. Kozlov, A.S., et al., *Target cell-specific modulation of neuronal activity by astrocytes.* Proc Natl Acad Sci U S A, 2006. **103**(26): p. 10058-63.
41. MacVicar, B.A., *Voltage-dependent calcium channels in glial cells.* Science, 1984. **226**(4680): p. 1345-7.
42. Verkhratsky, A., R.K. Orkand, and H. Kettenmann, *Glial Calcium: Homeostasis and Signaling Function.* Physiol. Rev., 1998. **78**(1): p. 99-141.
43. Fellin, T. and G. Carmignoto, *Neurone-to-astrocyte signalling in the brain represents a distinct multifunctional unit.* J Physiol, 2004. **559**(1): p. 3-15.
44. Perea, G. and A. Araque, *Astrocytes Potentiate Transmitter Release at Single Hippocampal Synapses.* Science, 2007. **317**(5841): p. 1083-1086.
45. Bains, J.S. and S.H.R. Oliet, *Glia: they make your memories stick!* Trends in Neurosciences, 2007. **30**(8): p. 417-424.
46. Todd, K.J., et al., *Glial cells in synaptic plasticity.* Journal of Physiology-Paris, 2006. **99**(2-3): p. 75-83.
47. Allen, N.J. and B.A. Barres, *Signaling between glia and neurons: focus on synaptic plasticity.* Current Opinion in Neurobiology, 2005. **15**(5): p. 542-548.
48. Kudoh, S.N., et al., *Long-lasting enhancement of synaptic activity in dissociated cerebral neurons induced by brief exposure to Mg2+-free conditions.* Neuroscience Research, 1997. **28**(4): p. 337-344.
49. Heidemann, S.R., et al., *The culture of chick forebrain neurons.* Methods Cell Biol, 2003. **71**: p. 51-65.
50. Dotti, C.G., C.A. Sullivan, and G.A. Banker, *The establishment of polarity by hippocampal neurons in culture.* J. Neurosci., 1988. **8**(4): p. 1454-1468.
51. Vogt, A.K., et al., *Synaptic plasticity in micropatterned neuronal networks.* Biomaterials, 2005. **26**(15): p. 2549-2557.
52. Li, Y., et al., *Characterization of synchronized bursts in cultured hippocampal neuronal networks with learning training on microelectrode arrays.* Biosensors and Bioelectronics, 2007. **22**(12): p. 2976-2982.
53. Ullian, E.M., et al., *Schwann cells and astrocytes induce synapse formation by spinal motor neurons in culture.* Mol Cell Neurosci, 2004. **25**(2): p. 241-51.

54. Zhang, H. and R.H. Miller, *Density-Dependent Feedback Inhibition of Oligodendrocyte Precursor Expansion.* J. Neurosci., 1996. **16**(21): p. 6886-6895.
55. Louis, J.C., D. Muir, and S. Varon, *Autocrine inhibition of mitotic activity in cultured oligodendrocyte-type-2 astrocyte (O-2A) precursor cells.* Glia, 1992. **6**(1): p. 30-8.
56. Zu-Cheng Ye, H.S., *Astrocytes protect neurons from neurotoxic injury by serum glutamate.* Glia, 1998. **22**(3): p. 237-248.
57. Grove, J., et al., *Catecholaminergic Expression in 2N27 Immortal Neural Cell Line Is Enhanced by Glial-Derived Factors.* Neurochemical Research, 1997. **22**(3): p. 267-271.
58. Sugiyama, K., A. Brunori, and M.L. Mayer, *Glial uptake of excitatory amino acids influences neuronal survival in cultures of mouse hippocampus.* Neuroscience, 1989. **32**(3): p. 779-91.
59. Janique Guiramand, A.M.M.-C.d.J.F.C.C.-S.M.V.M.R., *Gliotoxicity in hippocampal cultures is induced by transportable, but not by nontransportable, glutamate uptake inhibitors.* Journal of Neuroscience Research, 2005. **81**(2): p. 199-207.
60. Lisman, J.E., *Relating hippocampal circuitry to function: recall of memory sequences by reciprocal dentate-CA3 interactions.* Neuron, 1999. **22**(2): p. 233-42.
61. Kleinfeld, D., K.H. Kahler, and P.E. Hockberger, *Controlled outgrowth of dissociated neurons on patterned substrates.* J. Neurosci., 1988. **8**(11): p. 4098-4120.
62. Mansur, H.S., et al., *Biomaterial with chemically engineered surface for protein immobilization.* Journal of Materials Science: Materials in Medicine, 2005. **16**(4): p. 333-340.
63. Bani-Yaghoub, M., et al., *Neurogenesis and neuronal communication on micropatterned neurochips.* Biotechnol Bioeng, 2005. **92**(3): p. 336-45.
64. J. Cooper McDonald, D.C.D.J.R.A.D.T.C.H.W.O.J.A.S.G.M.W., *Fabrication of microfluidic systems in poly(dimethylsiloxane).* Electrophoresis, 2000. **21**(1): p. 27-40.
65. Vickers, J.A., M.M. Caulum, and C.S. Henry, *Generation of Hydrophilic Poly(dimethylsiloxane) for High-Performance Microchip Electrophoresis.* Anal. Chem., 2006. **78**(21): p. 7446-7452.
66. Millet, L.J., Matthew E. Stewart, Jonathan V. Sweedler, Ralph G. Nuzzo and Martha U. Gillette, *Microfluidic devices for culturing primary mammalian neurons at low densities.* Lab on a Chip, 2007. **7**: p. 987-994.
67. Lom, B., K.E. Healy, and P.E. Hockberger, *A versatile technique for patterning biomolecules onto glass coverslips.* J Neurosci Methods, 1993. **50**(3): p. 385-97.
68. Garbassi, F., M. Morra, and E. Occhiello, *Polymer surfaces : from physics to technology*. Rev. and updated ed. 1998, Chichester ; New York: Wiley. ix, 486 p.
69. Morra, M., et al., *The characterization of plasma-modified polydimethylsiloxane interfaces with media of different surface energy.* Clin Mater, 1990. **5**(2-4): p. 147-56.

70. Brumbach, M., et al., *Surface Composition and Electrical and Electrochemical Properties of Freshly Deposited and Acid-Etched Indium Tin Oxide Electrodes.* Langmuir, 2007.
71. Vancha, A.R., et al., *Use of polyethyleneimine polymer in cell culture as attachment factor and lipofection enhancer.* BMC Biotechnol, 2004. **4**: p. 23.
72. Vleggeert-Lankamp, C.L., et al., *Adhesion and proliferation of human Schwann cells on adhesive coatings.* Biomaterials, 2004. **25**(14): p. 2741-51.
73. Lakard, S., et al., *Adhesion and proliferation of cells on new polymers modified biomaterials.* Bioelectrochemistry, 2004. **62**(1): p. 19-27.
74. Ruegg, U.T. and F. Hefti, *Growth of dissociated neurons in culture dishes coated with synthetic polymeric amines.* Neurosci Lett, 1984. **49**(3): p. 319-24.
75. Bledi, Y., A.J. Domb, and M. Linial, *Culturing neuronal cells on surfaces coated by a novel polyethyleneimine-based polymer.* Brain Research Protocols, 2000. **5**(3): p. 282-289.
76. He, W. and R.V. Bellamkonda, *Nanoscale neuro-integrative coatings for neural implants.* Biomaterials, 2005. **26**(16): p. 2983-2990.
77. Wei, H., C.M. George, and V.B. Ravi, *Nanoscale laminin coating modulates cortical scarring response around implanted silicon microelectrode arrays.* Journal of Neural Engineering, 2006(4): p. 316.
78. Hirokazu Kaji, S.S.M.H.T.K.M.N., *Stepwise formation of patterned cell co-cultures in silicone tubing.* Biotechnology and Bioengineering, 2007. **98**(4): p. 919-925.
79. Kim, Y.-H., et al., *Performance and stability of electroluminescent device with self-assembled layers of poly(3,4-ethylenedioxythiophene)-poly(styrenesulfonate) and polyelectrolytes.* Thin Solid Films, 2006. **510**(1-2): p. 305-310.
80. Ruardij, T.G., M.H. Goedbloed, and W.L. Rutten, *Adhesion and patterning of cortical neurons on polyethylenimine- and fluorocarbon-coated surfaces.* IEEE Trans Biomed Eng, 2000. **47**(12): p. 1593-9.
81. Oka, H., et al., *A new planar multielectrode array for extracellular recording: application to hippocampal acute slice.* J Neurosci Methods, 1999. **93**(1): p. 61-7.
82. Shimono, K., et al., *Chronic multichannel recordings from organotypic hippocampal slice cultures: protection from excitotoxic effects of NMDA by non-competitive NMDA antagonists.* Journal of Neuroscience Methods, 2002. **120**(2): p. 193-202.
83. He, Y. and P.W. Baas, *Growing and working with peripheral neurons.* Methods Cell Biol, 2003. **71**: p. 17-35.
84. Brewer, G.J. and C.W. Cotman, *Survival and growth of hippocampal neurons in defined medium at low density: advantages of a sandwich culture technique or low oxygen.* Brain Research, 1989. **494**(1): p. 65-74.
85. Romanova, E.V., et al., *Self-assembled monolayers of alkanethiols on gold modulate electrophysiological parameters and cellular morphology of cultured neurons.* Biomaterials, 2006. **27**(8): p. 1665-1669.
86. Richert, L., et al., *Cell Interactions with Polyelectrolyte Multilayer Films.* Biomacromolecules, 2002. **3**(6): p. 1170-1178.

87. Kam, L., et al., *Axonal outgrowth of hippocampal neurons on micro-scale networks of polylysine-conjugated laminin.* Biomaterials, 2001. **22**(10): p. 1049-1054.
88. Bonner, J. and T.P. O'Connor, *The Permissive Cue Laminin Is Essential for Growth Cone Turning In Vivo.* J. Neurosci., 2001. **21**(24): p. 9782-9791.
89. Lee, H.K., et al., *Nidogen is a prosurvival and promigratory factor for adult Schwann cells.* Journal of Neurochemistry, 2007. **102**(3): p. 686-698.
90. Bozkurt, A., et al., *In Vitro Assessment of Axonal Growth Using Dorsal Root Ganglia Explants in a Novel Three-Dimensional Collagen Matrix.* Tissue Engineering. **0**(0).
91. Blewitt, M. and R. Willits, *The Effect of Soluble Peptide Sequences on Neurite Extension on 2D Collagen Substrates and Within 3D Collagen Gels.* Annals of Biomedical Engineering.
92. Cullen, D., M. Lessing, and M. LaPlaca, *Collagen-Dependent Neurite Outgrowth and Response to Dynamic Deformation in Three-Dimensional Neuronal Cultures.* Annals of Biomedical Engineering, 2007. **35**(5): p. 835-846.
93. Schnell, E., et al., *Guidance of glial cell migration and axonal growth on electrospun nanofibers of poly-[epsilon]-caprolactone and a collagen/poly-[epsilon]-caprolactone blend.* Biomaterials, 2007. **28**(19): p. 3012-3025.
94. Holly Colognato, P.D.Y., *Form and function: The laminin family of heterotrimers.* Developmental Dynamics, 2000. **218**(2): p. 213-234.
95. Yurchenco, P.D., Y.S. Cheng, and H. Colognato, *Laminin forms an independent network in basement membranes [published erratum appears in J Cell Biol 1992 Jun;118(2):493]*. J. Cell Biol., 1992. **117**(5): p. 1119-1133.
96. Rivas, R.J., D.W. Burmeister, and D.J. Goldberg, *Rapid effects of laminin on the growth cone.* Neuron, 1992. **8**(1): p. 107-115.
97. Armstrong, S.J., et al., *ECM Molecules Mediate Both Schwann Cell Proliferation and Activation to Enhance Neurite Outgrowth.* Tissue Engineering. **0**(0).
98. Lee, J.N., C. Park, and G.M. Whitesides, *Solvent compatibility of poly(dimethylsiloxane)-based microfluidic devices.* Anal Chem, 2003. **75**(23): p. 6544-54.
99. Vickers, J.A., M.M. Caulum, and C.S. Henry, *Generation of hydrophilic poly(dimethylsiloxane) for high-performance microchip electrophoresis.* Anal Chem, 2006. **78**(21): p. 7446-52.
100. Lee, J.N., et al., *Compatibility of Mammalian Cells on Surfaces of Poly(dimethylsiloxane).* Langmuir, 2004. **20**(26): p. 11684-11691.
101. Thibault, C., et al., *Poly(dimethylsiloxane) Contamination in Microcontact Printing and Its Influence on Patterning Oligonucleotides.* Langmuir, 2007. **23**(21): p. 10706-10714.
102. Morin, F., et al., *Constraining the connectivity of neuronal networks cultured on microelectrode arrays with microfluidic techniques: A step towards neuron-based functional chips.* Biosensors and Bioelectronics, 2006. **21**(7): p. 1093-1100.

103. Yoonkey, N., M. Katherine, and C.W. Bruce, *Application of a PDMS microstencil as a replaceable insulator toward a single-use planar microelectrode array.* Biomedical Microdevices, 2006. **V8**(4): p. 375-381.
104. Claverol-Tinture, E., J. Cabestany, and X. Rosell, *Multisite recording of extracellular potentials produced by microchannel-confined neurons in-vitro.* IEEE Trans Biomed Eng, 2007. **54**(2): p. 331-5.
105. Francisco, H., et al., *Regulation of axon guidance and extension by three-dimensional constraints.* Biomaterials, 2007. **28**(23): p. 3398-3407.
106. Clark, P., et al., *Topographical control of cell behaviour. I. Simple step cues.* Development, 1987. **99**(3): p. 439-48.
107. Vorobjev, I.A., et al., *Optical trapping for chromosome manipulation: a wavelength dependence of induced chromosome bridges.* Biophys. J., 1993. **64**(2): p. 533-538.
108. Liang, H., et al., *Wavelength dependence of cell cloning efficiency after optical trapping.* Biophys. J., 1996. **70**(3): p. 1529-1533.
109. Odde, D.J. and M.J. Renn, *Laser-guided direct writing of living cells.* Biotechnol Bioeng, 2000. **67**(3): p. 312-8.
110. Mohanty, S.K., et al., *Comet Assay Measurements of DNA Damage in Cells by Laser Microbeams and Trapping Beams with Wavelengths Spanning a Range of 308 nm to 1064 nm.* Radiation Research, 2002. **157**(4): p. 378-385.
111. Ashkin, A., *History of optical trapping and manipulation of small-neutral particle, atoms, and molecules.* Selected Topics in Quantum Electronics, IEEE Journal of, 2000. **6**(6): p. 841-856.
112. Lang, M.J. and S.M. Block, *Resource Letter: LBOT-1: Laser-based optical tweezers.* Am J Phys, 2003. **71**(3): p. 201-215.
113. Ashkin, A. and J.M. Dziedzic, *Optical trapping and manipulation of viruses and bacteria.* Science, 1987. **235**(4795): p. 1517-1520.
114. Ashkin, A., J.M. Dziedzic, and T. Yamane, *Optical trapping and manipulation of single cells using infrared laser beams.* Nature, 1987. **330**(6150): p. 769-771.
115. Konig, K., et al., *Andrology: Effects of ultraviolet exposure and near infrared laser tweezers on human spermatozoa.* Hum. Reprod., 1996. **11**(10): p. 2162-2164.
116. Liu, Y., et al., *Evidence for localized cell heating induced by infrared optical tweezers.* Biophys. J., 1995. **68**(5): p. 2137-2144.
117. Ringeisen, B.R., Christina M. Othon Jason A. Barron Daniel Young Barry J. Spargo, *Jet-based methods to print living cells.* Biotechnology Journal, 2006. **1**(9): p. 930-948.
118. Renn, M.J. and R. Pastel. *Particle manipulation and surface patterning by laser guidance*. in *Papers from the 42nd international conference on electron, ion, and photon beam technology and nanofabrication*. 1998. Chicago, Illinois (USA): AVS.
119. Renn, M.J., R. Pastel, and H.J. Lewandowski, *Laser Guidance and Trapping of Mesoscale Particles in Hollow-Core Optical Fibers.* Physical Review Letters, 1999. **82**(7): p. 1574.

120. Nahmias, Y., et al., *Laser-guided direct writing for three-dimensional tissue engineering.* Biotechnol Bioeng, 2005. **92**(2): p. 129-36.
121. Thomas, C.A., Jr., et al., *A miniature microelectrode array to monitor the bioelectric activity of cultured cells.* Exp Cell Res, 1972. **74**(1): p. 61-6.
122. Gross, G.W., *Simultaneous Single Unit Recording in vitro with a Photoetched Laser Deinsulated Gold Multimicroelectrode Surface.* Biomedical Engineering, IEEE Transactions on, 1979. **BME-26**(5): p. 273-279.
123. Pine, J., *Recording action potentials from cultured neurons with extracellular microcircuit electrodes.* J Neurosci Methods, 1980. **2**(1): p. 19-31.
124. Potter, S.M. and T.B. DeMarse, *A new approach to neural cell culture for long-term studies.* J Neurosci Methods, 2001. **110**(1-2): p. 17-24.
125. Borkholder, D.A., et al., *Microelectrode arrays for stimulation of neural slice preparations.* J Neurosci Methods, 1997. **77**(1): p. 61-6.
126. Bai, Q., K.D. Wise, and D.J. Anderson, *A high-yield microassembly structure for three-dimensional microelectrode arrays.* IEEE Trans Biomed Eng, 2000. **47**(3): p. 281-9.
127. Taketani, M. and M. Baudry, *Advances in network electrophysiology : using multiple-electrode arrays*. 2006, New York, NY: Springer. xvii, 478 p.
128. Gramowski, A., et al., *Substance identification by quantitative characterization of oscillatory activity in murine spinal cord networks on microelectrode arrays.* European Journal of Neuroscience, 2004. **19**(10): p. 2815-2825.
129. Prasad, S., et al., *Separation of individual neurons using dielectrophoretic alternative current fields.* Journal of Neuroscience Methods, 2004. **135**(1-2): p. 79-88.
130. Buitenweg, J.R., et al., *Extracellular detection of active membrane currents in the neuron-electrode interface.* Journal of Neuroscience Methods, 2002. **115**(2): p. 211-221.
131. Wagenaar, D.A., J. Pine, and S.M. Potter, *Effective parameters for stimulation of dissociated cultures using multi-electrode arrays.* Journal of Neuroscience Methods, 2004. **138**(1-2): p. 27-37.
132. Jimbo, Y., et al., *A system for MEA-based multisite stimulation.* IEEE Trans Biomed Eng, 2003. **50**(2): p. 241-8.
133. Wagenaar, D.A. and S.M. Potter, *Real-time multi-channel stimulus artifact suppression by local curve fitting.* Journal of Neuroscience Methods, 2002. **120**(2): p. 113-120.
134. Chiappalone, M., et al., *Dissociated cortical networks show spontaneously correlated activity patterns during in vitro development.* Brain Research, 2006. **1093**(1): p. 41-53.
135. Rieke, F., *Spikes : exploring the neural code*. Computational neuroscience. 1997, Cambridge, Mass.: MIT Press. xvi, 395 p.
136. Maeda, E., H.P. Robinson, and A. Kawana, *The mechanisms of generation and propagation of synchronized bursting in developing networks of cortical neurons.* J. Neurosci., 1995. **15**(10): p. 6834-6845.

137. Wagenaar, D.A., et al., *Controlling Bursting in Cortical Cultures with Closed-Loop Multi-Electrode Stimulation.* J. Neurosci., 2005. **25**(3): p. 680-688.
138. Wagenaar, D.A., J. Pine, and S.M. Potter, *An extremely rich repertoire of bursting patterns during the development of cortical cultures.* BMC Neurosci, 2006. **7**: p. 11.
139. Li, X., et al., *Long-term recording on multi-electrode array reveals degraded inhibitory connection in neuronal network development.* Biosensors and Bioelectronics, 2007. **22**(7): p. 1538-1543.
140. van den Pol, A.N., et al., *Early synaptogenesis in vitro: role of axon target distance.* J Comp Neurol, 1998. **399**(4): p. 541-60.
141. Braga, M.F., et al., *Lead increases tetrodotoxin-insensitive spontaneous release of glutamate and GABA from hippocampal neurons.* Brain Res, 1999. **826**(1): p. 10-21.
142. Chow, C.C. and J.A. White, *Spontaneous action potentials due to channel fluctuations.* Biophys J, 1996. **71**(6): p. 3013-21.
143. Arnold, F.J.L., et al., *Microelectrode array recordings of cultured hippocampal networks reveal a simple model for transcription and protein synthesis-dependent plasticity.* The Journal of Physiology, 2005. **564**(1): p. 3-19.
144. Latham, P.E., et al., *Intrinsic dynamics in neuronal networks. II. experiment.* J Neurophysiol, 2000. **83**(2): p. 828-35.
145. Jimbo, Y., et al., *The dynamics of a neuronal culture of dissociated cortical neurons of neonatal rats.* Biol Cybern, 2000. **83**(1): p. 1-20.
146. DeMarse, T., et al., *The Neurally Controlled Animat: Biological Brains Acting with Simulated Bodies.* Autonomous Robots, 2001. **11**(3): p. 305-310.
147. Shahaf, G. and S. Marom, *Learning in Networks of Cortical Neurons.* J. Neurosci., 2001. **21**(22): p. 8782-8788.
148. Ribeiro, M.J., et al., *Activation of MAPK is necessary for long-term memory consolidation following food-reward conditioning.* Learn. Mem., 2005. **12**(5): p. 538-545.
149. Korneev, S.A., et al., *Timed and Targeted Differential Regulation of Nitric Oxide Synthase (NOS) and Anti-NOS Genes by Reward Conditioning Leading to Long-Term Memory Formation.* J. Neurosci., 2005. **25**(5): p. 1188-1192.
150. Jones, N.G., et al., *A Persistent Cellular Change in a Single Modulatory Neuron Contributes to Associative Long-Term Memory.* Current Biology, 2003. **13**(12): p. 1064-1069.
151. Eytan, D., et al., *Dopamine-induced dispersion of correlations between action potentials in networks of cortical neurons.* J Neurophysiol, 2004. **92**(3): p. 1817-24.
152. Feber, J.l., et al., *Conditional firing probabilities in cultured neuronal networks: a stable underlying structure in widely varying spontaneous activity patterns.* Journal of Neural Engineering, 2007. **4**(2): p. 54.
153. Del Giudice, P., S. Fusi, and M. Mattia, *Modelling the formation of working memory with networks of integrate-and-fire neurons connected by plastic synapses.* Journal of Physiology-Paris, 2003. **97**(4-6): p. 659-681.

154. Giugliano, M., et al., *Single-Neuron Discharge Properties and Network Activity in Dissociated Cultures of Neocortex.* J Neurophysiol, 2004. **92**(2): p. 977-996.
155. Wagenaar, D.A., Z. Nadasdy, and S.M. Potter, *Persistent dynamic attractors in activity patterns of cultured neuronal networks.* Physical Review E (Statistical, Nonlinear, and Soft Matter Physics), 2006. **73**(5): p. 051907-8.
156. Compte, A., *Computational and in vitro studies of persistent activity: Edging towards cellular and synaptic mechanisms of working memory.* Neuroscience, 2006. **139**(1): p. 135-151.
157. Hopfield, J.J., *Neural networks and physical systems with emergent collective computational abilities.* Proc Natl Acad Sci U S A, 1982. **79**(8): p. 2554-8.
158. Hebb, D.O., *The organization of behavior; a neuropsychological theory*. 1949, New York,: Wiley. xix, 335 p.
159. Finkel, L.H., *Neuroengineering models of brain disease.* Annu Rev Biomed Eng, 2000. **2**: p. 577-606.
160. Tsodyks, M., *Attractor Neural Networks and Spatial Maps in Hippocampus.* Neuron, 2005. **48**(2): p. 168-169.
161. Costa Lda, F. and E.T. Manoel, *A percolation approach to neural morphometry and connectivity.* Neuroinformatics, 2003. **1**(1): p. 65-80.
162. Breskin, I., et al., *Percolation in living neural networks.* Phys Rev Lett, 2006. **97**(18): p. 188102.
163. Eckmann, J.-P., et al., *The physics of living neural networks.* Physics Reports, 2007. **449**(1-3): p. 54-76.
164. Jimbo, Y., H.P. Robinson, and A. Kawana, *Simultaneous measurement of intracellular calcium and electrical activity from patterned neural networks in culture.* IEEE Trans Biomed Eng, 1993. **40**(8): p. 804-10.
165. Curtis, A.S., et al., *Making real neural nets: design criteria.* Med Biol Eng Comput, 1992. **30**(4): p. CE33-6.
166. Chang, J.C., G.J. Brewer, and B.C. Wheeler, *Neuronal network structuring induces greater neuronal activity through enhanced astroglial development.* J Neural Eng, 2006. **3**(3): p. 217-26.
167. Chang, J.C., G.J. Brewer, and B.C. Wheeler, *Modulation of neural network activity by patterning.* Biosensors and Bioelectronics, 2001. **16**(7-8): p. 527-533.
168. Feinerman, O. and E. Moses, *Transport of Information along Unidimensional Layered Networks of Dissociated Hippocampal Neurons and Implications for Rate Coding.* J. Neurosci., 2006. **26**(17): p. 4526-4534.
169. Feinerman, O., M. Segal, and E. Moses, *Identification and Dynamics of Spontaneous Burst Initiation Zones in Unidimensional Neuronal Cultures.* J Neurophysiol, 2007. **97**(4): p. 2937-2948.
170. Pirlo, R.K., et al., *Cell deposition system based on laser guidance.* Biotechnol J, 2006. **1**(9): p. 1007-13.
171. Susan Kentroti, A.V., *Differential expression in glial cells derived from chick embryo cerebral hemispheres at an advanced stage of development.* Journal of Neuroscience Research, 1997. **47**(3): p. 322-331.

172. Barnea, A., et al., *Interleukin-1[beta] induces expression of neuropeptide Y in primary astrocyte cultures in a cytokine-specific manner: induction in human but not rat astrocytes.* Brain Research, 2001. **896**(1-2): p. 137-145.
173. Taylor, A.R., et al., *Astrocyte and Muscle-Derived Secreted Factors Differentially Regulate Motoneuron Survival.* J. Neurosci., 2007. **27**(3): p. 634-644.
174. Smeal, R.M., et al., *Substrate curvature influences the direction of nerve outgrowth.* Ann Biomed Eng, 2005. **33**(3): p. 376-82.
175. Mahoney, M.J., et al., *The influence of microchannels on neurite growth and architecture.* Biomaterials, 2005. **26**(7): p. 771-778.
176. Lawrence, C.J., *The mechanics of spin coating of polymer films.* Physics of Fluids, 1988. **31**(10): p. 2786-2795.
177. Emslie, A.G., F.T. Bonner, and L.G. Peck, *Flow of a Viscous Liquid on a Rotating Disk.* Journal of Applied Physics, 1958. **29**(5): p. 858-862.
178. Vogt, A.K., et al., *Impact of micropatterned surfaces on neuronal polarity.* Journal of Neuroscience Methods, 2004. **134**(2): p. 191-198.
179. Stenger, D.A., et al., *Microlithographic determination of axonal/dendritic polarity in cultured hippocampal neurons.* Journal of Neuroscience Methods, 1998. **82**(2): p. 167-173.
180. Brewer, G.J. and P.J. Price, *Viable cultured neurons in ambient carbon dioxide and hibernation storage for a month.* Neuroreport, 1996. **7**(9): p. 1509-12.